



AN ABSTRACT OF THE DISSERTATION OF

Holly Rene Barnard for the degree of Doctor of Philosophy in Forest Science  
and Forest Engineering presented on June 4, 2009

Title: Inter-relationships of Vegetation, Hydrology and Micro-climate in a Young,  
Douglas-fir Forest

Abstract approved:

---

Barbara J. Bond

Jeffrey J. McDonnell

The links between forests, streamflow, and climate are poorly understood. Despite hundreds of studies over the past 60 years, fundamental questions of forests' effects on the hydrologic cycle remain unanswered. The hydrological cycle involves mutually-dependent biological and physical processes that operate at multiple scales of time and space, and this principle is the foundation for research in ecohydrology. The objective of this research was to determine how vegetation processes (especially transpiration) affect subsurface water flow dynamics in hillslopes, and conversely how soil moisture and environmental variables affect vegetation function.

This dissertation used multiple approaches to mechanistically assess the inter-relationships between vegetation water use, hydrology, and climate. I found that transpiration on hillslopes played an important role in diel variation in subsurface discharge in headwater catchment. However, the amount of influence transpiration had on discharge was strongly dependent upon soil moisture properties. In addition, plot-scale transpiration across a steep topographic gradient could not be predicted from measured variations in environmental variables alone. Heterogeneity in biophysical drivers, edaphic properties and whole tree conductance controlled plot scale transpiration. Last, I applied a dual isotope ( $^{13}\text{C}$  and  $^{18}\text{O}$ ) approach to infer physiological response of trees to changing environmental conditions. I found that stable isotopes of oxygen were directly related to stomatal conductance and inversely related to relative humidity; however, the relationship with relative humidity more

apparent. The correlation of stable isotopes in tree rings with environmental variables can be particularly useful for assessing the impacts of environmental change on vegetation over short time series. Results demonstrated that the physiological interpretation of stable isotope in tree rings continues to be challenging in uncontrolled environments. This work represents one step forward in elucidating the linkages between vegetation processes, hydrology, and climate.

© Copyright by Holly Rene Barnard

June 4, 2009

All Rights Reserved

Inter-relationships of Vegetation, Hydrology and Micro-climate in a Young,  
Douglas-fir forest

by

Holly Rene Barnard

A DISSERTATION

Submitted to

Oregon State University

In partial fulfillment of  
the requirements for the  
degree of

Doctor of Philosophy

Presented June 4, 2009

Commencement June 2009

Doctor of Philosophy dissertation of Holly Rene Barnard presented on June 4, 2009.

APPROVED:

---

Co-Major Professor, representing Forest Science

---

Co-Major Professor, representing Forest Engineering

---

Head of the Department of Forest Ecosystems and Society

---

Head of the Department of Forest Engineering, Resources and Management

---

Dean of the Graduate School

I understand that my dissertation will become part of the permanent collection of Oregon State University libraries. My signature below authorizes release of my dissertation to any reader upon request.

---

Holly Rene Barnard, Author

## CONTRIBUTION OF AUTHORS

Chapter 2: Dr. Barbara Bond, Dr. Jeffrey McDonnell and Dr. J. Renee Brooks provided assistance with data interpretation and editing of the manuscript. Chris Graham and Willem VanVerseveld provided logistical support and assisted with editing.

Chapter 3: Dr. Barbara Bond, Dr. Jeffrey McDonnell, Dr. J. Renee Brooks and Dr. Frederick Meinzer provided assistance with data interpretation and editing of the manuscript. Dr. Thomas Pypker provided assistance with data interpretation. Adam Kennedy provided soil moisture and environmental data. Claire Phillips provided soil moisture retention data. Dr. Takahiro Sayama provided radiation data interpretation of the results.

Chapter 4: Dr. Barbara Bond and Dr. J. Renee Brooks provided assistance with data interpretation and editing of the manuscript.

## ACKNOWLEDGEMENTS

First and foremost, I am grateful for my loving partner, Matt Findley. Matt took the biggest career risk, sacrificed the most personal time, and has endured the hardships of me attaining this degree in ways most people would find hard to imagine.

My deep appreciation goes out to my co-advisors, Barbara Bond and Jeff McDonnell. Barbara was the first to introduce me to the field of ecohydrology and correctly convinced me that OSU would best be the place to pursue my interests. Jeff accepted me into his lab and always encouraged me to pursue the research that excited me. J. Renee Brooks deserves special recognition for being an exceptional unofficial advisor, mentor, and friend. This research would not have been possible without Renee's generosity with her time, ideas, and laboratory. This dissertation greatly benefited from the helpful comments of and discussions with Rick Meinzer and Jim Wigington. Tom Hinckley and Linda Brubaker were my undergraduate advisors nearly a decade ago and they continue to be willing to guide and mentor me through my academic highs and lows. I would like to recognize Elizabeth Sulzman who is dearly missed by friends and colleagues and served as an inspiration to many young, female scientists including myself.

Very special thanks to the McDonnell and Bond lab members for making coming into work each day a pleasure. Without Adam Mazurkiewicz, Chris Graham, Zac Kayler, Tom Pypker, Willem vanVerseveld, Cody Hale, Luisa Hopp, Dave Alley, Dave Callery, Takahiro Sayama, and Rosemary Fanelli, I would have learned a lot less, laughed a lot less, played a lot less, and saved a lot more money throughout my PhD. Numerous people assisted me with field work, but I especially appreciate the efforts of Aidan Padilla. I thank Sierra Wolfenbarger for cutting and grinding hundreds of tree rings. Last, Jack T. Beagle has been my constant companion throughout all my academic endeavors. Thanks for being the best, best-friend.

Financial support was provided by the Ford Foundation, the OSU Graduate School, OSU Institute for Water and Watersheds, the American Geophysical Union and by Bond and McDonnell research funds. Data and facilities were provided by the HJ Andrews Experimental Forest research program, funded by the National Science

Foundation's Long-Term Ecological Research Program (DEB 08-23380), US Forest Service Pacific Northwest Research Station, and Oregon State University.

## TABLE OF CONTENTS

	<u>Page</u>
Chapter 1 Introduction .....	1
Introduction .....	2
Chapter 2 Mechanistic assessment of hillslope transpiration controls of diel sub-surface flow: a steady-state irrigation approach .....	8
Introduction .....	9
Methods .....	11
Study Site Description .....	11
Irrigation Experiment .....	12
Hillslope discharge and lateral subsurface flow .....	13
Xylem Water Flux, Transpiration, and Canopy Reference Evapotranspiration .....	13
Soil Moisture .....	15
Analysis .....	15
Results .....	16
Hillslope discharge .....	16
Xylem Water Flux, Transpiration, and Canopy Reference Evapotranspiration .....	17
Soil Moisture .....	18
Discussion .....	18
Conclusion .....	22
References .....	23
Chapter 3 The response of Douglas-fir transpiration to variation in environmental drivers in complex terrain .....	30
Introduction .....	31
Methods .....	33
Study Site .....	33
Transpiration .....	34
Micro-climate .....	36
Soil Moisture and Retention Curves .....	37
Predawn Tree Water Potential ( $\Psi_{PD}$ ) .....	37
Soil Depth and Resistance to Penetration .....	38
Analyses .....	38
Results .....	40
Transpiration .....	40
Micro-climate .....	41
Soil Moisture and Soil Water Retention Curves .....	42
Predawn Tree Water Potential .....	42
Soil Depth and Resistance to Penetration .....	43

## TABLE OF CONTENTS (Continued)

	<u>Page</u>
Effects of Environmental Predictor Variables on Daily Transpiration .....	43
Examining the response of E to micro-environment using a mechanistic model ..	44
Discussion .....	46
Insights gained from the statistical model .....	46
Insights gained using a mechanistic modeling approach.....	47
Spatial variability in edaphic properties .....	48
Conclusion.....	49
References .....	51
Chapter 4 A dual isotope ( $^{13}\text{C}$ and $^{18}\text{O}$ ) approach to infer annual aboveground biomass increment in young Douglas-fir.....	68
Introduction .....	69
Methods .....	72
Study site .....	72
Tree ring sampling and processing.....	72
Xylem water sampling.....	74
Isotope analysis.....	74
Environmental variables .....	75
Estimating $g_s$ from environmental data and $\delta^{18}\text{O}$ data .....	75
Estimating A from $\delta^{13}\text{C}_{\text{cell}}$ and $g_s$ derived from $\delta^{18}\text{O}_{\text{cell}}$ .....	76
Aboveground biomass and leaf area estimates.....	76
Foliar Nitrogen .....	77
Application of the Scheidegger Conceptual Model.....	77
Statistics.....	79
Results .....	79
Time series of $\delta^{13}\text{C}_{\text{cell}}$ , $\delta^{18}\text{O}_{\text{cell}}$ , and BAI .....	79
A derived from $\delta^{13}\text{C}_{\text{cell}}$ and $\delta^{18}\text{O}_{\text{cell}}$ versus BMI.....	80
Correlations between environmental variables and $\delta^{13}\text{C}_{\text{cell}}$ , $\delta^{18}\text{O}_{\text{cell}}$ , and BAI.....	81
Conceptual Model of $\delta^{13}\text{C}_{\text{cell}}$ and $\delta^{18}\text{O}_{\text{cell}}$ relationships.....	82
Discussion .....	83
Can $^{13}\text{C}$ and $^{18}\text{O}$ be used to estimate aboveground net primary production? .....	83
The relationship between $\delta^{13}\text{C}_{\text{cell}}$ , $\delta^{18}\text{O}_{\text{cell}}$ and environmental variables .....	84
Do variations in $\delta^{13}\text{C}_{\text{cell}}$ and $\delta^{18}\text{O}_{\text{cell}}$ correspond to the Scheidegger conceptual model? .....	85
On the importance of stand dominance in tree ring isotope research.....	86
Conclusion .....	87

TABLE OF CONTENTS (Continued)

	<u>Page</u>
References .....	89
Chapter 5 Conclusion .....	104
Conclusion .....	105
Summary of main dissertation findings .....	105
Future research .....	106
References .....	108
Appendix A Stable isotope theory .....	109
Isotopic Theory .....	110
References .....	113
Bibliography .....	115

## LIST OF FIGURES

<u>Figure</u>	<u>Page</u>
Figure 2-1: Map of study site with outline of irrigated area with 24 time domain reflectometry rods, meteorological station and instrumented trees.....	26
Figure 2-2: (A) Hillslope irrigation rate, (B) Hillslope discharge, (C) Difference in xylem flux density between irrigated and control Douglas-fir trees, and (D) Soil volumetric water content versus Time.....	27
Figure 2-3: Total diel reduction in hillslope discharge ('missing trenchflow'), total daily hillslope transpiration, and average daily canopy reference evapotranspiration for 3 irrigation periods.....	28
Figure 2-4: Phase (time lag) relationship between maximum transpiration and minimum hillslope discharge for 3 irrigation periods.....	29
Figure 3-1: Map of the location of the HJ Andrews Experimental Forest and Watershed 1.....	60
Figure 3-2: Transpiration (A-B), mean 0800-1430 $D$ (C-D), total daily $Q$ (E-F), soil volumetric water content at 30 cm depth (G-H), $\Psi_{PD}$ (symbols with connecting lines) and $\Psi_S$ (solid lines, no symbols) (I-J) throughout the growing season for our four study plots.....	61
Figure 3-3: The relationship between mean 0800-1430 $D$ and $E$ for early (DOY 100-181; open symbols), mid- (DOY 182-256; gray symbols), and late (DOY 257-300; black symbols) growing season.....	62
Figure 3-4: The relationship between total daily $Q$ and $E$ for early (DOY 100-181; open symbols), mid- (DOY 182-256; gray symbols), and late (DOY 257-300; black symbols) growing season.....	63
Figure 3-5: Soil moisture retention curves for the four study plots.....	64
Figure 3-6: The relationship between $\Psi_S$ at 30 cm depth and $E$ for early (DOY 100-181; open symbols), mid- (DOY 182-256; gray symbols), and late (DOY 257-300; black symbols) growing season.....	65
Figure 3-7: Results of the Bond-Kavanagh model for six model scenarios (see Table 3-2) examining the relative decline in $E$ through time for each of the four study plots.....	66
Figure 3-8: Estimated mid-day $K_L$ through time for each of the four study plots.....	67
Figure 4-1: Conceptual application of the Scheidegger model (adapted from Scheidegger et al. (2000)).....	95
Figure 4-2: Map of the location of the HJ Andrews Experimental Forest and Watershed 1.....	96
Figure 4-3: Temperature ( $T$ ), relative humidity ( $RH$ ), $\delta^{18}O_{cell}$ and $\delta^{13}C_{cell}$ through time.....	97

LIST OF FIGURES (Continued)

<u>Figure</u>	<u>Page</u>
Figure 4-4: Annual basal area increment by crown class. Circles = dominant, Squares = co-dominant, triangles = intermediate, and summer precipitation (May-October). Error bars equal the standard error of the means. ....	98
Figure 4-5: Aboveground biomass increment (BMI) relative to maximum aboveground BMI versus isotope derived $A$ relative to maximum isotope derived $A$ for earlywood (Panel A) and latewood (Panel B). ....	99
Figure 4-6: $\delta^{13}\text{C}_{\text{cell}}$ and $\delta^{18}\text{O}_{\text{cell}}$ Cellulose $\delta^{13}\text{C}$ value minus the mean $\delta^{13}\text{C}$ value for all samples versus $\delta^{18}\text{O}$ minus mean $\delta^{18}\text{O}$ for all samples for earlywood (Panels A-C) and latewood (Panel D-F). ....	100
Figure 4-7: $\delta^{13}\text{C}_{\text{cell}}$ minus mean $\delta^{13}\text{C}_{\text{cell}}$ versus $\delta^{18}\text{O}_{\text{cell}}$ minus mean $\delta^{18}\text{O}_{\text{cell}}$ for earlywood (Panels A-C) and latewood (Panel D-F). ....	101
Figure 4-8: $\delta^{13}\text{C}_{\text{cell}}$ minus mean $\delta^{13}\text{C}_{\text{cell}}$ versus $\delta^{18}\text{O}_{\text{cell}}$ minus mean $\delta^{18}\text{O}_{\text{cell}}$ for earlywood (Panels A-C) and latewood (Panel D-F). ....	102
Figure 4-9: The difference between latewood and earlywood $\delta^{13}\text{C}_{\text{cell}}$ and $\delta^{18}\text{O}_{\text{cell}}$ for dominant (A), co-dominant (B), and intermediate (C) crown classes. ....	103

## LIST OF TABLES

<u>Table</u>	<u>Page</u>
Table 3-1: The site characteristics for each of the four plots. ....	57
Table 3-2: Summary of parameters used in the Bond-Kavanagh model and how they were varied during six different model scenarios. ....	58
Table 3-3: Regression coefficients ( $\beta$ ), p-values and coefficients of partial determination ( $r^2_{PD}$ ) of models for early-, mid-, and late-season prediction of daily transpiration. ....	59
Table 4-1: Pearson correlation coefficient (r), p-value (p), and number of observations (N) for the relationship between normalized cellulose $\delta^{13}C_{cell}$ , $\delta^{18}O_{cell}$ , BAI, and climate variables for both earlywood and latewood. ....	93
Table 4-2: The nitrogen composition (%) of current year (2006) foliage, 1-yr-old foliage (2005). ....	94

## DEDICATION

In loving memory of  
Kathleen G. and Everett P. Barnard

## **Chapter 1 Introduction**

## **Introduction**

The links between forests, streamflow, and climate are poorly understood. Despite hundreds of studies over the past 60 years examining vegetation function, soil hydrologic processes, and micro-environment independently, the feedbacks between these core areas have only recently become a research priority (Berry et al., 2005). The interdisciplinary field of ecohydrology has begun to bring the perspectives of ecosystem scientists and hydrologists together. Historically, ecosystem scientists have tended to approach the soil-plant-atmosphere-continuum from a one dimensional perspective, with water entering a system vertically as precipitation and leaving vertically by evaporation or transpiration. In complex topography with steep hillslopes, this conceptual model is often inadequate, as it does not take account of either the lateral flows of water across a landscape or advective movements of airmasses above ground. Hydrologists, on the other hand, have a strong history and capability in measuring and modeling 3-dimensional flows of water through the ground, but the incorporation of vegetation processes into these measurements and models has been limited (Bond, 2003). Because the inter-relationships between hydrology and ecology affect the quantity, quality, timing and distribution of water of available to humans, ecohydrology is a new research framework to be used by water managers in the sustainable development and management of water resources (Nuttle, 2002, Zalewski, 2002). Indeed, water management practices have begun to shift from more hydrotechnical approaches to those that integrate ecosystem attributes into hydrologic processes (Zalewski, 2000).

Until recently, the paired watershed approach has been the primary means to evaluate forest influences on hydrology. Results from this black-box approach (where only inputs and outputs are characterized) have been highly equivocal where studies have shown that decreases in forest cover result in increased (Bosch and Hewlett, 1982, Calder, 1998), decreased (Bosch and Hewlett, 1982, Cosandey et al., 2005), or no net change in stream discharge (Rich et al., 1961, Harr and McCorison, 1979, Bosch and Hewlett, 1982). In semi-arid zones where paired watershed approaches are infeasible due to limited streamflow, studies of ecohydrological coupling are more advanced and have shown strong relationships between plant physiology and soil infiltration, run-off

obstruction, erosion, groundwater depth and discharge (Pierson et al., 2002, Huxman et al., 2005, Ludwig et al., 2005, Williams et al., 2005). However, in humid, upland regions dominated by forests, detailed process-based studies that explore the interface between plant physiological function and watershed flowpaths and flow sources, have not been widely attempted.

Forest water use (transpiration) is a large component of the annual water balance, and can account for over half of the water that exits mature forested catchments (Hewlett, 1982). Forests within catchments differ from their flat land counterparts due to large spatial variability in solar radiation, slope, and sub-surface hydrology. Transpiration is dependent not only on these topographic properties, but also physiological responses to environmental drivers (Adelman et al., 2008, Lorant et al., 2008). Quantifying the spatial and temporal variation in forest transpiration with regard to topography is central to understanding the influence of complex terrain on both biological and hydrological function.

The goal of this dissertation research is to determine some of the ways that vegetation processes (especially transpiration) affect subsurface water flow dynamics in hillslopes, and conversely how soil moisture and environmental variables affect vegetation function. This research uses multiple approaches to mechanistically assess some of the inter-relationships between vegetation water use, hydrology, and climate. Chapter 2 describes a steady-state irrigation experiment performed at the instrumented hillslope in Watershed 10, in the H.J. Andrews Experimental Forest. The experiment was conducted to quantify the relationships among soil moisture, transpiration, and hillslope subsurface flow. The objectives were to: 1) determine the phase shift (time lag) between maximum transpiration and minimum hillslope discharge with regard to soil moisture, 2) quantify the relationships between diel hillslope discharge and daily transpiration, and 3) identify the soil depth from which trees extract water for transpiration. Findings indicate that transpiration on hillslopes plays an important role in diel variation in subsurface discharge. However, the amount of influence transpiration has on discharge is strongly dependent upon soil moisture properties.

Chapter 3 examines both the spatial and temporal variation in forest transpiration with regard to aspect and hillslope position in a steep catchment. The

specific objectives were to: 1) quantify the variation in transpiration of young, mature Douglas-fir stands across a steep elevation gradient through a growing season, 2) examine the relative importance of vapor pressure deficit, photosynthetically active radiation, and soil matric potential ( $\Psi_s$ ) on transpiration through early, mid-, and late periods of the growing season and 3) use a simple, process-based model, *a posteriori*, to identify physiological mechanisms that may explain observed patterns of spatial variation in transpiration that cannot be explained by differences in microclimate. Findings indicated that plot-scale transpiration across a steep topographic gradient could not be predicted from measured variations in environmental variables alone. Furthermore, spatial variations in soil moisture and  $\Psi_s$  did not conform to preconceived expectations based simply upon topographic gradients. Results of this study demonstrate that models of catchment hydrological processes should not assume that transpiration is spatially uniform or that biophysical drivers alone accurately predict transpiration

Chapter 4 uses a dual isotope ( $^{13}\text{C}$  and  $^{18}\text{O}$ ) approach to infer physiological response of trees to changing environmental conditions. While several studies have clearly shown that the isotopic composition of cellulose in tree rings ( $\delta^{13}\text{C}_{\text{cell}}$  and  $\delta^{18}\text{O}_{\text{cell}}$ ) can be a valuable source of information for the reconstruction of both, plant water relations and environmental variability, most investigations to date have been generally based on the analysis of either  $\delta^{13}\text{C}_{\text{cell}}$  or  $\delta^{18}\text{O}_{\text{cell}}$ , but only infrequently using both. Examination of inter-relationships between  $\delta^{13}\text{C}_{\text{cell}}$ ,  $\delta^{18}\text{O}_{\text{cell}}$ , and tree ring width has the potential to illuminate new physiological information. Our specific objectives were to 1) to test the hypothesis that aboveground net primary production is equal to the product of the assimilation to stomatal conductance ratio ( $A/g_s$ ), derived from  $\delta^{13}\text{C}_{\text{cell}}$  and stomatal conductance ( $g_s$ ), derived from  $\delta^{18}\text{O}_{\text{cell}}$ , 2) to examine how  $\delta^{13}\text{C}_{\text{cell}}$  and  $\delta^{18}\text{O}_{\text{cell}}$  responds to environmental variations with regard to crown dominance within a stand, and 3) to compare our observed values of  $\delta^{13}\text{C}_{\text{cell}}$  and  $\delta^{18}\text{O}_{\text{cell}}$  to a qualitative conceptual model of the  $^{13}\text{C}$ - $^{18}\text{O}$  relationship. We used natural environmental gradients in a steep catchment dominated by a single species to maximize variation in aboveground net primary production, while at the same time reducing the isotopic variation in source water and source  $\text{CO}_2$ . Findings indicated that using both isotopes to

interpret physiology appears to fit the expected temporal and spatial variation we found. However, expanding the theory to predict relative rates of photosynthesis from isotopes does not conform to theory, potentially due to tree to tree differences in isotopic baselines. In addition, these isotopic estimates of photosynthesis did not match patterns of above ground productivity.

## References

- Adelman, J. D., Ewers, B. E. & Mackay, D. S. (2008) Use of temporal patterns in vapor pressure deficit to explain spatial autocorrelation dynamics in transpiration. *Tree Physiology*, **28**, 647-658.
- Berry, S. L., Farquhar, G. D. & Roderick, M. L. (2005) Co-evolution of climate, vegetation, soil and air. *Encyclopedia of Hydrological Sciences*, pp. 177-192. John Wiley & Sons Inc., Hoboken, NJ.
- Bond, B. J. (2003) Hydrology and ecology meet - and the meeting is good. *Hydrological Processes*, **17**, 2087-2089.
- Bosch, J. M. & Hewlett, J. D. (1982) A review of catchment experiments to determine the effect of vegetation changes on water yield and evapotranspiration. *Journal of Hydrology*, **55**, 3-23.
- Calder, I. R. (1998) Water use by forests, limits and controls. *Tree Physiology*, **18**, 625-631.
- Cosandey, C., Andreassian, V., Martin, C., Didon-Lescot, J., Lavabre, J., Folton, N., Mathys, N. & Richard, D. (2005) The hydrologic impact of the Mediterranean forest: a review of French research. *Journal of Hydrology*, **301**, 235-249.
- Ford, C. R., Hubbard, R. M., Kloeppel, B. D. & Vose, J. M. (2007) A comparison of sap flux based evapotranspiration estimates with catchment-scale water balance. *Agricultural and Forest Meteorology*, **145**, 176-185.
- Harr, R. D. & McCorison, F. M. (1979) Initial effects of clearcut logging on size and timing of peak flows in a small watershed in western Oregon. *Water Resources Research*, **15**, 90-94.
- Hewlett, J. D. (1982) *Principles of forest hydrology*. The University of Georgia Press, Athens.
- Huxman, T. E., Wilcox, B. P., Breshears, D. D., Scott, R. L., Snyder, K. A., Small, E. E., Hultine, K., Pockman, W. T. & Jackson, R. B. (2005) Ecohydrological implications of woody plant encroachment. *Ecology*, **86**, 308-319.
- Loranty, M. M., Mackay, D. S., Ewers, B. E., Adelman, J. D. & Kruger, E. L. (2008) Environmental drivers of spatial variation in whole-tree transpiration in an aspen-dominated upland-to-wetland forest gradient. *Water Resources Research*, **44**, W02441, doi:10.1029/2007WR00627, 2008.
- Ludwig, J. A., Wilcox, B. P., Breshears, D. D., Tongway, D. J. & Imeson, A. C. (2005) Vegetation patches and runoff-erosion as interacting ecohydrological processes in semiarid landscapes. *Ecology*, **85**, 288-297.
- Nuttle, W. K. (2002) Is ecohydrology one idea or many? *Hydrological Sciences*, **47**, 805-807.
- Pierson, F., Carlson, D. & Spaeth, K. (2002) Impacts of wildfire on soil hydrologic properties of steep sagebrush-stepp rangeland. *International Journal of Wildland Fire* **11**, 145-151.
- Rich, L., Reynolds, H. & West, J. (1961) The Workman Creek experimental watershed. pp. 188.
- Williams, D., Scott, R., Huxman, T. & Goodrich, D. (2005) Multi-scale eco-hydrology of riparian ecosystems in the desert southwest. *The 58th Annual Meeting, Society for Range Management*. Fort Worth, Texas.

- Zalewski, M. (2000) Ecohydrology – the scientific background to use ecosystem properties as management tools toward sustainability of water resources. *Ecological Engineering* **16**, 1-8.
- Zalewski, M. (2002) Ecohydrology - the use of ecological and hydrological processes for sustainable management of water resources. *Hydrological Sciences*, **47**, 823-832.

**Chapter 2 Mechanistic assessment of hillslope transpiration  
controls of diel sub-surface flow: a steady-state irrigation  
approach**

## **Introduction**

The hydrological cycle involves mutually-dependent biological and physical processes that operate at multiple scales of time and space, and this principle is the foundation for research in Ecohydrology. Early studies of paired watersheds operated at the whole-basin spatial scale and at annual to decadal time scales – highlighting the importance of vegetation to streamflow, with demonstrations of increased streamflow (in most cases) following complete removal of vegetation (Bosch and Hewlett, 1982). While paired-watershed manipulations have been implemented in many regions, much of the work to date has focused only on inputs and outputs. These studies demonstrate strong influences of vegetation on streamflow, but this black-box approach fails to explain the mechanisms controlling water flow paths within the catchment. Mechanistic assessment of the relationships between transpiration and discharge is necessary to advance our understanding of catchment hydrology. A fruitful approach may be to look at processes at smaller scales of time and space.

A number of recent studies have begun to explore the mechanistic link between transpiration and streamflow via the analysis of diel variations in streamflow. While vegetation-induced diel fluctuations in stream discharge have been noted for many decades, this behavior is especially pronounced during baseflow periods in mountainous, forested watersheds (White, 1932, Troxell, 1936). A growing body of work has suggested that evapotranspiration (ET) losses from riparian zones characterized with shallow groundwater tables caused these diel fluctuations (Dunford and Fletcher, 1947, Federer, 1973, Kobayashi et al., 1990, Bren, 1997, Chen, 2007, Gribovszki et al., 2008, Loheide, 2008, Szilágyi et al., 2008). Many of these studies have reported time lags between the time of maximum transpiration and minimum stream discharge on the order of 4 – 6 hours, and the authors infer that this is a manifestation of a strong hydrologic connection between riparian vegetation water use and water draining into the stream channel.

Bond et al. (2002) found strong diel patterns in stream discharge in the spring that persisted through late summer in a small catchment in western Oregon. These observed diel patterns were hypothesized to be the result of extraction of water by vegetation in the riparian zone. Xylem water flux measurements indicated that

transpiration within less than 0.3 % of the total basin area accounted for the diel reduction in streamflow. Cross-correlations between transpiration and stream discharge were highest and the time lag between maximum transpiration and minimum stream discharge was shortest in the early summer, at which time transpiration explained nearly 80% of the daily variation in stream discharge. As summer drought conditions progressed, the apparent connectedness of the vegetation and the stream was greatly diminished; transpiration was not significantly related to discharge at any time lag by mid-August. Wondzell et al. (2007) conducted further analysis of diel fluctuations in the same stream examined by Bond et al. (2002) and suggested that shifts in time lags between transpiration and discharge were strongly dependent on stream flow velocity. Wondzell et al. (2007) found that high flow velocities occurring during high baseflow periods resulted in constructive wave interference that amplifies the diel signal generated by ET along the stream channel. These different interpretations highlight the need for further experimental work to elucidate the first-order controls on transpiration-streamflow interactions. While prior studies have reported strong linkages between stream discharge and riparian vegetation dynamics, many questions still remain concerning the mechanistic relationship between transpiration and water yield. What causes the seasonal change in the timing and magnitude of diel fluctuations in discharge in relation to transpiration? By what mechanism does soil moisture influence the hydrologic connection between transpiration and subsurface flow? At what soil depth do roots take up water?

We know that diel fluctuations are not unique to streams with riparian vegetation and/or shallow groundwater tables. In a classic study by Dunford and Fletcher (1947), a damped diel signal persisted in stream discharge even after the complete removal of riparian vegetation. Since that study, however, little if any research has focused on the potential for hillslope transpiration to contribute to observed diel dynamics of streamflow. The role that hillslope transpiration plays in the diel subsurface flow (and hence streamflow) is difficult to identify in complex terrain with a hillslope-riparian area interface. Circumstantial evidence for hillslope control of stream diel dynamics is shown in the long term stream discharge data from the H.J. Andrews Experimental Forest (HJA), the site of the field analyses presented in this paper. Long

term records at HJA demonstrate diel fluctuations in Watershed 10, a first order 10 ha headwater watershed devoid of any riparian zone (due to its excavation by debris flows—see Van Verseveld et al., 2009 for details).

Resolving the mechanisms causing diel variations will reveal fundamental properties of vegetation-hydrological coupling in catchments. Examining the link between transpiration and subsurface flow at the hillslope scale is necessary to further our understanding of the potential mechanisms that are likely to operate at the catchment scale. We approached this issue experimentally, using an irrigation treatment to induce saturated conditions and examined the relationships of soil moisture, transpiration, and hillslope subsurface flow before, during and after the treatment. The overall goal of this experiment was to quantify the relationship between hillslope transpiration and diel hillslope discharge and how soil moisture modulates the timing and magnitude of the relationship. Our objectives were to: 1) examine the phase shift (time lag) between maximum transpiration and minimum hillslope discharge at different levels of soil moisture, 2) quantify the relationships between diel hillslope discharge and daily transpiration, and 3) identify the soil depths from which trees extract water for transpiration.

## **Methods**

### *Study Site Description*

This study was conducted in a 10.2 ha headwater catchment (Watershed 10 - WS10), located on the western boundary of the HJA, in the western-central Cascade Mountains of Oregon, USA (44.2° N, 122.25° W). The HJA is part of the Long Term Ecological Research program and has a continuous meteorological and stream discharge data record from 1958 to the present. The HJA has a Mediterranean climate, with wet, mild winters and dry summers. Average annual rainfall is 2220 mm, of which about 80% falls between October and April during storms characterized by long duration and low rainfall intensity. Elevations in WS10 range from 470 m at the watershed gauging station to a maximum of 680 m at the southeastern ridge line. The watershed was harvested during May-June 1975 and is now dominated by naturally-regenerated, second-growth Douglas-fir (*Pseudotsuga menziesii*). Several seep areas along the stream have been identified (Harr, 1977, Triska et al., 1984). These seep areas are

related to the local topography of bedrock, or to the presence of vertical, andesitic dikes (Swanson and James, 1975b, Harr, 1977). Frequent debris flows at WS10 (most recently in 1996) have scoured the stream channel to bedrock removing the riparian area in the lower 200 meters of the stream.

The study hillslope is located on the south aspect, 91 m upstream from the stream gauging station. The 125 m stream-to-ridge slope has an average gradient of 37°, ranging from 27° near the ridge to 48° adjacent to the stream (McGuire, 2004). The bedrock is of volcanic origin with andesitic and dacitic tuff and coarse breccia (Swanson and James, 1975b). The soils vary across the watershed as either Typic Hapludands or as Andic Dystrudepts (Yano *et al.*, 2005), and are underlain by low permeability subsoil (saprolite), formed from the highly weathered coarse breccia (Ranken, 1974, Sollins *et al.*, 1981). Soil depth on the study hillslope ranges from 0.1 m adjacent to the stream, to 2.4 meters at the upper limit of the irrigated area. Soils have distinct pore size distribution shifts at 0.3, 0.7 and 1.0 m, resulting in transient lateral subsurface flow at these depths (Harr, 1977, van Verseveld, 2007). Soils are well aggregated, tending towards massive structure at depth (0.7 -1.1 m) (Harr, 1977). Soil texture changes little with depth. Surface soils are gravelly loams, lower soil layers are gravelly, silty, clay loams or clay loams and subsoils are characterized by gravelly loams or clay loams (Harr, 1977).

#### *Irrigation Experiment*

We conducted an irrigation experiment for 24 continuous days beginning on Julian day of year (DOY) 208 (July 27), 2005. Monitoring began one week before we began irrigating and continued for two weeks after irrigation stopped. The irrigation treatment area was located directly upslope from the soil-bedrock channel interface at the toe of the hillslope and was approximately 8 m by 20 m (174.3 m<sup>2</sup>) (Figure 2-1). A rectangular grid of 36 (9 rows of 4) 360° micro-sprinklers (with approximately 1 m spray radius) was installed on the hillslope, with sprinkler heads spaced 2 m apart and approximately 0.4 m above the soil surface. Sprinklers were controlled with an automatic timer to maintain a consistent application rate throughout the experiment. Sprinkler rate was measured by an array of 72 (5 and 10 cm diameter) cups that were sampled every 4-12 hours during days 12 through 19 of the experiment. Additionally, 3

tipping-bucket rain gauges (TruTrack, Inc, Pronamic Rain Guage) recorded irrigation rates throughout the experiment. The cups and tipping buckets were placed randomly in the sprinkled area, between 0.1 and 0.8 m from the sprinkler heads. We applied a total of 2107 mm of water at an average rate ( $\pm$ SD) of 3.6 (0.5) mm h<sup>-1</sup> continuously except for minor malfunction periods on days 210, 225, 228, 229, and 230 (Figure 2-2(A)).

#### *Hillslope discharge and lateral subsurface flow*

A 10 m trench consisting of sheet metal anchored 5 cm into bedrock and sealed with cement was constructed in 2002 to measure lateral subsurface flow at a natural seepage face (McGuire et al., 2007). Intercepted subsurface water was routed to a calibrated 30° V-notch weir that recorded stage at 10-minute time intervals using a 1-mm resolution capacitance water-level recorder (TruTrack, Inc., model WT-HR). Thirty-two manual measurements of discharge covered the range of values experienced during the irrigation experiment, and allowed for a stage-discharge relationship ( $R^2=0.997$ ). We report hillslope discharge and lateral subsurface flow on a per unit irrigation area basis.

#### *Xylem Water Flux, Transpiration, and Canopy Reference Evapotranspiration*

Transpiration was estimated from xylem water flux measurements of the dominant trees located within or bordering the sprinkled area (n=9) beginning 10 days prior to irrigation (DOY 199) and continuing for 60 days after irrigation stopped (DOY 293) (Figure 2-1). Of the mature trees located within the irrigation area Douglas-fir (n=6), western hemlock (*Tsuga heterophylla*) (n=2) and cascara (*Rhamnus purshiana*) (n=1) represented 67-, 27-, and 6 % of the total basal area, respectively. As a control for the trees in the experimental irrigation area, xylem water flux of three dominant Douglas-fir trees was measured 10 -20 m outside the irrigation area. Xylem water flux was measured using the heat-dissipation method (Granier, 1985, Granier, 1987) every 15 s and data were stored in a CR-10x datalogger (Campbell Scientific, Logan, UT) as 15 min means. We used 2 cm probes for the flux measurements. Sapwood depths were measured on tree cores extracted at the same height as the sap flux sensors on each tree. For trees with sapwood depths greater than 2 cm, corrections for radial variations in

flux were estimated from measured radial flux profiles of trees of the same species and age at another location (Moore et al., 2004, Domec et al., 2006).

We scaled measurements from individual sensors to water flux per unit ground area ( $\text{mm day}^{-1}$ ). For each tree, the total xylem area at each depth interval (0-2, 2-3, >3 cm) was calculated. The flux within each depth interval of xylem was calculated as the product of the area of that interval and the measured or predicted flux; we then summed the fluxes for each xylem depth interval to estimate total flux per tree. Last, we summed the fluxes of all the trees and divided by the ground area of the irrigation experiment to estimate mean water flux per unit ground area.

Meteorological conditions were monitored near the center of the irrigation treatment area from DOY 205 to 262 (Figure 2-1). Net radiation, relative humidity, air and soil temperature and wind speed and direction were measured every 15 s and stored to a datalogger (CR-10x, Campbell Scientific) as 15 min means. To estimate total daily evapotranspiration, we calculated canopy reference evapotranspiration (CRET) using the Penman-Monteith equation:

$$CRET = \frac{\Delta(R_n - G) + \rho c_p \{VPD\} / r_a}{\lambda(\Delta + \gamma(1 + r_c / r_a))} \quad (1)$$

where,  $\Delta$  is the rate change of saturation vapor pressure with temperature ( $\text{Pa K}^{-1}$ ),  $R_n$  is net radiation measured at the hillslope ( $\text{W m}^{-2}$ ),  $G$  is the ground heat flux ( $\text{W m}^{-2}$ ),  $\rho$  is the density of air ( $\text{kg m}^{-3}$ ),  $c_p$  is the heat capacity of air ( $\text{J kg}^{-1} \text{K}^{-1}$ ),  $VPD$  is vapor pressure deficit (Pa),  $r_a$  is the aerodynamic resistance of the canopy ( $\text{s m}^{-1}$ ),  $\lambda$  is the latent heat of evaporation ( $\text{J kg}^{-1}$ ),  $\gamma$  is the psychrometer constant ( $\text{Pa K}^{-1}$ ) and  $r_c$  is the average canopy stomatal resistance ( $\text{s m}^{-1}$ ). Average canopy stomatal resistance was estimated to be  $150 \text{ s m}^{-1}$  (Monteith and Unsworth, 2008; T. Pypker personal communication). Relative to  $E$  and the sensible heat flux,  $G$  is usually small in forested ecosystems (Oke, 1992). Thus, we assumed  $G$  was only 10% of  $R_n$ . The aerodynamic resistance ( $r_a$ ) was estimated using:

$$r_a = \frac{\ln[(z - d)/z_o]}{ku(z)} \quad (2)$$

where  $z$  is the height of the canopy (m),  $d$  is the zone of zero displacement,  $k$  is von Karman's constant (0.41),  $z_o$  is the roughness length and  $u(z)$  is the wind speed at the hillslope. In using Equations 1 and 2 we assumed that  $d = 0.65h$ , where  $h$  is canopy height ( $h = 22$  m),  $z_o = 0.1h$  (Campbell and Norman, 1998, Monteith and Unsworth, 2008)).

### *Soil Moisture*

Soil volumetric water content (hereafter referred to as soil moisture) was measured at 24 locations within the irrigated area with a profiling time domain reflectometry (TDR) system (Environmental Sensors, Inc., model PRB-A). The system consisted of 1.2 m TDR probes that measured multiple depth segments (0.0-0.3 m, 0.3-0.6 m, 0.6-0.9 m, and 0.9-1.2 m) in a single profile. The probes have a manufacturer-reported precision within 3%. Since the probes were not calibrated for our site-specific soil type, we examined relative changes in moisture content. Measurement locations were in a 4 by 6 sensor grid (parallel and perpendicular to the stream channel, respectively), with probes installed 2 meters apart in each direction (Figure 2-1). Soil moisture was measured every hour for the duration of the experiment. Of the 96 measurements (locations x depth), 49 of the probe segments gave consistent results. Poor electrical connections or poor contact between the probe and soil caused inconsistent readings from the remaining 47 measurement segments. Only the data from consistently-working segments were analyzed.

### *Analysis*

We took a statistical process control approach to evaluating differences between xylem water flux density within and outside the irrigation treatment throughout the experiment (Deming, 1950, Shewhart, 1993). Using this approach, we measured the difference in the 24 hr running mean of xylem water flux density at 15 min intervals between treatment ( $n = 6$ ) and control ( $n = 3$ ) Douglas-fir trees prior to irrigation. A significant ( $p \leq 0.05$ ) treatment effect was defined to occur when the difference between treatment and control trees exceeded the mean difference prior to irrigation plus two standard deviations.

We followed methods similar to those used by Bond et al. (2002) to examine the correlations between transpiration and hillslope discharge. Hillslope discharge and transpiration measurements were averaged over 30 minute time intervals for statistical analysis. The correlations were analyzed separately for three, 4-7 day time periods: pre-irrigation (DOY 199 – 203), steady-state irrigation (DOY 218 - 223), and post-irrigation (DOY 238 – 245). For each period, the Pearson's correlation coefficient between transpiration and hillslope discharge was calculated for each 30 min lag (relating discharge to transpiration at progressively earlier time periods) from 0 to 12 hrs.

We estimated the diel reduction in hillslope discharge associated with evapotranspiration for each day during the 3 irrigation periods. Following methods of Bond et al. (2002), we interpolated a straight line between successive daily maximum trenchflows. The difference between the interpolated line and the observed discharge was calculated at 10 min intervals and summed for each day to calculate the amount of water that was “missing” from the actual daily discharge compared with the presumed potential discharge without evapotranspiration.

## **Results**

### *Hillslope discharge*

Hillslope discharge measured at the trench responded quickly to irrigation, with a detectable rise in discharge within an hour of initiation on DOY 208 (Figure 2-2 B). Steady-state was defined as the period when average discharge remained relatively constant and only diel fluctuations were recorded. Discharge rose from a pre-sprinkling average rate of 0.2 mm h<sup>-1</sup> to a steady-state average rate of 1.2 mm h<sup>-1</sup> within 8 days. Steady-state discharge was maintained for 13 days (with one malfunction that increased discharge on DOY 225), after which a series of sprinkler malfunctions increased discharge over the steady state rate. Irrigation was terminated on DOY 232. Distinct diel patterns in hillslope discharge were apparent prior to the onset of irrigation. These became more pronounced as the system entered steady-state during the treatment, (DOY 216) and persisted after irrigation ceased (Figure 2-2 B). The mean daily amplitude (+/- 1 SD) of the diel fluctuation was 0.03 (0.002) mm h<sup>-1</sup> prior to irrigation, 0.22 (0.03) during steady state, and 0.08 (0.02) after irrigation ended.

The amount of diel reduction ('missing trenchflow') in hillslope discharge varied greatly between the three analyzed time periods (Figure 2-3). During the 4 day pre-irrigation period, the calculated diel reduction averaged ( $\pm$  1 SD) 0.2 (0.1) mm day<sup>-1</sup>. During steady-state irrigation, there was a ten-fold increase in the amount of 'missing trenchflow' with an average of 2.4 (0.5) mm day<sup>-1</sup>. Post-irrigation diel flow reduction averaged 0.9 (0.3) mm day<sup>-1</sup>. Minimum diel reduction occurred on days (DOY 202 and 241) when there were small (< 2 mm) natural rain events supporting the idea that these daily reductions result from evapotranspiration.

#### *Xylem Water Flux, Transpiration, and Canopy Reference Evapotranspiration*

The difference in xylem water flux between irrigated and control Douglas-fir trees increased with time during irrigation and differences persisted after irrigation ceased (Figure 2-2 C). The difference was significant ( $p > 0.05$ ) within seven days after irrigation began. The observed differences in xylem water flux density resulted from a decline in the xylem water flux density of the control trees through time that is likely a result in declining soil moisture outside the irrigation area.

Total daily transpiration of the nine dominant trees in the experimental plot showed little daily variation before, during and after the irrigation treatment, averaging 1.1 mm day<sup>-1</sup>, 1.2 mm day<sup>-1</sup> and 1.0 mm day<sup>-1</sup> during the pre-treatment, treatment and post-treatment periods, respectively (Figure 2-3). Daily maximum transpiration rates occurred at 1300 hours, 1230 hours, and 1315 hours (Pacific Standard Time), respectively. These results contrast with diel reduction in hillslope discharge (i.e., 'missing trenchflow') which varied with irrigation. Prior to irrigation, transpiration was greater than the diel reduction in discharge by about 0.3 mm, but during the irrigation, the diel reduction was almost twice that of transpiration. Post treatment, the two were similar in magnitude.

Estimated CRET within the irrigation plot varied from 0.1 mm h<sup>-1</sup> at night to 0.7 mm h<sup>-1</sup> during the day, with a daily average rate of 5.2 mm day<sup>-1</sup> during the steady-state irrigation period. Post-irrigation CRET rates ranged from 1.6 to 13.9 mm day<sup>-1</sup> with an average rate of 4.2 mm day<sup>-1</sup> (Figure 2-3). Data were not available to calculate hillslope-specific CRET for the pre-irrigation period; however, environmental data (temperature, relative humidity, and total solar radiation) from the HJA long term

meteorological sites suggests that CRET during this period was unlikely to differ greatly from post-irrigation period (data not shown).

Correlations between transpiration and hillslope discharge shifted through the experiment (Figure 2-4). Prior to irrigation, maximum transpiration was correlated ( $r = -0.51$ ,  $p < 0.01$ ) to minimum hillslope discharge with a 6.5 hr time lag between the two variables. During the experiment at steady-state conditions, the correlation increased ( $r = -0.89$ ,  $p < 0.01$ ) and the time lag decreased to 4hr. For the seven-day period following irrigation, the time lag decreased further, with maximum transpiration most highly correlated with minimum hillslope discharge 2 hr later ( $r = -0.86$ ,  $p < 0.01$ ).

### *Soil Moisture*

Soil moisture increased rapidly in response to the onset of irrigation, with time lags at depth. Soil moisture in the upper 0.6 m of soil increased within the first 30 minutes of irrigation, whereas soil moisture in 0.6 - 0.9 m increased after 90 minutes, and below 0.9 m within 150 min. Soil moisture reached steady-state within 5-6 days after irrigation was initiated (DOY 213-214), and steady-state conditions persisted until DOY 228, when the first of the sprinkler malfunctions caused an increase in soil moisture (Figure 2-2 D). After irrigation ceased on DOY 232, the soil profile drained quickly for the first 8 - 12 hours, followed by a slower, more sustained water loss for the duration of monitoring.

Diel fluctuations in the soil moisture varied with soil depth and irrigation-state. Diel fluctuations were most evident at 0.3 – 0.6 m depth prior to irrigation and post-irrigation. Diel fluctuations were not apparent during the steady-state period of the experiment (Figure 2-2 D). Diel fluctuations in soil moisture were also observed at depths greater than 0.6 m beginning 5 days after irrigation ceased.

### **Discussion**

Examining the link between transpiration and subsurface flow at the hillslope scale is necessary to further our understanding of the potential mechanisms that are likely to operate at the catchment scale. Irrigation experiments at the hillslope scale provide an opportunity to isolate the relationships between hillslope transpiration and runoff from riparian and instream processes. In addition, irrigation reveals transpiration-

subsurface flow processes under conditions that are difficult to capture for extended periods under natural conditions (e.g., prolonged soil saturation and rapid transition states).

By directly measuring hillslope discharge via a gauged trench at the hillslope-streambed interface, we observed time lags between maximum transpiration and minimum discharge on the hillslope scale that were similar to those reported by Bond et al. (2002) for the whole catchment scale in a nearby basin. In our study, pre-irrigation time lags were 6.5 hours and lags during steady-state and post-irrigation were 2 - 4 hours. These time lags correspond with measurements reported by Bond et al. (2002) for late July and June, respectively. The change in time lags we observed were not likely caused by increases in transpiration rate in response to soil moisture. For the range of soil moisture conditions observed during this experiment, daily total transpiration remained relatively constant with the exception of reductions due to cloud cover. The observed decline in transpiration by trees in close proximity to, but outside the irrigated area, further suggests that irrigated trees transpired at a rate higher than they would have under natural soil moisture conditions. Wondzell et al. (2007) recently modeled the effects of stream flow velocity on time lags between transpiration and streamflow and found that as flow velocities decreased, time lags increased. Due to the short flow paths lengths (< 20 m) from the hillslope to the trench, subsurface flow velocity is not likely to explain the shifts in time lags that we observed. Furthermore, the shortest time lag we measured (two hours) occurred post treatment, not during the irrigation, when the highest flow velocities would be expected. We speculate that the interaction of hillslope and soil properties with tree roots under different moisture regimes are mechanisms behind the variation in lag time.

Although total daily transpiration remained relatively constant throughout the irrigation experiment, the total amount of diel reduction in subsurface flow varied among the three irrigation periods. During the pre-irrigation period, transpiration exceeded the calculated amount of diel reduction in hillslope discharge. The average daily reduction in hillslope discharge was 60% of total daily transpiration. We propose two possible mechanisms to explain why transpiration would exceed the reduction in discharge. The first explanation corresponds with the conceptual model in Bond et al.

(2002), which suggests that as soil moisture storage declines throughout rain-free periods, vegetation from locations farther upslope become hydrologically disconnected from subsurface flow paths that contribute to discharge. As a result, only vegetation located in close proximity to the trench would influence diel fluctuations, so rate of transpiration within the entire irrigation plot exceeds transpiration of the small zone of influence.

A second explanation centers on the drainable pore space within the soil. In late July, the large-volume, fast-draining pore space within the shallow soil layers is generally air-filled, and soil moisture within this area resides in small pore areas where it is tightly bound by adhesive and cohesive forces. While this tightly-bound water is slow to move to the trench due to relatively low water potentials and low hydraulic conductivity in unsaturated soil, the water is available for uptake by roots located in this zone. Our study shows that the depth at which water is taken up by roots is 0.3 to 0.6 m as indicated by the distinct diel soil moisture fluctuations at this depth. This physical disconnection may be responsible for the observed long lag times between transpiration and discharge.

During the steady-state irrigation period, the diel reduction in discharge was nearly double the daily total transpiration in the irrigated plot, suggesting potential limitations in the simple mass balance approach of the conceptual model advanced by Bond et al. (2002). The combination of very high soil moisture status and high evapotranspiration during this period is unlikely to occur under natural conditions, but the experiment allowed us to identify mechanisms that would be difficult to observe otherwise. The diel reduction was likely larger than transpiration for several reasons: greater direct evaporation during the day and soil filling and draining processes. The CRET was on average seven times higher during the day compared to the night. With the soil surface and understory vegetation being continually wet during the irrigation, daytime evaporation greatly exceeded night time evaporation creating a greater diel reduction. Another reason for the large diel reduction in discharge was likely driven by the non-linearity and hysteresis with filling and draining between soil water content and soil water potential. While the soils would be largely saturated during the irrigation period, preferential flow paths and heterogeneity within the soil would likely cause

some areas to remain unsaturated where daily filling and draining processes could contribute to the diel reductions and lag times (Selker et al., 1999). During the day, increased evapotranspiration would reduce daily inputs and could allow for greater drainage and eventually reducing gravitational flow. At night when evaporative demand was lower, a greater proportion of irrigation inputs infiltrated into the soil, pores refilled, and ultimately subsurface flow and discharge increased. Since much of the soil pore volume was filled during steady-state irrigation, tree roots had a direct hydrologic connection to water that contributes to subsurface flow and discharge. This direct connection resulted in an apparent increased coupling between transpiration and discharge with time lags between the maximum transpiration and minimum hillslope discharge becoming much shorter than observed prior to irrigation. However, as a consequence to much of the soil pore volume being filled, hydraulic conductivity was high and water within the profile was rapidly transmitted through the subsurface to the trench.

We observed the greatest coupling between transpiration and hillslope discharge in a seven-day period after irrigation. The time lag between maximum transpiration and minimum hillslope discharge was shortened to 2 hrs and the daily reduction in hillslope discharge was 90% of total daily transpiration. In our conceptual model of soil drainage, this period would correspond to large-volume soil pore space being fully drained while small pore volumes continue to contribute to discharge. Our conceptual model of soil drainage is consistent with measurements made of hillslope drainage by Harr (1977) at the same study site. Harr (1977) found a distinct decrease in hillslope discharge corresponding to the draining of larger soil pores 10 h after the end of natural rainfall events. We observed a rapid draining of the soil profile for 8-12 h after irrigation had stopped followed by a slower and more prolonged drainage for the duration of monitoring. Harr (1977) also observed that subsurface water flux was predominately in the vertical direction between rain events, in contrast to downslope flux during events. Tree roots intersecting these more slowly draining pore volumes are in direct competition with vertically draining water where soil-to-root water potential gradients work against the gravitational potential within the soil profile. Since a large proportion of the excess water in the hillslope has already drained, water losses via

transpiration become even more apparent and coupled to the diel reduction in hillslope discharge. Presumably, this coupling would become progressively less pronounced (and time lags between maximum transpiration and minimum discharge longer) as the pore spaces within the rooting zone become air-filled, and trees begin to rely on soil moisture within this area where water is very tightly bound by adhesive and cohesive forces. We conclude that the soil pore size distribution, hydraulic conductivity, and slope of the study site coupled with the ability of roots to take up water at low water potentials are responsible for the diel dynamics observed in hillslope discharge during the experiment.

### **Conclusion**

This work represents one step forward in elucidating the linkages between vegetation water use and (sub) surface flow processes. A mechanistic understanding of the role forests play in controlling subsurface flow and streamflow patterns is needed to further our understanding of hydrologic processes in headwater catchments. We demonstrated in this paper that transpiration on hillslopes plays an important role in diel variation in subsurface discharge. However, the amount of influence transpiration has on discharge is strongly dependent upon soil moisture properties. During saturated conditions subsurface flow is characterized as a fast moving pool held at relatively weak matric tensions, making flow more subject to gravitational transport and preferential flow to streams when more water is added to the system. As soil moisture declines, water becomes more tightly bound to soil peds, and there is an increased likelihood it will be taken up by plants rather than draining to the stream. Our study hillslope represents only one contributing unit to streamflow. Given the spatial heterogeneity of watersheds, it is unlikely that transpiration signal inputs are synchronous at the watershed scale. Additional work is necessary to deconvolve hillslope, riparian, and in stream processes that contribute to diel fluctuations in low-order streams.

## References

- Adelman, J. D., Ewers, B. E. & Mackay, D. S. (2008) Use of temporal patterns in vapor pressure deficit to explain spatial autocorrelation dynamics in transpiration. *Tree Physiology*, **28**, 647-658.
- Berry, S. L., Farquhar, G. D. & Roderick, M. L. (2005) Co-evolution of climate, vegetation, soil and air. *Encyclopedia of Hydrological Sciences*, pp. 177-192. John Wiley & Sons Inc., Hoboken, NJ.
- Bond, B. J. (2003) Hydrology and ecology meet - and the meeting is good. *Hydrological Processes*, **17**, 2087-2089.
- Bond, B. J., Jones, J. A., Moore, G., Phillips, N., Post, D. & McDonnell, J. J. (2002) The zone of vegetation influence on baseflow revealed by diel patterns of streamflow and vegetation water use in a headwater basin. *Hydrological Processes*, **16**, 1671-1677.
- Bosch, J. M. & Hewlett, J. D. (1982) A review of catchment experiments to determine the effect of vegetation changes on water yield and evapotranspiration. *Journal of Hydrology*, **55**, 3-23.
- Bren, L. J. (1997) Effects of slope vegetation removal on the diurnal variations of a small mountain stream. *Water Resources Research*, **33**, 321-331.
- Calder, I. R. (1998) Water use by forests, limits and controls. *Tree Physiology*, **18**, 625-631.
- Campbell, G. S. & Norman, J. M. (1998) *An introduction to environmental biophysics*. Springer, New York.
- Chen, X. (2007) Hydrologic connections of a stream-aquifer-vegetation zone in south-central Platte River valley, Nebraska. *Journal of Hydrology* **333**, 554-568.
- Cosandey, C., Andreassian, V., Martin, C., Didon-Lescot, J., Lavabre, J., Folton, N., Mathys, N. & Richard, D. (2005) The hydrologic impact of the Mediterranean forest: a review of French research. *Journal of Hydrology*, **301**, 235-249.
- Deming, W. E. (1950) *Some theory of sampling*. Wiley and Sons, New York.
- Domec, J. C., Meinzer, F. C., Gartner, B. L. & Woodruff, D. (2006) Transpiration-induced axial and radial tension gradients in trunks of Douglas-fir trees. *Tree Physiology* **26**, 275-284.
- Dunford, E. G. & Fletcher, P. W. (1947) Effect of removal of stream-bank vegetation upon water yield. *Eos transactions, American Geophysical Union* **28**, 105-110.
- Federer, C. A. (1973) Forest transpiration greatly speeds streamflow recession. *Water Resources Research*, **9**, 1599-1604.
- Granier, A. (1985) Une nouvelle méthode pour la mesure du flux de sève brute dans le tronc des arbres. *Annales Des Sciences Forestieres*, **42**, 193-200.
- Granier, A. (1987) Evaluation of transpiration in a Douglas-fir stand by means of sap flow measurements. *Tree Physiology*, **3**, 309-320.
- Gribovszki, Z., Kalicz, P., Szilágyi, J. & Kucsara, M. (2008) Riparian zone evapotranspiration estimation from diurnal groundwater fluctuations. *Journal of Hydrology* **349**, 6-17.
- Harr, R. D. (1977) Water flux in soil and subsoil on a steep forested slope. *Journal of Hydrology*, **33**, 37-58.

- Harr, R. D. & McCorison, F. M. (1979) Initial effects of clearcut logging on size and timing of peak flows in a small watershed in western Oregon. *Water Resources Research*, **15**, 90-94.
- Hewlett, J. D. (1982) *Principles of forest hydrology*. The University of Georgia Press, Athens.
- Huxman, T. E., Wilcox, B. P., Breshears, D. D., Scott, R. L., Snyder, K. A., Small, E. E., Hultine, K., Pockman, W. T. & Jackson, R. B. (2005) Ecohydrological implications of woody plant encroachment. *Ecology*, **86**, 308-319.
- Kobayashi, D., Suzuki, K. & Nomura, M. (1990) Diurnal fluctuations in streamflow and in specific electric conductance during drought periods. *Journal of Hydrology*, **115**, 105-114.
- Loheide, S. P. (2008) A method for estimating subdaily evapotranspiration of shallow groundwater using diurnal water table fluctuations. *Ecohydrology*, **1**, 59-66.
- Loranty, M. M., Mackay, D. S., Ewers, B. E., Adelman, J. D. & Kruger, E. L. (2008) Environmental drivers of spatial variation in whole-tree transpiration in an aspen-dominated upland-to-wetland forest gradient. *Water Resources Research*, **44**, W02441, doi:10.1029/2007WR00627, 2008.
- Ludwig, J. A., Wilcox, B. P., Breshears, D. D., Tongway, D. J. & Imeson, A. C. (2005) Vegetation patches and runoff-erosion as interacting ecohydrological processes in semiarid landscapes. *Ecology*, **85**, 288-297.
- McGuire, K. J. (2004) *Water residence time and runoff generation in the western Cascades of Oregon*. PhD Dissertation, Oregon State University, Corvallis.
- McGuire, K. J., McDonnell, J. J. & Weiler, M. (2007) Integrating tracer experiments with modeling to infer water transit times. *Advances in Water Resources*, **30**, 824-837.
- Monteith, J. L. & Unsworth, M. H. (2008) *Principles of Environmental Physics*. Academic Press, New York.
- Moore, G. W., Bond, B. J., Jones, J. A., Phillips, N. & Meinzer, F. C. (2004) Structural and compositional controls on transpiration in a 40- and 450-yr-old riparian forest in western Oregon, USA. *Tree Physiology*, **24**, 481-491.
- Nuttle, W. K. (2002) Is ecohydrology one idea or many? *Hydrological Sciences*, **47**, 805-807.
- Oke, T. R. (1992) *Boundary Layer Climates*. Routledge, New York.
- Pierson, F., Carlson, D. & Spaeth, K. (2002) Impacts of wildfire on soil hydrologic properties of steep sagebrush-stepp rangeland. *International Journal of Wildland Fire* **11**, 145-151.
- Ranken, D. W. (1974) *Hydrologic properties of soil and subsoil on a steep, forested slope*. M.S., Oregon State University, Corvallis.
- Rich, L., Reynolds, H. & West, J. (1961) The Workman Creek experimental watershed. pp. 188.
- Selker, J. S., Keller, C. K. & McCord, J. T. (1999) *Vadose zone processes*. Lewis Publishers, Boca Raton, FL.
- Shewhart, W. A. (1993) The role of statistical method in economic standardization. *Econometrica*, **1**, 23-25.

- Sollins, P., Cromack, K. J., McCorison, F. M., Waring, R. H. & Harr, R. D. (1981) Changes in nitrogen cycling at an old-growth Douglas-fir site after disturbance. *Journal of Environmental Quality*, **10**, 37-42.
- Swanson, F. J. & James, M. E. (1975) Geology and geomorphology of the H.J. Andrews Experimental Forest, western Cascades, Oregon., pp. 14. U.S. Department of Agriculture, Forest Service, Pacific Northwest Forest and Range Experiment Station, Portland, OR.
- Szilágyi, J., Gribovszki, Z., Kalicz, P. & Kucsara, M. (2008) On diurnal riparian zone groundwater-level and streamflow fluctuations. *Journal of Hydrology*, **349**, 1-5.
- Triska, F. J., Sedell, J. R., Cromack, K., Gregory, S. V. & McCorison, F. M. (1984) Nitrogen budget for a small coniferous forest stream. *Ecological Monographs*, **54**, 119-140.
- Troxell, M. C. (1936) The diurnal fluctuations in the groundwater and flow of the Santa Ana River and its meaning. *Eos transactions, American Geophysical Union* **17**, 496-504.
- van Verseveld, W. (2007) *Hydro-biogeochemical coupling at the hillslope and catchment scale*. PhD, Oregon State University, Corvallis.
- White, W. N. (1932) A method of estimating ground-water supplies based on discharge by plants and evaporation from soil: Results of investigations in Escalante Valley, Utah. pp. 1-105.
- Williams, D., Scott, R., Huxman, T. & Goodrich, D. (2005) Multi-scale eco-hydrology of riparian ecosystems in the desert southwest. *The 58th Annual Meeting, Society for Range Management*. Fort Worth, Texas.
- Wondzell, S. M., Gooseff, M. N. & McGlynn, B. L. (2007) Flow velocity and the hydrologic behavior of streams during baseflow. *Geophysical Research Letters*, **34**.
- Zalewski, M. (2000) Ecohydrology – the scientific background to use ecosystem properties as management tools toward sustainability of water resources. *Ecological Engineering* **16**, 1-8.
- Zalewski, M. (2002) Ecohydrology - the use of ecological and hydrological processes for sustainable management of water resources. *Hydrological Sciences*, **47**, 823-832.

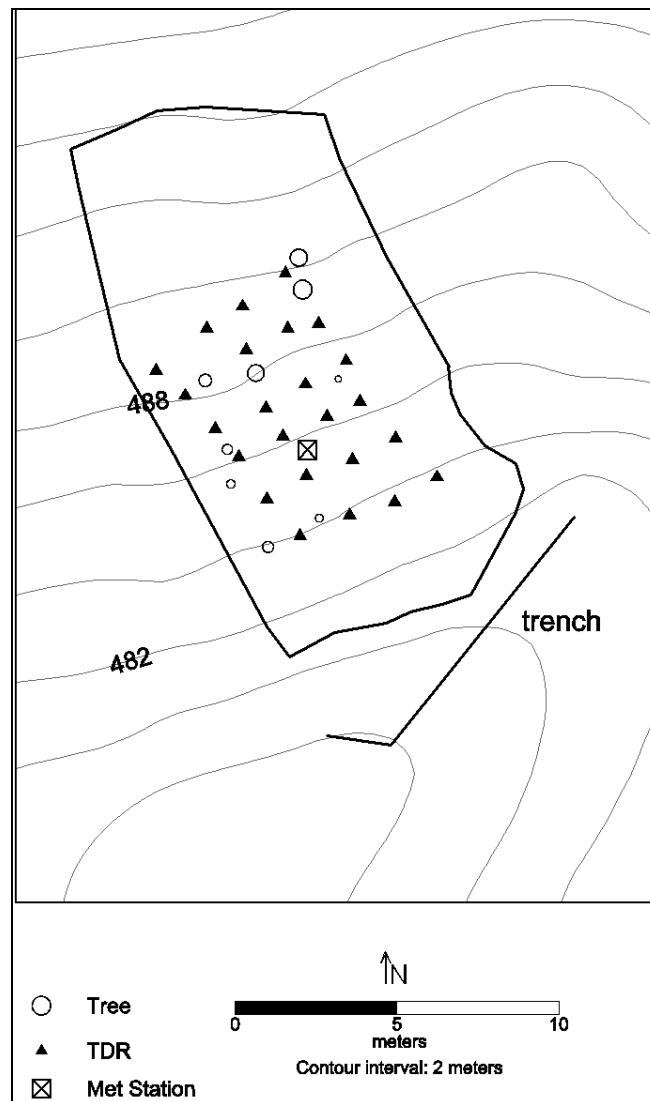


Figure 2-1: Map of study site with outline of irrigated area with 24 time domain reflectometry rods, meteorological station and instrumented trees. The relative size of circle symbol represents the diameter of the tree (minimum = 4.4 cm, maximum = 28 cm).

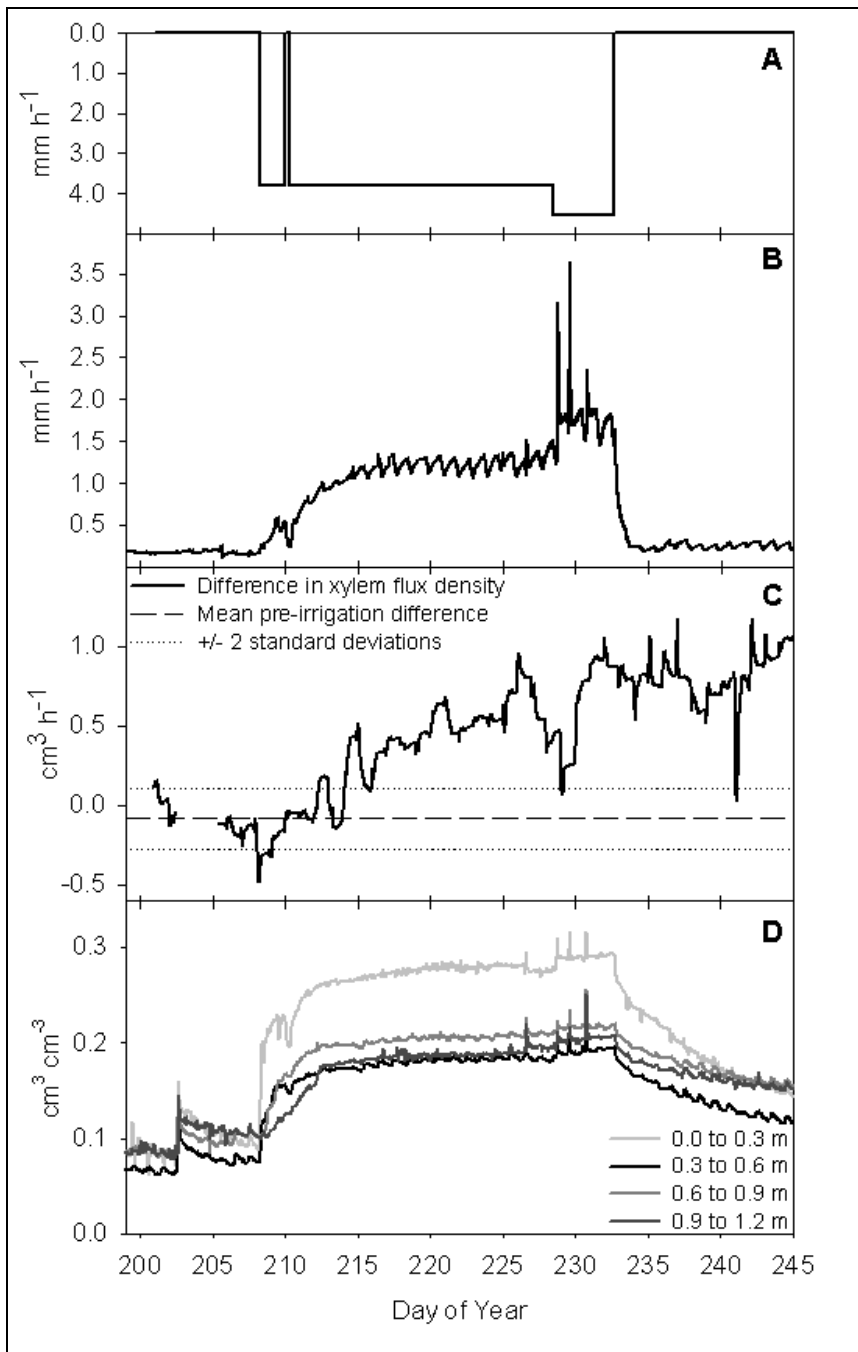


Figure 2-2: (A) Hillslope irrigation rate, (B) Hillslope discharge, (C) Difference in xylem flux density between irrigated and control Douglas-fir trees, and (D) Soil volumetric water content versus Time.

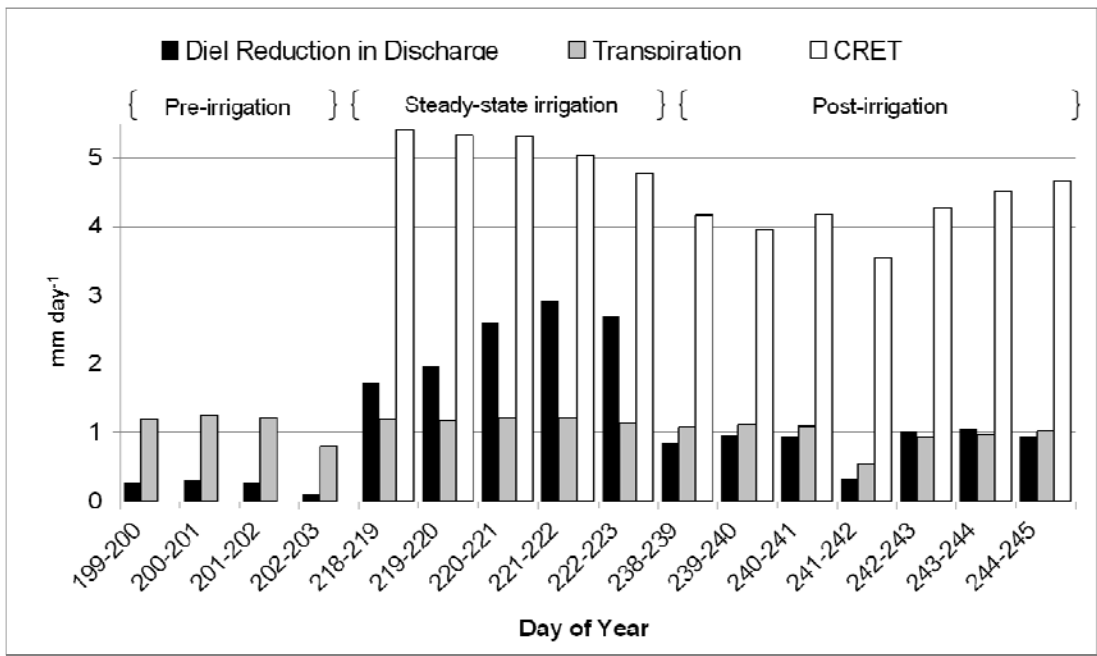


Figure 2-3: Total diel reduction in hillslope discharge (‘missing trenchflow’), total daily hillslope transpiration, and average daily canopy reference evapotranspiration for 3 irrigation periods.

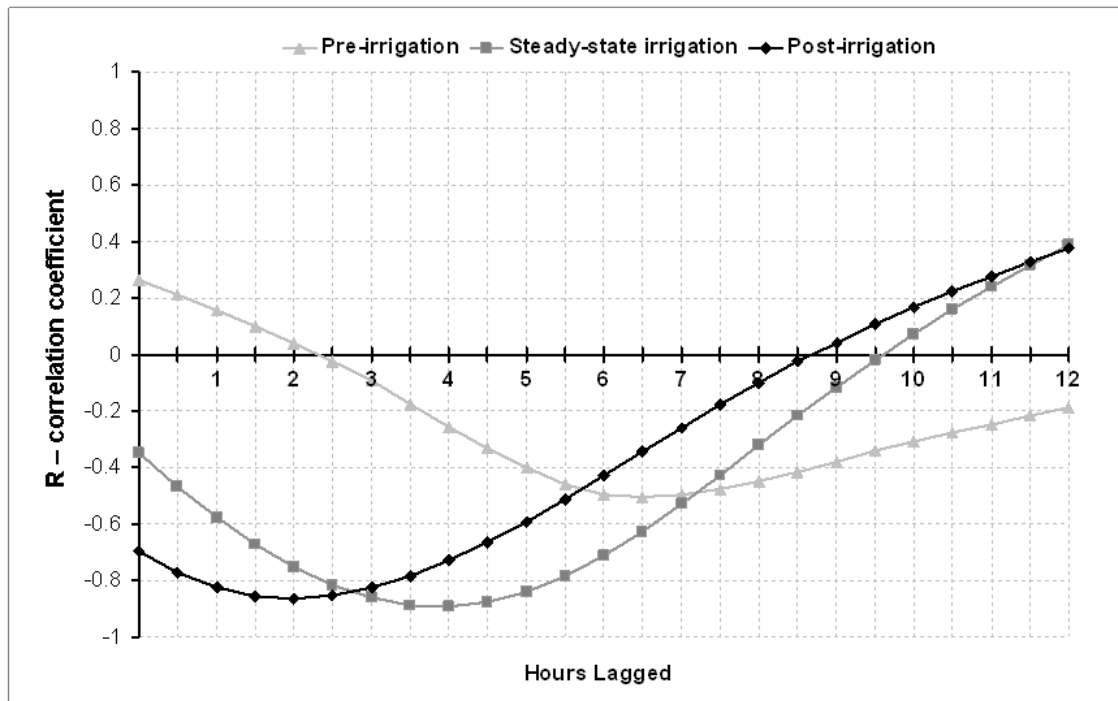


Figure 2-4: Phase (time lag) relationship between maximum transpiration and minimum hillslope discharge for 3 irrigation periods.

**Chapter 3 The response of Douglas-fir transpiration to  
variation in environmental drivers in complex terrain**

## Introduction

Transpiration ( $E$ ) is a large component of the annual water balance in forested watersheds in humid regions (Hewlett, 1982) and quantifying the spatial variation in forest transpiration is central to understanding the linkages between biological and hydrological function. Nevertheless, response of transpiration to variation in environmental drivers in complex terrain is still poorly understood. Forested, mountainous catchments differ from their flat land counterparts due to large spatial variability in solar radiation, slope, and sub-surface hydrology. Traditional methods of measuring large-scale ecosystem fluxes (using eddy flux towers) are difficult to employ in mountainous terrain due to this spatial heterogeneity and to complexities in airflow patterns (Aubinet et al., 2003). Topography and geology define gravity-driven water flow paths within three-dimensional (3-D) physical landscapes. These water flow paths influence, and are influenced by, ecological and biogeochemical processes (Hooper et al., 1998, McDonnell and Tanaka, 2001, van Verseveld, 2007). Clearly we need a similar 3-D framework for characterizing soil-plant-atmosphere interactions if we are to understand the first principles controlling transpiration in complex terrain (Bond, 2003, Ford et al., 2007).

Recent ecohydrological work at the hillslope scale has demonstrated the potential for  $E$  to vary greatly over relatively short distances. Variations in soil depth, available soil moisture, and subsurface lateral flow were strongly correlated to differences in tree transpiration rates across an approximately 900 m<sup>2</sup> hillslope in the Southern Piedmont of Georgia, USA (Tromp-van Meerveld and McDonnell, 2006a, Tromp-van Meerveld and McDonnell, 2006b). These findings indicated that when soil moisture was uniformly high across the hillslope, transpiration rates were similar irrespective of the location of the trees on the hillslope. In contrast, during periods of drought, trees growing in shallow soils rapidly depleted soil moisture stores, and consequently, their transpiration declined to 40% of the rate of trees growing in deeper soils. Topographical controls on  $E$  would be expected to generate distinct spatial patterns in  $E$ , and indeed other studies utilizing geostatistical methods found distinct spatial autocorrelation of  $E$  within hillslopes of both sub-alpine forest and mixed hardwood forests (Adelman et al., 2008, Loranty et al., 2008). Both of these studies

observed declines in spatial autocorrelation with increasing vapor pressure deficits ( $D$ ), indicating that spatial variation in  $E$  was dependent not only on topographic properties, but also physiological responses to environmental drivers.

The response of  $E$  and stomatal conductance to water vapor to environmental drivers has been studied intensively for several decades (reviewed in Whitehead, 1998, Wullschleger et al., 1998, Meinzer, 2003). In coniferous forests that are well coupled to the atmosphere,  $E$  is regulated primarily by the stomatal response to photosynthetically active radiation ( $Q$ ),  $D$ , and soil moisture (Jarvis and McNaughton, 1986, Monteith, 1995). Photosynthetically active radiation influences water loss from plants since stomatal aperture increases as a function of the amount of radiation reaching the leaf surface up to a saturation point (Taiz and Zeiger, 1991). In contrast, stomata partially close in response to increases in  $D$  and as a result, conductance to water vapor declines. In a conifer canopy with high boundary layer conductance, the relationship between  $E$ , canopy-averaged stomatal conductance of water vapor for the canopy ( $G_c$ ), and  $D$  is expressed mathematically as:

$$E = G_c * D \quad (1)$$

Transpiration is driven by the environmental factors  $D$  and  $Q$ , as well as, the water potential difference between the soil and the leaf, but it is also limited by the conductance of the entire soil to leaf pathway ( $K$ ) and. Therefore, the flow of water along the soil to leaf pathway can be expressed as:

$$E = K_L * (\Psi_S - \Psi_L - h\rho g) \quad (2)$$

where,  $K_L$  is average conductance for the whole tree from the soil to the leaf (per unit leaf area) and  $\Psi_S - \Psi_L$  is the average water potential gradient from the soil to the leaves and  $h\rho g$  is the average gravitational pull on the water column for leaves of height  $h$  and density  $\rho$  (Whitehead, 1998). In isohydric species, including Douglas-fir trees, where stomata regulate water loss to prevent  $\Psi_L$  from dropping below a species-specific minimum,  $E$  decreases as  $K_L$  or  $G_c$  decreases after  $\Psi_L$  reaches its minimum (Hinckley et al., 1978, Tyree and Sperry, 1988, Tardieu, 1993, Bond and Kavanagh, 1999).

Explaining the causes of spatial heterogeneity in  $E$  with regard to variability in environmental variables as well as topographic features is a first step in developing scaling approaches to be used within a 3-D framework.

In a small catchment dominated by a single, even-aged species, one might assume that the trees are generally exposed to the same macro-environment where precipitation inputs are uniform and soil moisture gradients are driven predominately by gravitational potential (Quinn et al., 1991, Hjerdt et al., 2004). Under this assumption, we would expect that spatial variation in  $E$  would be driven primarily by micro-environmental variations in  $Q$  and  $D$  when soil moisture conditions are not limiting. Furthermore, during periods without precipitation, we would expect that sites located in upslope locations, closer to ridgelines, would experience soil drought conditions more quickly and perhaps more intensely than their downslope counterparts as a result of being exposed to greater solar radiation and evaporative demand, as well as having a greater gravitational potential leading to rapid sub-surface drainage and ultimately lower soil moisture content.

Here we report on a study that tests these assumptions by measuring transpiration across a ridge-to-ridge transect running perpendicular to the stream in a headwater catchment in western Oregon. The aim of this study was to examine both the spatial and temporal variation in forest transpiration with regard to aspect and hillslope position in a steep catchment. Our specific goals were: 1) to quantify the variation in transpiration of young, mature Douglas-fir stands across a steep elevation gradient through a growing season, 2) to examine the relative importance of  $D$ ,  $Q$ , and  $\Psi_s$  on transpiration through early, mid-, and late periods of the growing season and 3) to use a simple, process-based model, *a posteriori*, to identify physiological mechanisms that may explain observed patterns of spatial variation in transpiration that cannot be explained by differences in microclimate.

## **Methods**

### *Study Site*

The study area is a 96 ha catchment (Watershed One - WS1), located in the H J Andrews Experimental Forest (HJA) in the western Cascades of central Oregon, USA (44.2 °N, 122.2 °W) (Figure 3-1). Elevations in WS1 range from 430 m at the watershed gauging station to a maximum of 1010 m at the eastern ridge line. The HJA is part of the Long Term Ecological Research program and has a continuous

meteorological and stream discharge data record from 1958 to the present. WS-1 is covered predominately by young, mature Douglas-fir (*Psuedotsuga menziesii* (Mirb.) Franco) replanted following clear-cut harvesting in the late 1960s. Smaller components of the forest basal area consist of western hemlock (*Tsuga heterophylla* (Raf.) Sarg), bigleaf maple (*Acer macrophyllum* Pursh), vine maple (*Acer circinatum* Pursh) and red alder (*Alnus rubra* Bong.); the angiosperm populations are greatest within the riparian area (Moore et al., 2004). At the time of our study, the maximum height of canopy ranged from approximately 22 to 31 m. The HJA has a Mediterranean climate, with wet, mild winters and dry summers. Annual rainfall averages 2220 mm, of which about 80% falls between October and April (Rothacher et al., 1967). Soils in WS1 are Andic, and are seasonally reduced (Swanson and James, 1975a). Soils on the south-facing slope have a loam to silt loam texture in the upper 30 cm and silt textured sub-soil below 30 cm. The average C:N ratio for the upper 30 cm of soil on the south-facing slope ranges from 4 to 14 and soil pore space makes up an average 46 % of the volume. Soils on the north-facing slope have a sandy loam texture in the upper 30 cm and loamy sand textured sub-soil below 30 cm. The average C:N ratio for the upper 30 cm of soil on the north-facing slope ranges from 2 to 5 and soil pore space makes up an average 45 % of the volume (Kleber, unpublished data).

A transect of eight plots (four on each slope) with a radius of 10 m were established perpendicular to the axis of the valley in the spring of 2005 (Figure 3-1). Four plots from this transect were instrumented intensively for this study: Plot 501 (South-facing Upslope – SF↑), Plot 505 (South-facing Downslope – SF↓), Plot 507 (North-facing Downslope - NF↓), and Plot 510 (North-facing Upslope – NF↑). Table 3-1 includes a summary of individual plot characteristics.

### *Transpiration*

We used heat-dissipation sensors (Granier, 1985, Granier, 1987) from April to October, 2006 (day of year (DOY) 100 – 300) to measure the water flux of 10 trees per plot in four plots along the transect (Figure 3-1, Table 3-1). Dominant trees have substantially more sapwood conducting area and leaf area than smaller trees within stands, and thus represent most of the water flux for a stand. For this reason, the sampling design was weighted most heavily towards the large trees within each plot

with six dominant, two intermediate and two suppressed trees being selected. Trees within the plot were selected by establishing 10 rays uniformly distributed around the plot center and selecting a tree along that ray from within the randomly assigned dominance class. This tree selection method ensured that the trees were distributed throughout the plot. In each tree, a 2 cm-long sensor was inserted into the xylem at the 0-2 cm depth interval at 1.4 m above ground. In three dominant trees per plot, 1-cm-long sensors were installed at two additional depth intervals (2-3 cm, and 3-4 cm) to account for radial flux profiles (Phillips et al., 1996). Sapwood depths determined visually from increment cores, indicated that none of the sensors crossed the heartwood boundary. Measurements were recorded by a datalogger (CR23X, Campbell-Scientific Inc.) every 15 s and averaged over 15 min intervals. Sensor measurements were converted to sap flux ( $\text{g H}_2\text{O m}^{-2} \text{ sapwood s}^{-1}$ ). Sap flux in the inner (>2 cm depth) xylem of trees that were not equipped with inner sap flow probes was estimated from a ratio between the outer 0-2 cm flux and the inner 2-3 cm or 3-4 cm fluxes from the measured trees. The ratio of outer 0-2 cm flux to inner 2-3 cm flux was 0.22, 0.14, 0.61, and 0.57 for the SF $\uparrow$ , SF $\downarrow$ , NF $\downarrow$ , and NF $\uparrow$  plots, respectively. The ratio of outer 0-2 cm flux to inner 3-4 cm flux was 0.29, 0.09, 0.46, and 0.49 for the SF $\uparrow$ , SF $\downarrow$ , NF $\downarrow$ , and NF $\uparrow$  plots, respectively. We assumed that there was no change in flux between the depth of the 3-4 cm sensor and the heartwood boundary.

We scaled measurements from individual sensors to average water flux per tree and then to a unit ground area basis ( $\text{mm day}^{-1}$ ). First, for each plot, diameter at breast height (DBH, measured 1.37 m above ground) was measured for all trees. Sapwood depth for each tree was calculated using a diameter to sapwood depth relationship developed from over 200 tree cores taken across the watershed (Equation 1,  $R^2 = 0.77$ ,  $p < 0.01$ ; Woolley, unpublished data):

$$\text{Sapwood depth} = e^{(-1.81 + 1.02(\ln(\text{DBH}))} \quad (3)$$

where DBH is measured in cm. For each tree, the cross-sectional sapwood area was calculated for three depth intervals (0-2, 2-3, >3cm). The flux within each depth interval of sapwood was calculated as the product of the area of that interval and the measured or predicted flux; we then summed the fluxes for each sapwood depth interval

to estimate total flux per tree. Last, we summed the fluxes of all the trees on each plot and divided by the ground area to estimate mean water flux per unit ground area.

We did not estimate nighttime transpiration. Recent work demonstrates that trees often transpire at night when the  $D$  is above 0.6 kPa (Kavanagh et al., 2007). Within the study watershed, nighttime  $D$  was greater than 0.6 kPa on less than 4% of nights during the growing season and was greater than 0.2 kPa on less than 25% of the nights. Even on the nights when  $D$  was greater than 0.2 kPa, transpiration is likely minimal, as past research demonstrates that nocturnal transpiration by Douglas-fir trees is only 1-7% of daytime transpiration (Dawson et al., 2007).

### *Micro-climate*

At each plot, air temperature ( $T_a$ ) and relative humidity (RH) were measured at mid-canopy (HMP45c, Campbell-Scientific Inc., Logan, UT, USA) from which  $D$  was calculated. Plot-level measurements were recorded by a datalogger (CR23X, Campbell-Scientific Inc.) every 15 s and averaged over 15 min intervals. To examine the relationship between  $D$  and  $E$ , we calculated the daily mean  $D$  for hours 0800 – 1430. This period represents the time of day with the greatest water vapor flux. In addition, climatic conditions ( $T_a$ , RH,  $Q$ , and precipitation (PPT)) were monitored at a nearby weather station (HJA Primary Meteorological Station - PRIMET) within 0.75 km of the study area. Meteorological data sets were provided by the Forest Science Data Bank, a partnership between Oregon State University and the U.S. Forest Service Pacific Northwest Research Station, Corvallis, Oregon.

We estimated daily, plot-specific, above-canopy  $Q$  based on the ratio of  $Q$  predicted at PRIMET to  $Q$  predicted at each plot from the clear sky solar radiation analysis tools in the ArcGIS Spatial Analyst Extension (ESRI, Redlands, CA, USA). After calculating the plot-specific ratio for each day, we applied the ratio to  $Q$  measured at PRIMET to estimate  $Q$  for each plot throughout the growing season. The Spatial Analyst Extension accounts for atmospheric effects, site latitude and elevation, slope and aspect, daily and seasonal shifts of the sun angle, and effects of shadows cast by surrounding topography. Topographic parameters were estimated based on a 1 m grid digital elevation model (DEM) derived from 1 m resolution light detection and ranging (LIDAR) bare earth return data.

### *Soil Moisture and Retention Curves*

We measured soil volumetric water content (hereafter referred to as soil moisture) (Echo-20, Decagon Devices, Pullman, WA) continuously within each plot at 30 and 100 cm depths during 2005 and 2006. Calibration equations specific to local soils were used to convert the millivolt signal from the soil moisture sensors to volumetric water content (Czarnomski et al., 2005). Measurements were recorded by a datalogger (CR23X, Campbell-Scientific Inc.) every 15 s and averaged over 15 minute intervals. We used the 30 cm sensor values to estimate the soil moisture depletion throughout the growing season at the 0- 30 cm depth interval and the 100 cm sensor values to estimate the soil moisture depletion for the 30 – 100 cm depth interval. Total soil moisture depletion was calculated as the sum of depletion across these two depth intervals.

Because up to 80 % of fine to medium sized root biomass occurs in the upper 40 cm of soil (Warren et al., 2005), we estimated  $\Psi_s$  at the 30 cm depth for each plot from laboratory-generated soil moisture retention curves in combination with soil moisture from field-based measurements. Three to four soil cores per plot were sampled with a bulk density corer centered at 30 cm depth below the mineral soil surface. Soil cores (4.9cm ID x 4.9cm long) were kept intact in aluminum rings and supported on the bottom with nylon screen. Moisture retention was determined using the pressure plate method as described by Klute (1986). The cores were saturated before each pressure measurement by wetting overnight in a shallow pan of water to allow capillary draw to refill micropores. Volumetric water content was determined at nine pressure levels: 0.01, 0.04, 0.08, 0.14, 0.20, 0.28, 0.38, 0.5, and 1.5 MPa (1.5 MPa was only available for the NF $\uparrow$  plot).

### *Predawn Tree Water Potential ( $\Psi_{PD}$ )*

Approximately every three weeks, we measured the water potential of three small, cut stems (each from a different tree) 1–3 h prior to sunrise in each of the four plots where transpiration was measured using a field portable pressure chamber (PMS systems, Corvallis, OR, USA). Twigs were sampled by shotgun from the outside of the upper half of the canopy and measurements were conducted within two to three minutes of sampling. Predawn water potential measurements were not corrected for

gravitational potential since the exact height of sampling was difficult to determine, but the height was relatively consistent over time so variation in  $\Psi_{PD}$  was not related to variation in sampling height.

#### *Soil Depth and Resistance to Penetration*

We used a 2 m dynamic cone penetrometer to measure soil depth and resistance to penetration in each measurement plot. Soil resistance to penetration has been shown to be directly related to bulk density and inversely related to saturated hydraulic conductivity (Yoshinaga and Ohnuki, 1995, Shanley et al., 2003). We used the resistance profile with soil depth to gain insight into possible subsurface drainage behavior. In each plot, a total of 20 measurements were taken along two transects oriented in a direction perpendicular to the elevation contour lines and each located 2 m east and west from the plot center. The cone penetrometer consists of a 1.5-cm-diameter stainless steel rod with a cone tip and gradations marked every 5 cm along the length of the rod. A 5 kg sliding weight was dropped from a fixed height onto a strike plate fixed to the top of the rod. Measurements were recorded as the number of blows (knocks) that were needed to insert the rod 5 cm into the soil. The soil-bedrock interface was assumed to be the point where 15 drops did not move the rod deeper into the subsurface. Additional details of cone penetrometer methods can be found in Shanley et al. 2003.

#### *Analyses*

To analyze the effects of mean daytime  $D$ , total daily  $Q$  and  $\Psi_S$  on daily  $E$  throughout the growing season, we used a multiple linear regression approach. We analyzed the data for three distinct periods during the growing season separately based on precipitation: 1) early season (DOY 100 - 181) when soil moisture was high and precipitation events were common, 2) mid-season (DOY 182 – 256) when no precipitation events occurred and soil moisture continuously declined, and 3) late season (DOY 257 – 300) which marked the onset of Fall precipitation events. First,  $E$  was regressed against each predictor variable ( $D$ ,  $Q$  and  $\Psi_S$ ) separately and residual analysis was used to determine necessary transformations of the predictor variable. A square root transformation provided the best fit for all predictor variables using a simple

linear regression. Since the objective was to evaluate the relative importance of each of the predictor variables, all three of the variables and all interaction terms were included in a multiple regression model. We used a backward-model selection process until all remaining variables in the model were significant at  $\alpha = 0.05$  level. We analyzed the residuals of the selected models for auto-correlation. To account for auto-correlation between daily values, we used a non-random holdout sample for model selection and validation where a subset of the time series data was used for model selection and the remaining data set was used for model validation. Data points for model selection were systematically chosen so that data points were sufficiently distant from each other in time to remove auto-correlation. Next, we added indicator (dummy) variables to the model representing each plot to examine differences in the intercepts and slopes for each plot (Neter et al., 1996). Last, we measured the relative contribution of each of the predictor variables by the coefficient of partial determination ( $R^2_{PD}$ ) (Neter et al., 1996, Brooks et al., 1996). The coefficient of partial determination is a measure of the correlation between a single predictor variable and the dependent variable when the other predictor variables in the model are held constant. All statistical analyses were performed using SPSS (SPSS 15.0 for Windows, SPSS Inc., Chicago, IL, USA).

To identify physiological mechanisms that may explain observed patterns of spatial variation in  $E$  that cannot be explained by differences in environmental variables, we used a mechanistic model as described by Bond and Kavanagh (1999). The Bond-Kavanagh model uses whole-tree hydraulic properties and species-specific characteristics (such as maximum stomatal conductance) to estimate responses of stomatal conductance and  $E$  to variations in  $Q$ ,  $D$ ,  $\Psi_s$ ,  $K_L$  and minimum  $\Psi_L$  ( $\Psi_{L-MIN}$ ). It assumes that boundary layer resistance as well as the utilization of stored water for transpiration are negligible, which are both reasonable for Douglas-fir of this age (Bond and Kavanagh, 1999, Phillips et al., 2003).

We systematically varied parameters in Bond-Kavanagh model to test whether the observed variability in environmental drivers between study plots could explain the observed declines in  $E$  throughout the growing season, or alternatively, to examine whether there is evidence for change or variation in physiological parameters. The

Bond-Kavanagh model is a leaf-specific model where estimates of  $E$  are calculated on a per unit leaf area basis. Not every unit of foliage is equally exposed to the driving forces for transpiration, and therefore the functional leaf area (the amount of leaf area that is transpiring the most) is less than total leaf area of a tree (Cermak, 1989, Brooks et al., 2003). Since the functional leaf area for each of the plots in this study was not known, we did not attempt to scale results from the Bond-Kavanagh model from the leaf to the plot level. Instead, we examined the relative change in  $E$  in response to plot-specific environmental variables. We treated the SF $\uparrow$  plot as the reference base case where all parameters in the model were set equal to those measured in SF $\uparrow$  with the exception of the variables being tested for response. Parameters being tested for response were set to their plot-specific values measured in the field. We examined the response of six different scenarios for the seven days selected through the season for when we had concurrent measurements of  $\Psi_{PD}$  and all other parameters. The scenarios are outlined in Table 3-2. For scenarios one through four, both  $K_L$  and minimum leaf water potential ( $\Psi_{L-MIN}$ ) were held at constant values that are typical for young Douglas-fir.  $K_L$  was assumed to equal  $0.3 \text{ mmol m}^{-2} \text{ s}^{-1} \text{ MPa}^{-1}$  (Phillips et al., 2002) and  $\Psi_{L-MIN}$  assumed to equal  $-2.1 \text{ MPa}$  (Bond and Kavanagh, 1999). In scenarios five and six, we varied  $K_L$  based on field-based, mid-day estimates and then we varied  $\Psi_{L-MIN}$  since although Douglas-fir is isohydric, the  $\Psi_{L-MIN}$  can differ among trees (McDowell et al., 2002).

## Results

### *Transpiration*

Transpiration was highly variable both temporally and spatially (Figure 3-2A-B). From April 10, 2006 (DOY 100) to October 27, 2006 (DOY 300), the average transpiration rate of all four plots combined decreased from a high of  $1.7 \text{ (SE = 0.17) mm d}^{-1}$  in late April to a low of  $0.1 \text{ (SE = 0.03) mm d}^{-1}$  in October. Plots in the upslope locations (SF $\uparrow$  and NF $\uparrow$ ) had rates that over the measurement period averaged approximately 40% greater than those of valley bottom plots ( $1.0 \text{ mm per day}$  vs.  $0.6 \text{ mm per day}$ , respectively). The lowest transpiration rates were observed on the north-facing aspect near the bottom of the valley (Plot NF $\downarrow$ , Figure 3-2B). Average

transpiration was 25% greater in south-facing plots (SF $\uparrow$  and SF $\downarrow$ ) in comparison to north-facing plots (NF $\uparrow$  and NF $\downarrow$ ).

### *Micro-climate*

While the environmental drivers of transpiration followed similar seasonal trends for each plot, the drivers did vary significantly and consistently between plots. Mean daytime  $D$  (0800-1430 h) was highest during the mid-summer drought period (Figure 3-2 C-D). At mid-season, mean daytime  $D$  was 1.61, 1.38, 1.33, and 1.37 kPa for the SF $\uparrow$ , SF $\downarrow$ , NF $\downarrow$ , and NF $\uparrow$  plots, respectively. The two north-facing plots (NF $\uparrow$  and NF $\downarrow$ ) had the most similar values of  $D$  throughout the season, and the regression of NF $\uparrow$  versus NF $\downarrow$  was not significantly different from the 1:1 line ( $p = 0.51$ ). The downslope plots (SF $\downarrow$  and NF $\downarrow$ ) were similar in  $D$  (but significantly different from 1:1) with a regression slope that diverged from the 1:1 by 6 % ( $p < 0.01$ ). Vapor pressure deficit was consistently greater in Plot SF $\uparrow$  than in all other plots ( $p < 0.01$ , for all pairwise regressions). During the early season,  $D$  was 14% greater in SF $\uparrow$  than in the other three plots. As solar angle declined late in the growing season, differences in  $D$  between the SF $\uparrow$  plot and all other plots increased to 25 – 65 %. The plots ranked in order of highest to lowest  $D$  were SF $\uparrow$ , NF $\uparrow$ , SF $\downarrow$ , and NF $\downarrow$ .

Transpiration at a given value of daytime  $D$  declined in both the SF $\downarrow$  and NF $\downarrow$  plots as the growing season progressed from early- to mid-season (Figure 3-3). The response of  $E$  to daytime  $D$  was more consistent across the growing season for the SF $\uparrow$  and NF $\downarrow$  plots.

Rankings among research plots with respect to total daily  $Q$  were similar to those observed for  $D$ . Photosynthetically active radiation was always greatest in the SF $\uparrow$  and lowest in the NF $\downarrow$  as expected from basic topographic principles (Figure 3-2 E-F). The north-facing plots had lower  $Q$  than the south-facing plots. On average, the NF $\downarrow$  plot received 39- 74% less  $Q$  than the other three plots. With the exception of the SF $\uparrow$  plot,  $E$  was greater in the early season at high  $Q$  in comparison to the mid-season (Figure 3-4).  $E$  was highly variable at high levels of  $Q$  indicating that even under high light conditions  $E$  was likely affected by additional variables.

### *Soil Moisture and Soil Water Retention Curves*

Soil moisture declined throughout the growing season in response to water uptake by roots and reduced precipitation (Figure 3-2 G-H). Surprisingly, the NF↓ plot had much lower soil moisture in comparison to all other plots. Soil moisture at 30 cm depth was generally lower and declined more rapidly than at 100 cm for all plots (data not shown). Total soil moisture depletion in the upper 100 cm over the measured growing season was 234, 245, 273, and 345 mm for plots NF↑, NF↓, SF↓, and SF↑, respectively. Soil water retention curves showed an exponential decline in soil moisture in response to increases in pressure plate suction. Soil from the SF↓ plot had the greatest reductions in soil moisture in response to increased suction resulting in the most negative predicted soil matric potentials based on field measured soil moisture (Figure 3-5 and 3-2 I). Because  $\Psi_{PD}$  is commonly used as a proxy for  $\Psi_S$ , we compared values of  $\Psi_S$  to  $\Psi_{PD}$ . Soil matric potentials predicted from retention curves at 30 cm depth were consistently higher than  $\Psi_{PD}$  for both the SF↑ and NF↑ plots. In comparison, retention curves predicted  $\Psi_S$  values more negative than measure  $\Psi_{PD}$  for both downslope locations although  $\Psi_S$  and  $\Psi_{PD}$  were more similar in the NF↓ plot than the SF↓ plot (Figure 3-2 I-J).

### *Predawn Tree Water Potential*

Predawn tree water potential differed by only 0.2 MPa between plots for much of the growing season (Figure 3-2 I-J), and averaged -0.54 MPa early in the season. However, in the late summer differences between plots became more pronounced with the  $\Psi_{PD}$  of plot NF↑ decreasing rapidly to a minimum value of -1.3 MPa in late August (DOY 240). Predawn water potential of Plot NF↓ also showed a marked decrease in  $\Psi_{PD}$  over time with a minimum value of -1.0 MPa in late August. The  $\Psi_{PD}$  of south-facing plots (SF↑ and SF↓) decreased less over the summer compared with north-facing plots, declining by about 0.2 MPa throughout the growing season, indicating less soil moisture stress at the south-facing plots. As mentioned previously,  $\Psi_{PD}$  and  $\Psi_S$  were similar only for the NF↓ plot and  $\Psi_{PD}$  was consistently lower than  $\Psi_S$  for all other plots. This difference between  $\Psi_{PD}$  and  $\Psi_S$  was frequently greater than 0.5 MPa even early in the season when soils had high moisture content. Although we did not account for the

hydrostatic gradient in our  $\Psi_{PD}$  values, the difference of 0.5 MPa exceeds the hydrostatic gradient for 30 m tall tree (0.3MPa).

#### *Soil Depth and Resistance to Penetration*

Depth to bedrock exceeded 2 m in all four plots. The true depth to bedrock could not be detected in any of the four plots because the length of the cone penetrometer was restricted to 2 m and refusal was not typically encountered prior to that depth. Although absolute depth to bedrock could not be determined, we observed distinct differences in resistance profiles between the south-facing (SF $\uparrow$  and SF $\downarrow$ ) and north-facing plots (NF $\downarrow$  and NF $\uparrow$ ). For all plots, resistance to penetration was low in the surface soils, and increased with depth. For the 0-100 cm depth interval, the SF $\uparrow$  plot averaged four knocks per 5 cm depth interval, whereas all other plots averaged just two knocks per 5 cm. At depths below 100 cm, the differences between plots was more apparent and resistance to penetration increased more in the south-facing slopes than in the north-facing slopes, indicating greater bulk density and lower saturated hydraulic conductivity at depth in the south-facing plots. For the 100 – 200 cm depth interval, the SF $\uparrow$  plot had the greatest resistance to penetration averaging 14 knocks per 5 cm interval. The SF $\downarrow$ , NF $\downarrow$ , and NF $\uparrow$  plots averaged nine, six and four knocks, respectively.

#### *Effects of Environmental Predictor Variables on Daily Transpiration*

As a first approach, the effects of  $D$ ,  $Q$ , and  $\Psi_S$  were assessed using a multiple linear regression with analysis of coefficients of partial determination to evaluate the relative importance of each predictor variable. Caution must be used when interpreting  $R^2_{PD}$  when predictor variables are highly correlated to each other (co-linearity). Co-linearity does not reduce the ability to obtain a good model fit or the inferences about the mean responses. However, co-linearity tends to make regression coefficients ( $\beta$ ) and  $R^2_{PD}$  imprecise (Neter et al., 1996). For this reason, we were conservative in our interpretations of  $R^2_{PD}$  when the predictor variables were highly correlated.

During the early season, variation in the environmental variables explained 49 % of the variation in  $E$ . However, the model was improved to explain 66 % by including separate intercepts for SF $\downarrow$  and NF $\uparrow$ , indicating that these plots had higher  $E$  for a given

set of environmental variables compared to SF $\uparrow$  (Table 3-3).  $D$  and  $Q$  were the only highly correlated predictor variables (Pearson's  $r = 0.70$ ,  $p < 0.01$ ); however,  $Q$  was not significant as a predictor variable ( $p=0.25$ ), but was included in the full model because the SF $\downarrow$  plot had a significantly different response to  $Q$  than the other plots ( $p < 0.01$ , Table 3-3, Figure 3-4). The  $R^2_{PD}$  of  $D$  was much greater than that of both  $Q$  and  $\Psi_S$  indicating that  $D$  was the most influential variable explaining variation in  $E$  during that early period (Table 3-3).

As the summer progressed to the mid-season, variation in the environmental variables explained 69 % of the variation in transpiration. By including separate intercepts for SF $\downarrow$ , NF $\downarrow$  and NF $\uparrow$ , the model was improved to explain 89 % (Table 3-3). The impact of  $Q$  and  $\Psi_S$  increased, and all three predictor variables had nearly the same values of  $R^2_{PD}$  indicating they were equally influential in predicting  $E$  (Table 3-3).  $Q$  and  $\Psi_S$  were highly correlated during this period ( $r = -0.75$ ,  $p < 0.01$ ), but no other pairwise comparisons of predictor variables were significantly correlated. During the late season,  $\Psi_S$  was not a significant predictor variable, and  $D$  returned to being the most influential variable in predicting  $E$  ( $R^2_{PD} = 0.69$ ). Interactions between plot indicator variables and environmental predictor variables ( $Q$  and  $D$ ) were significant for most interaction terms indicating that response (slope) of  $E$  varied between the plots (Table 3-3). Interaction terms were not consistently significant from the early to late season. This is an indication that after intermittent precipitation events, environmental variables returned to values similar to those in the early season, but plot-level  $E$  responded to the environmental variables differently. This difference in response was most evident when examining the relationship between  $E$  and  $\Psi_S$  (Figure 3-6) where during the late season,  $\Psi_S$  increased in response to precipitation, but  $E$  remained consistently lower than early or mid-season values.

#### *Examining the response of $E$ to micro-environment using a mechanistic model*

We systematically varied parameters in Bond-Kavanagh model to test whether the observed variability in environmental drivers between study plots could explain the observed declines in  $E$  throughout the growing season, or alternatively, to examine whether there is evidence for change or variation in physiological parameters. We

treated the SF $\uparrow$  plot as the reference base case where all parameters in the model were set equal to those measured in SF $\uparrow$  with the exception of the variables being tested for response. Parameters being tested for response were set to their plot-specific values measured in the field. First, we examined the relative changes in  $E$  in response to plot-specific environmental factors. Differences between plots in environmental variables alone did not result in the same relative amount of decline in  $E$  as we observed with field measurements (Figure 3-7A-D). The average seasonal decline in  $E$  for all four plots was 65%, ranging from 57% in the NF $\downarrow$  plot to 79% in the NF $\uparrow$  plot. Plot-specific differences in  $Q$  and  $D$  (Scenario 2) resulted in average decline of only 42%. The addition of plot-specific values of  $\Psi_{PD}$  as a surrogate for  $\Psi_S$  only resulted in an additional 4% decline (Scenario 3) whereas, the addition of  $\Psi_S$  predicted from soil retention curves resulted in an average decline of 58% (Scenario 4). The seasonal trends in  $E$  generated by the model did not capture the measured seasonal patterns when only plot-specific environmental variables were included in the model. For example, the modeled declines in  $E$  for the SF $\uparrow$  and NF $\uparrow$  plots were much more linear than the measured declines in  $E$  (Figure 3-7A-B).

To understand the possible mechanism behind the measured seasonal pattern, we varied two physiological variables:  $K_L$  and  $\Psi_{L-MIN}$ . The observed seasonal variability in  $E$  was accounted for once plot- and DOY-specific estimates of  $K_L$  were included in the model (Figure 3-7E-H).  $K_L$  ranged from 0.19 (SF $\downarrow$ ) to 0.25 (NF $\uparrow$ ) mmol m<sup>-2</sup> s<sup>-1</sup> MPa<sup>-1</sup> during the early season and from 0.08 (SF $\downarrow$ ) to 0.15 (NF $\downarrow$ ) mmol m<sup>-2</sup> s<sup>-1</sup> MPa<sup>-1</sup> in the late season. Although the magnitude of the range was similar at beginning and end of the growing season, differences between plots in  $K_L$  were much greater throughout the mid-season (Figure 3-8). In the early season,  $K_L$  tended to be higher in the upslope plots relative to downslope, and higher in northfacing relative to southfacing plots. In the late season,  $K_L$  dropped dramatically in the upslope plots. Although including plot- and DOY-specific estimates of  $K_L$  in the model accounted for relative day to day shifts in  $E$ , when  $\Psi_{L-MIN}$  was set to -2.1 MPa, the model tended to underestimate  $E$ , especially during the mid-season, except for the NF $\downarrow$  plot where  $E$  was overestimated (Figure 3-7E-H). In the final scenario, we varied  $\Psi_{L-MIN}$  by +/- 0.2MPa. The observed  $E$  in the SF $\uparrow$  and NF $\uparrow$  plots was most similar to model results when  $\Psi_L$ .

$\Psi_{L-MIN}$  was set equal to -1.9 MPa whereas SF $\downarrow$  may have had an even higher  $\Psi_{L-MIN}$  than we modeled. The NF $\downarrow$  plot was most similar the model with a  $\Psi_{L-MIN} = -2.3$  MPa setpoint. These results indicate that  $\Psi_{L-MIN}$  might not be the same for all the plots despite the trees being of similar size class and age.

## Discussion

Our study demonstrates the large spatial variability in  $E$  across relatively short distances within a steep, headwater catchment. We found that spatial variability in micro-environment did not fully explain the observed variability in  $E$ . Thus, even within an even-aged forest dominated by one species, the trees differed significantly in their responses to environmental drivers and not always as expected based on differences in aspect and hillslope position. Although the study was not designed to examine the spatial variability in  $K_L$  and  $\Psi_{L-MIN}$ , results from the mechanistic Bond-Kavanagh model suggest that both of these factors varied over time and space and were important determinants of the observed variability in  $E$ .

### *Insights gained from the statistical model*

Although the relationship between micro-environment and  $E$  is complex, we were able to examine the influence of  $Q$ ,  $D$ , and  $\Psi_S$  on  $E$  through time using a relatively simple regression-based approach. It was not surprising to find that  $D$  was consistently influential in predicting  $E$  throughout all three growing season periods. When the canopy is well coupled to the atmosphere,  $E$  of conifers is highly responsive to  $D$  (Jarvis and McNaughton, 1986). However, during the precipitation-free mid-season,  $\Psi_S$  became equally influential in the prediction of  $E$  as both  $D$  and  $Q$ . Recent work by Warren et al. (2005) demonstrated the importance of  $\Psi_S$  in estimating tree water uptake for Douglas-fir, and found that although trees used water from deep in the soil, daily water uptake from the entire soil profile was strongly dependent on  $\Psi_S$  at 20 cm depth. Our findings are consistent with other studies where transpiration declines with decreasing  $\Psi_S$  (Wullschleger et al., 1998, Meinzer et al., 2004). In general, we observed that the relationship between micro-environment and  $E$  became more complex as the growing season progressed. The number of significant interaction terms between plot and  $Q$ , and plot and  $D$  in the model increased from the early season to the late-

season indicating that even after  $Q$ ,  $D$ , and  $\Psi_S$  were accounted for, differences in  $E$  existed between plots. We used the Bond-Kavanagh model to mechanistically assess what physiological differences between plots might additionally explain the observed spatial and temporal variation observed in  $E$ .

*Insights gained using a mechanistic modeling approach*

By systematically varying the plot-specific parameters within the Bond-Kavanagh model framework, we found that varying  $K_L$  in both time and space in conjunction with environmental variables could account for the observed declines in  $E$ . Our estimates of  $K_L$  are similar to those observed for Douglas-fir of similar age and size. Several other studies have found  $K_L$  to vary in response to drought; however, we are unaware of another study that has examined the spatial variability in  $K_L$  with regard to topography (Reich and Hinckley, 1989, Cochard et al., 1996, Irvine et al., 1998, Phillips et al., 2002, Addington et al., 2004). Declines in  $K_L$  with declining soil moisture (and  $\Psi_S$ ) can be attributed to reductions in rhizosphere conductance and xylem cavitation. Reductions in rhizosphere conductance have been shown to be important in limiting the total water flux in plants especially in coarse soils such as those at HJA (Sperry et al., 1998). Sperry (1997) found Douglas-fir roots are more vulnerable to cavitation than stems. In addition, Domec et al. (2004) reported root embolism increased from 20 to 55 % loss of conductivity from July to September in young Douglas-fir in southwestern Washington, and loss of conductivity was linearly related to decreased stomatal conductance suggesting that root xylem embolism acted in concert with stomata to limit water loss. It is likely that the initial declines we observed in  $K_L$  are the result of reductions in rhizosphere conductance. Reduction in  $K_L$  over the course of the growing season may be a result of xylem cavitation and incomplete refilling of large conduits (Addington et al., 2004).

Although our results indicate that spatial and temporal variability in  $K_L$  is equally important as microclimatic factors in determining spatial patterns in  $E$ , the results of our modeling also indicated that  $\Psi_{L-MIN}$  may vary spatially as well. It is well documented that Douglas-fir trees regulate  $\Psi_{L-MIN}$ . However, Hacke et al. (2000) demonstrated that  $\Psi_{L-MIN}$  varies in response to edaphic conditions such as soil texture. In addition,  $\Psi_{L-MIN}$  has been shown to decline with increasing tree height and/or age

(Bauerle et al., 1999, McDowell et al., 2002, Barnard and Ryan, 2003, Ewers et al., 2005). These observed declines in  $\Psi_{L-MIN}$  seem to be one compensatory mechanism employed by trees in response to increased resistance and hydrostatic water potential along the soil-plant-atmosphere continuum. Our results from the Bond-Kavanagh model are consistent with this conceptual framework. We found that the model most closely matched the observed declines in  $E$  for the NF↓ plot when  $\Psi_{L-MIN}$  was set to -2.3 MPa whereas, variation in  $E$  for the other plots best represented by the model when  $\Psi_{L-MIN}$  was -1.9 MPa. The NF↓ plot consistently had the lowest soil moisture and  $\Psi_S$  was never as high as the other three plots indicating that trees growing in this plot likely experienced greater moisture stress and likely higher resistance in the rhizosphere. Unfortunately, we do not have measurements of mid-day  $\Psi_L$ , so we cannot determine if the implications of the model were actually applicable to the field.

#### *Spatial variability in edaphic properties*

Stand  $E$  of Douglas-fir forests is reduced strongly when soil moisture availability becomes limited (Lassoie et al., 1977, Unsworth et al., 2004). Soil moisture varied considerably among the four plots in our study. Surprisingly, plots on the south-facing slope had greater soil moisture content than north-facing slope, especially in the late summer. We expected south-facing slopes to have lower soil moisture availability due to greater solar radiation and water use by vegetation (Jones 1992). The differences in soil moisture between slopes was most likely due to soil physical properties such as clay and organic matter content, bulk density and hydraulic conductivity. Soil resistance to penetration has been shown to be inversely related to saturated hydraulic conductivity ( $K_{sat}$ ) (Shanley et al., 2003). If soil resistivity is inversely related to  $K_{sat}$  for WS1, then the soils of the north-facing slope have nearly uniform high  $K_{sat}$  throughout the soil profile. Previous work at HJA has shown that even on steep slopes, water flux directions are almost always vertical in the subsurface (van Verseveld, 2007). Thus, on the north-facing slope infiltrating water may percolate rapidly in a vertical direction down to the impeding layer or the soil-bedrock interface. In contrast, the more stratified resistance pattern on the south facing slope would result in water draining more slowly in the vertical direction and soil moisture would remain higher in comparison to the north-facing slope.

Observed differences in soil moisture did not translate to proportional differences in  $\Psi_S$ . Moisture retention curves varied greatly between plots; however, we acknowledge that differences are suspect because we had to extrapolate curves beyond the range of retention curve data. Soil texture is one of the primary determinants of soil moisture release properties (Saxton et al., 1986, Warren et al., 2005). Because soils across our transect fell within a relatively narrow range of soil textures, we did not expect to find large differences in moisture retention. Predawn water potential is often used as a proxy for  $\Psi_S$ , where it is assumed that leaf water potential equilibrates at night to that region of soil with the highest (least negative) water potential (Richter 1997, but see Donovan et al., 2003 and Kavanagh et al. 2007 for limitations to this assumption). Our measures of  $\Psi_{PD}$  and  $\Psi_S$  (at 30 cm) were only similar for the NF↓ plot. Since  $\Psi_{PD}$  is an integration of  $\Psi_S$  throughout the soil profile and we only estimated  $\Psi_S$  for 30 cm, it is reasonable for these two measures to differ. However, as mentioned previously, daily water uptake is strongly related to  $\Psi_S$  at 20 cm depth (Warren et al., 2005). Our data indicate that  $\Psi_{PD}$  does not reflect  $\Psi_S$  of shallow soil layers and we caution against using  $\Psi_{PD}$  as a surrogate for  $\Psi_S$  especially when relating  $\Psi_{PD}$  to  $E$ .

### **Conclusion**

We observed that plot-scale transpiration across a steep topographic gradient could not be predicted from measured variations in environmental variables alone. Furthermore, spatial variations in soil moisture and  $\Psi_S$  did not conform to preconceived expectations based simply upon topographic gradients. Spatial variability in  $E$  across even small distances can be high and it can not be assumed that a single, randomly selected plot will be representative of the catchment. In the case of WS1, heterogeneity in biophysical drivers ( $Q$  and  $D$ ), edaphic properties and  $K_L$  control plot scale transpiration. Although spatial variation in biophysical drivers may be easy to model, heterogeneous edaphic properties and  $K_L$  are difficult predict without extensive measurements. A better understanding of spatial variation in site characteristics is necessary to explain differences in transpiration throughout the watershed. Currently, very little detailed spatial data exist for edaphic properties and  $K_L$  beyond the hillslope

scale and therefore, it continues to be difficult to scale  $E$  from the plot to the catchment. Our results demonstrate that models of catchment hydrological processes should not assume that transpiration is spatially uniform or that biophysical drivers accurately predict transpiration. Future research should focus on understanding the inter-relationships and feedbacks between soil, vegetation and climate beyond the plot or hillslope scale.

## References

- Addington, R. N., Mitchell, R. J., Oren, R. & Donovan, L. A. (2004) Stomatal sensitivity to vapor pressure deficit and its relationship to hydraulic conductance in *Pinus palustris*. *Tree Physiology*, **24**, 561-569.
- Adelman, J. D., Ewers, B. E. & Mackay, D. S. (2008) Use of temporal patterns in vapor pressure deficit to explain spatial autocorrelation dynamics in transpiration. *Tree Physiology*, **28**, 647-658.
- Aubinet, M., Heinesch, B. & Yernaux, M. (2003) Horizontal and vertical CO<sub>2</sub> advection in a sloping forest. *Boundary-Layer Meteorology*, **108**, 397-417.
- Barnard, H. R. & Ryan, M. G. (2003) A test of the hydraulic limitation hypothesis in fast-growing *Eucalyptus saligna*. *Plant, Cell and Environment*, **26**, 1235-1245.
- Bauerle, W. L., Hinckley, T. M., Cermak, J., Kucera, J. & Bible, K. (1999) The canopy water relations of old-growth Douglas-fir trees. *Trees*, **13**, 211-217.
- Berry, S. L., Farquhar, G. D. & Roderick, M. L. (2005) Co-evolution of climate, vegetation, soil and air. *Encyclopedia of Hydrological Sciences*, pp. 177-192. John Wiley & Sons Inc., Hoboken, NJ.
- Bond, B. J. (2003) Hydrology and ecology meet - and the meeting is good. *Hydrological Processes*, **17**, 2087-2089.
- Bond, B. J., Jones, J. A., Moore, G., Phillips, N., Post, D. & McDonnell, J. J. (2002) The zone of vegetation influence on baseflow revealed by diel patterns of streamflow and vegetation water use in a headwater basin. *Hydrological Processes*, **16**, 1671-1677.
- Bond, B. J. & Kavanagh, K. L. (1999) Stomatal behavior of four woody species in relation to leaf-specific hydraulic conductance and threshold water potential. *Tree Physiology*, **19**, 502-510.
- Bosch, J. M. & Hewlett, J. D. (1982) A review of catchment experiments to determine the effect of vegetation changes on water yield and evapotranspiration. *Journal of Hydrology*, **55**, 3-23.
- Bren, L. J. (1997) Effects of slope vegetation removal on the diurnal variations of a small mountain stream. *Water Resources Research*, **33**, 321-331.
- Brooks, J. R., Schulte, P. J., Bond, B. J., Coulombe, R., Domec, J. C., Hinckley, T. M., McDowell, N. G. & Phillips, N. (2003) Does foliage on the same branch compete for the same water? Experiments on Douglas-fir trees. *Trees*, **17**, 101-108.
- Brooks, J. R., Sprugel, D. G. & Hinckley, T. M. (1996) The effects of light acclimation during and after foliage expansion on photosynthetic function of *Abies amabilis* foliage within the canopy. *Oecologia*, **107**, 21-32.
- Calder, I. R. (1998) Water use by forests, limits and controls. *Tree Physiology*, **18**, 625-631.
- Campbell, G. S. & Norman, J. M. (1998) *An introduction to environmental biophysics*. Springer, New York.
- Cermak, J. (1989) Solar equivalent leaf area as the efficient biometrical parameter of individual leaves, trees and stands. *Tree Physiology*, **5**, 269-289.

- Chen, X. (2007) Hydrologic connections of a stream–aquifer–vegetation zone in south-central Platte River valley, Nebraska. *Journal of Hydrology* **333**, 554-568.
- Cochard, H., Breda, N. & Granier, A. (1996) Whole tree hydraulic conductance and water loss regulation in *Quercus* during drought: evidence for stomatal control of embolism. *Annales Des Sciences Forestières*, **53**, 197-206.
- Cosandey, C., Andreassian, V., Martin, C., Didon-Lescot, J., Lavabre, J., Folton, N., Mathys, N. & Richard, D. (2005) The hydrologic impact of the Mediterranean forest: a review of French research. *Journal of Hydrology*, **301**, 235-249.
- Czarnomski, N. M., Moore, G. W., Pypker, T. G., Licata, J. & Bond, B. J. (2005) Precision and accuracy of three alternative soil water content instruments in two forest soils of the Pacific Northwest. *Canadian Journal of Forest Research*, **35**, 1867-1876.
- Dawson, T. E., Burgess, S. S. O., Tu, K. P., Oliveira, R. S., Santiago, L. S., Fisher, J. B., Simonin, K. A. & Ambrose, A. R. (2007) Nighttime transpiration in woody plants from contrasting ecosystems. *Tree Physiology*, **27**, 561-575.
- Deming, W. E. (1950) *Some theory of sampling*. Wiley and Sons, New York.
- Domec, J.-C., Warren, J. M., Meinzer, F. C., Brooks, J. R. & Coulombe, R. (2004) Native root xylem embolism and stomatal closure in stands of Douglas-fir and ponderosa pine: mitigated by hydraulic redistribution. *Oecologia*, **141**, 7-16.
- Domec, J. C., Meinzer, F. C., Gartner, B. L. & Woodruff, D. (2006) Transpiration-induced axial and radial tension gradients in trunks of Douglas-fir trees. *Tree Physiology* **26**, 275-284.
- Donovan, L. A., Richards, J. H. & Linton, M. J. (2003) Magnitude and mechanisms of disequilibrium between predawn plant and soil water potentials. *Ecology*, **84**, 463-470.
- Dunford, E. G. & Fletcher, P. W. (1947) Effect of removal of stream-bank vegetation upon water yield. *Eos transactions, American Geophysical Union* **28**, 105-110.
- Ewers, B. E., Gower, S. T., Bond-Lamberty, B. & Wang, C. K. (2005) Effects of stand age and tree species on canopy transpiration and average stomatal conductance of boreal forests. *Plant, Cell and Environment*, **28**, 660-678.
- Federer, C. A. (1973) Forest transpiration greatly speeds streamflow recession. *Water Resources Research*, **9**, 1599-1604.
- Ford, C. R., Hubbard, R. M., Kloeppel, B. D. & Vose, J. M. (2007) A comparison of sap flux based evapotranspiration estimates with catchment-scale water balance. *Agricultural and Forest Meteorology*, **145**, 176-185.
- Granier, A. (1985) Une nouvelle méthode pour la mesure du flux de sève brute dans le tronc des arbres. *Annales Des Sciences Forestières*, **42**, 193-200.
- Granier, A. (1987) Evaluation of transpiration in a Douglas-fir stand by means of sap flow measurements. *Tree Physiology*, **3**, 309-320.
- Gribovszki, Z., Kalicz, P., Szilágyi, J. & Kucsara, M. (2008) Riparian zone evapotranspiration estimation from diurnal groundwater fluctuations. *Journal of Hydrology* **349**, 6-17.
- Hacke, U. G., Sperry, J. S., Ewers, B. E., Ellsworth, D. S., Schafer, K. V. R. & Oren, R. (2000) Influence of soil porosity on water use in *Pinus taeda*. *Oecologia*, **124**, 495 - 505

- Harr, R. D. (1977) Water flux in soil and subsoil on a steep forested slope. *Journal of Hydrology*, **33**, 37-58.
- Harr, R. D. & McCorison, F. M. (1979) Initial effects of clearcut logging on size and timing of peak flows in a small watershed in western Oregon. *Water Resources Research*, **15**, 90-94.
- Hewlett, J. D. (1982) *Principles of forest hydrology*. The University of Georgia Press, Athens.
- Hinckley, T. M., Lassoie, J. P. & Running, S. W. (1978) Temporal and spatial variations in the water status of forest trees. *Forest Science*, **24**, 72.
- Hjerdt, K. N., McDonnell, J. J., Seibert, J. & Rodhe, A. (2004) A new topographic index to quantify downslope controls on local drainage. *Water Resources Research*, **40**, W05602, doi:10.1029/2004WR003130.
- Hooper, R. P., Aulenbach, B. T., Burns, D. A., McDonnell, J., Freer, J., Kendall, C. & Beven, K. (1998) Riparian control of stream-water chemistry: implications for hydrochemical basin models. *Conference HeadWater '98 Conf.* (eds K. Kovar, U. Tappeiner, N. Peters & R. Craig), pp. 451-458. IAHS, Meran, Italy.
- Huxman, T. E., Wilcox, B. P., Breshears, D. D., Scott, R. L., Snyder, K. A., Small, E. E., Hultine, K., Pockman, W. T. & Jackson, R. B. (2005) Ecohydrological implications of woody plant encroachment. *Ecology*, **86**, 308-319.
- Irvine, J., Perks, M. P., Magnani, F. & Grace, J. C. (1998) The response of *Pinus sylvestris* to drought: stomatal control of transpiration and hydraulic conductance. *Tree Physiology*, **18**, 393-402.
- Jarvis, P. G. & McNaughton, K. G. (1986) Stomatal control of transpiration: scaling up from leaf to region. *Advances in Ecological Research*, **15**, 1-49.
- Kavanagh, K. L., Pangle, R. & Schotzko, A. D. (2007) Nocturnal transpiration causing disequilibrium between soil and stem predawn water potential in mixed conifer forests of Idaho. *Tree Physiology*, **27**, 621-629.
- Klute, A. (1986) Water Retention: Laboratory Methods. *Methods of Soil Analysis Part 1 - Physical and Mineralogical Methods* (ed A. Klute), pp. 635-662. Soil Science Society of America, Inc., Madison, WI.
- Kobayashi, D., Suzuki, K. & Nomura, M. (1990) Diurnal fluctuations in streamflow and in specific electric conductance during drought periods. *Journal of Hydrology*, **115**, 105-114.
- Lassoie, J., Scott, D. & Fritschen, L. (1977) Transpiration Studies in Douglas-fir Using the Heat Pulse Technique. *Forest Science*, **23**, 377-390.
- Loheide, S. P. (2008) A method for estimating subdaily evapotranspiration of shallow groundwater using diurnal water table fluctuations. *Ecohydrology*, **1**, 59-66.
- Loranty, M. M., Mackay, D. S., Ewers, B. E., Adelman, J. D. & Kruger, E. L. (2008) Environmental drivers of spatial variation in whole-tree transpiration in an aspen-dominated upland-to-wetland forest gradient. *Water Resources Research*, **44**, W02441, doi:10.1029/2007WR00627, 2008.
- Ludwig, J. A., Wilcox, B. P., Breshears, D. D., Tongway, D. J. & Imeson, A. C. (2005) Vegetation patches and runoff-erosion as interacting ecohydrological processes in semiarid landscapes. *Ecology*, **85**, 288-297.
- McDonnell, J. J. & Tanaka, T. (2001) Hydrology and biogeochemistry of forested catchments. *Hydrological Processes*. John Wiley & Sons, New York.

- McDowell, N. G., Phillips, N., Lunch, C., Bond, B. J. & Ryan, M. G. (2002) An investigation of hydraulic limitation and compensation in large, old Douglas-fir trees. *Tree Physiology*, **22**, 763-774.
- McGuire, K. J. (2004) *Water residence time and runoff generation in the western Cascades of Oregon*. PhD Dissertation, Oregon State University, Corvallis.
- McGuire, K. J., McDonnell, J. J. & Weiler, M. (2007) Integrating tracer experiments with modeling to infer water transit times. *Advances in Water Resources*, **30**, 824-837.
- Meinzer, F. C. (2003) Functional convergence in plant responses to the environment. *Oecologia*, **134**, 1-11.
- Meinzer, F. C., Brooks, J. R., Bucci, S., Goldstein, G., Scholtz, F. G. & Warren, J. M. (2004) Converging patterns of uptake and hydraulic redistribution of soil water in contrasting woody vegetation types. *Tree Physiology*, **24**, 919-928.
- Monteith, J. L. (1995) A reinterpretation of stomatal responses to humidity. *Plant, Cell, and Environment*, **18**, 357-364.
- Monteith, J. L. & Unsworth, M. H. (2008) *Principles of Environmental Physics*. Academic Press, New York.
- Moore, G. W., Bond, B. J., Jones, J. A., Phillips, N. & Meinzer, F. C. (2004) Structural and compositional controls on transpiration in a 40- and 450-yr-old riparian forest in western Oregon, USA. *Tree Physiology*, **24**, 481-491.
- Neter, J., Kutner, M. H., Nachsheim, C. J. & Wasserman, W. (1996) *Applied Linear Statistical Models*. Irwin, Chicago, IL.
- Nuttle, W. K. (2002) Is ecohydrology one idea or many? *Hydrological Sciences*, **47**, 805-807.
- Oke, T. R. (1992) *Boundary Layer Climates*. Routledge, New York.
- Phillips, N., Bond, B., McDowell, N. & Ryan, M. G. (2002) Canopy and hydraulic conductance in young, mature, and old Douglas-fir trees. *Tree Physiology*, **22**, 205-211.
- Phillips, N., Oren, R. & Zimmerman, R. (1996) Radial patterns of xylem sap flow in non-diffuse and ring-porous tree species. *Plant Cell and Environment*, **19**, 983-990.
- Phillips, N., Ryan, M. G., Bond, B. J., McDowell, N. G., Hinkley, T. M. & Èermák, J. (2003) Reliance on stored water increases with tree size in three species in the Pacific Northwest. *Tree Physiology*, **23**, 237-245.
- Pierson, F., Carlson, D. & Spaeth, K. (2002) Impacts of wildfire on soil hydrologic properties of steep sagebrush-stepp rangeland. *International Journal of Wildland Fire* **11**, 145-151.
- Quinn, P. F., Beven, K. J., Chevallier, P. & Planchon, O. (1991) The prediction of hillslope flow paths for distributed hydrological modelling using digital terrain models. *Hydrological Processes*, **5**, 59-79.
- Ranken, D. W. (1974) *Hydrologic properties of soil and subsoil on a steep, forested slope*. M.S., Oregon State University, Corvallis.
- Reich, P. B. & Hinkley, T. M. (1989) Influence of pre-dawn water potential and soil-to-leaf hydraulic conductance on maximum daily leaf diffusive conductance in two oak species. *Functional Ecology*, **3**, 719-726.

- Rich, L., Reynolds, H. & West, J. (1961) The Workman Creek experimental watershed. pp. 188.
- Richter, H. (1997) Water relations of plants in the field: some comments on the measurement of select parameters. *Journal of Experimental Botany*, **48**, 1-7.
- Rothacher, J., Dyrness, C. T. & Fredriksen, F. L. (1967) Hydrologic and related characteristics of three small watersheds in the Oregon cascades. pp. 1-54. Forest Service, USDA.
- Saxton, K. E., Rawls, W. J., Romberger, J. S. & Papendick, R. I. (1986) Estimating generalized soil-water characteristics from texture. *Soil Science Society of America Journal*, **50**, 1031 - 1036.
- Selker, J. S., Keller, C. K. & McCord, J. T. (1999) *Vadose zone processes*. Lewis Publishers, Boca Raton, FL.
- Shanley, J. B., Hjerdt, K. N., McDonnell, J. J. & Kendall, C. (2003) Shallow water table fluctuations in relation to soil penetration resistance. *Ground Water*, **41**, 964 - 972.
- Shewhart, W. A. (1993) The role of statistical method in economic standardization. *Econometrica*, **1**, 23-25.
- Sollins, P., Cromack, K. J., McCorison, F. M., Waring, R. H. & Harr, R. D. (1981) Changes in nitrogen cycling at an old-growth Douglas-fir site after disturbance. *Journal of Environmental Quality*, **10**, 37-42.
- Sperry, J. S., Adler, F. R., Campbell, G. S. & Comstock, J. P. (1998) Limitation of plant water use by rhizosphere and xylem conductance: results form a model. *Plant Cell and Environ.*, **21**, 347-359.
- Sperry, J. S. & Ikeda, T. (1997) Xylem cavitation in roots and stems of Douglas-fir and white fir. *Tree Physiology*, **17**, 275-280.
- Swanson, F. J. & James, M. E. (1975a) Geology and geomorphology of the H.J. Andrews Experimental Forest, Western cascades, Oregon. *Pacific Northwest Forest and Range Experiment Station, Forest Service, U.S.D.A, Research Paper PNW-188*, 1-14.
- Swanson, F. J. & James, M. E. (1975b) Geology and geomorphology of the H.J. Andrews Experimental Forest, western Cascades, Oregon., pp. 14. U.S. Department of Agriculture, Forest Service, Pacific Northwest Forest and Range Experiment Station, Portland, OR.
- Szilágyi, J., Gribovszki, Z., Kalicz, P. & Kucsara, M. (2008) On diurnal riparian zone groundwater-level and streamflow fluctuations. *Journal of Hydrology*, **349**, 1-5.
- Taiz, L. & Zeiger, E. (1991) *Plant Physiology*. The Benjamin/Cummings Publishing Company, Inc., New York.
- Tardieu, F. a. W. J. D. (1993) Integration of hydraulic and chemical signalling in the control of stomatal conductance and water status of droughted plants. *Plant, Cell, and Environ.*, **16:341-349**.
- Triska, F. J., Sedell, J. R., Cromack, K., Gregory, S. V. & McCorison, F. M. (1984) Nitrogen budget for a small coniferous forest stream. *Ecological Monographs*, **54**, 119-140.
- Tromp-van Meerveld, H. J. & McDonnell, J. J. (2006a) On the interrelations between topography, soil depth, soil moisture, tranpiration rates and species distribution at the hillslope scale. *Advances in Water Resources*, **29**, 293-310.

- Tromp-van Meerveld, H. J. & McDonnell, J. J. (2006b) Threshold relations in subsurface stormflow: 2. The fill and spill hypothesis. *Water Resources Research*, **42**, doi:10.1029/2004WR003800.
- Troxell, M. C. (1936) The diurnal fluctuations in the groundwater and flow of the Santa Ana River and its meaning. *Eos transactions, American Geophysical Union* **17**, 496-504.
- Tyree, M. T. & Sperry, J. S. (1988) Do Woody plants operate near the point of catastrophic xylem dysfunction caused by dynamic water stress? *Plant Physiology*, **88**, 574-580.
- Unsworth, M. H., Phillips, N., Link, T. E., Bond, B. J., Falk, M., Harmon, M. E., Hinkley, T. M., Marks, D. & Paw U, K. (2004) Components and controls of water flux in an old-growth Douglas-fir/western hemlock ecosystem. *Ecosystems*, **7**, 468-481.
- van Verseveld, W. (2007) *Hydro-biogeochemical coupling at the hillslope and catchment scale*. PhD, Oregon State University, Corvallis.
- Warren, J. M., Meinzer, F. C., Brooks, J. R. & Domec, J. C. (2005) Vertical stratification of soil water storage and release dynamics in Pacific Northwest coniferous forests. *Agricultural and Forest Meteorology*, **130**, 39 - 58.
- White, W. N. (1932) A method of estimating ground-water supplies based on discharge by plants and evaporation from soil: Results of investigations in Escalante Valley, Utah. pp. 1-105.
- Whitehead, D. (1998) Regulation of stomatal conductance and transpiration in forest canopies. *Tree Physiology*, **18**, 633-644.
- Williams, D., Scott, R., Huxman, T. & Goodrich, D. (2005) Multi-scale eco-hydrology of riparian ecosystems in the desert southwest. *The 58th Annual Meeting, Society for Range Management*. Fort Worth, Texas.
- Wondzell, S. M., Gooseff, M. N. & McGlynn, B. L. (2007) Flow velocity and the hydrologic behavior of streams during baseflow. *Geophysical Research Letters*, **34**.
- Wullschleger, S. D., Meinzer, F. C. & Vertessy, R. A. (1998) A review of whole-plant water use studies in trees. *Tree Physiology*, **18**, 499-512.
- Yoshinaga, S. & Ohnuki, Y. (1995) Estimation of soil physical properties from a handy cone penetrometer test. *Japan Society of Erosion Control Engineering*, **48**, 22-28.
- Zalewski, M. (2000) Ecohydrology – the scientific background to use ecosystem properties as management tools toward sustainability of water resources. *Ecological Engineering* **16**, 1-8.
- Zalewski, M. (2002) Ecohydrology - the use of ecological and hydrological processes for sustainable management of water resources. *Hydrological Sciences*, **47**, 823-832.

Table 3-1: The site characteristics for each of the four plots. The table provides plot level descriptives for slope, stem density, basal area, canopy height, diameter at 1.37 m (DBH), sapwood depth and leaf area index (LAI), and soil moisture depletion.

<b>Plot</b>	<b>Slope (°)</b>	<b>Stem Density (stems ha<sup>-1</sup>)</b>	<b>Total Basal Area (m<sup>2</sup>)</b>	<b>% Basal Area PSME</b>	<b>Max Canopy Ht. (m)</b>	<b>Mean PSME DBH (cm) (S.E.)</b>	<b>Mean PSME sapwood depth (cm) (S.E.)</b>	<b>LAI (m<sup>2</sup> m<sup>-2</sup>) PSME Only</b>	<b>Soil Moisture Depletion (mm)</b>
SF↑	31.2	3055	1.04	93	22	11.3 (0.7)	3.7 (0.3)	7.8	234
SF↓	36.3	764	1.12	100	29	22.3 (2.0)	3.4 (0.4)	8.7	245
NF↓	43.4	859	0.85	82	24	18.7 (1.2)	3.3 (0.5)	5.2	273
NF↑	35.5	1304	1.00	96	31	16.8 (0.9)	3.5 (0.4)	7.5	345

Table 3-2: Summary of parameters used in the Bond-Kavanagh model and how they were varied during six different model scenarios.

Scenario	Parameters				
	$Q$ ( $\mu\text{mol m}^{-2} \text{s}^{-1}$ )	$D$ (kPa)	$\Psi_S$ (MPa)	$K_L$ ( $\text{mmol m}^{-2} \text{s}^{-1} \text{MPa}^{-1}$ )	$\Psi_{L-\text{MIN}}$ (MPa)
1	Plot-specific	= SF $\uparrow$	= SF $\uparrow$	0.3	-2.1
2	Plot-specific	Plot-specific	= SF $\uparrow$	0.3	-2.1
3	Plot-specific	Plot-specific	Plot-specific estimated from $\Psi_{PD}$	0.3	-2.1
4	Plot-specific	Plot-specific	Plot-specific $\Psi_S$ estimated from retention curves	0.3	-2.1
5	Plot-specific	Plot-specific	Plot-specific $\Psi_S$ estimated from retention curves	Plot-specific	-2.1
6	Plot-specific	Plot-specific	Plot-specific $\Psi_S$ estimated from retention curves	Plot-specific	-2.1 $\pm$ 0.2

Table 3-3: Regression coefficients ( $\beta$ ), p-values and coefficients of partial determination ( $r^2_{PD}$ ) of models for early-, mid-, and late-season prediction of daily transpiration.

Variable	Early Season ( $R^2 = 0.66$ )			Mid-Season ( $R^2 = 0.89$ )			Late Season ( $R^2 = 0.86$ )		
	$\beta$	p	$r^2_{PD}$	$\beta$	p	$r^2_{PD}$	$\beta$	p	$r^2_{PD}$
<sup>a</sup> $D$	1.281	<0.01	0.36	0.163	0.03	0.13	0.941	<0.01	0.69
<sup>a</sup> $Q$	0.007	0.25	0.03	0.007	0.02	0.14	0.001	0.61	<0.01
<sup>ab</sup> $\Psi_S$	1.057	0.04	0.08	-0.267	0.01	0.16	NS		
$D \times \Psi_S$	-1.397	0.01	0.13	NS			NS		
Plot SF↓	3.014	<0.01		-0.298	<0.01		0.610	<0.01	
Plot NF↓	NS			-0.326	<0.01		-0.042	0.81	
Plot NF↑	0.473	<0.01		-1.179	<0.01		-0.100	0.44	
$Q \times SF\downarrow$	-0.046	<0.01		NS			NS		
$Q \times NF\downarrow$	NS			NS			0.021	<0.01	
$Q \times NF\uparrow$	NS			0.019	<0.01		0.011	<0.01	
$D \times SF\downarrow$	NS			NS			-0.951	<0.01	
$D \times NF\downarrow$	NS			NS			-0.667	<0.01	
$D \times NF\uparrow$	NS			NS			-0.474	<0.01	
Intercept	-0.589	0.07		0.699	<0.01		-0.160	0.11	
n	69			44			88		
Mean Squared Error	0.10			0.01			0.01		

NS: the predictor variable was insignificant at the  $\alpha = 0.05$  level.

<sup>a</sup> A square root transformation was applied to  $D$ ,  $Q$ , and  $\Psi_S$ .

<sup>b</sup>  $\Psi_S$  values were inputted into the models as the absolute values.

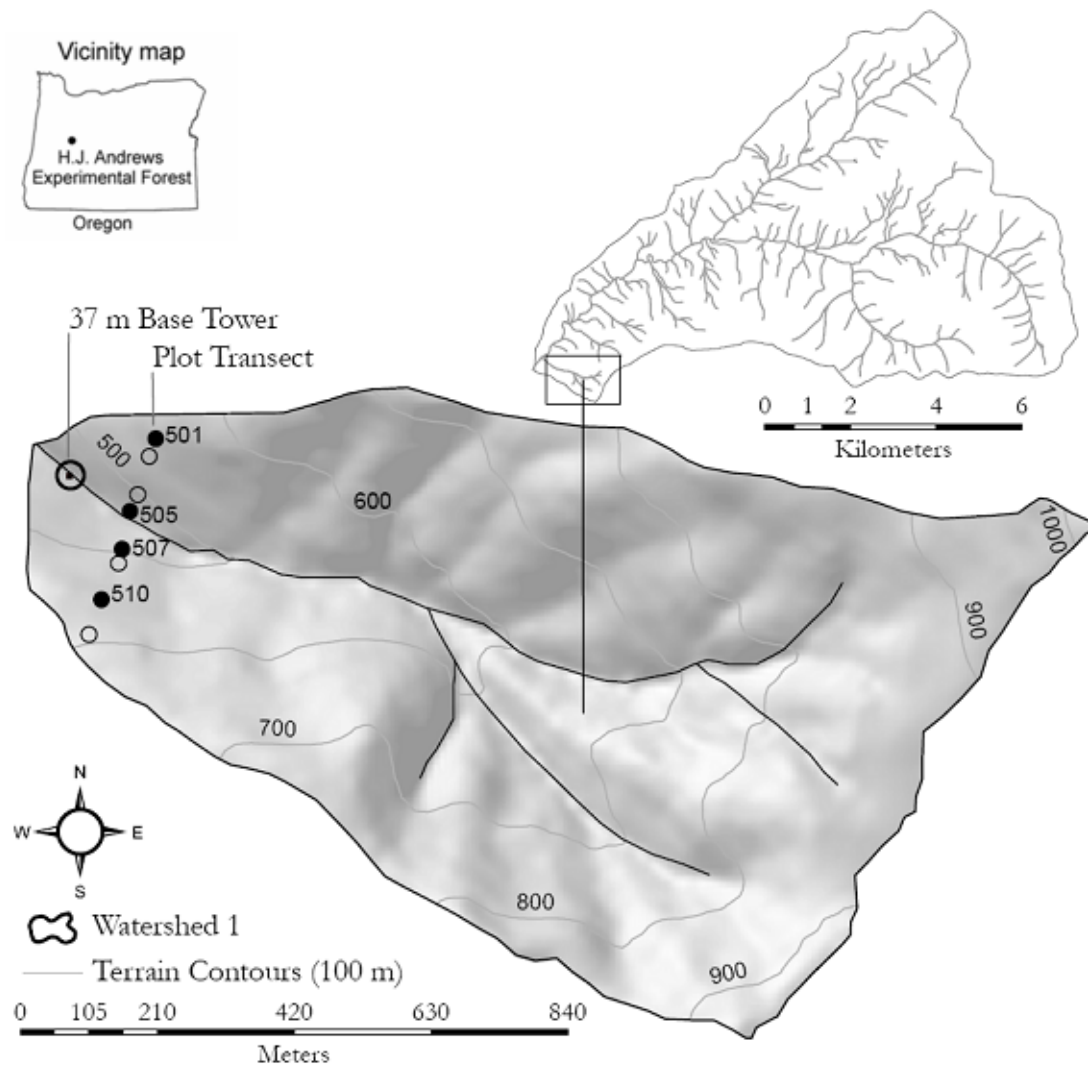


Figure 3-1: Map of the location of the HJ Andrews Experimental Forest and Watershed 1. The map of Watershed 1 shows the locations of the base tower and the eight research plot along the transect. The dark circles indicate the four research plots along the transect that were used in this study (501 - SF $\uparrow$ , 505 - SF $\downarrow$ , 507 - NF $\downarrow$  and 510 - NF $\uparrow$ ).

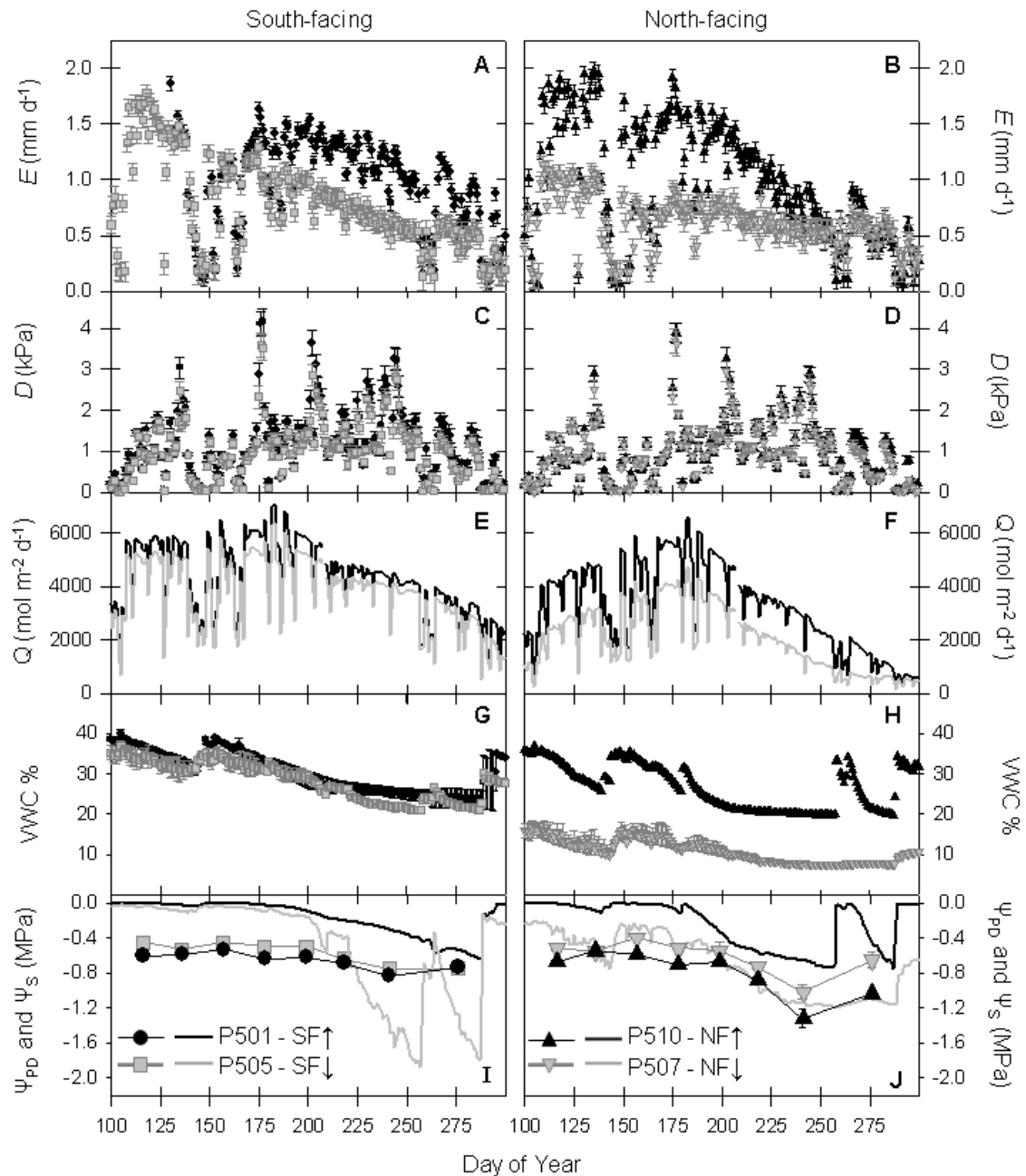


Figure 3-2: Transpiration (A-B), mean 0800-1430  $D$  (C-D), total daily  $Q$  (E-F), soil volumetric water content at 30 cm depth (G-H),  $\Psi_{PD}$  (symbols with connecting lines) and  $\Psi_S$  (solid lines, no symbols) (I-J) throughout the growing season for our four study plots. Error bars = standard error.

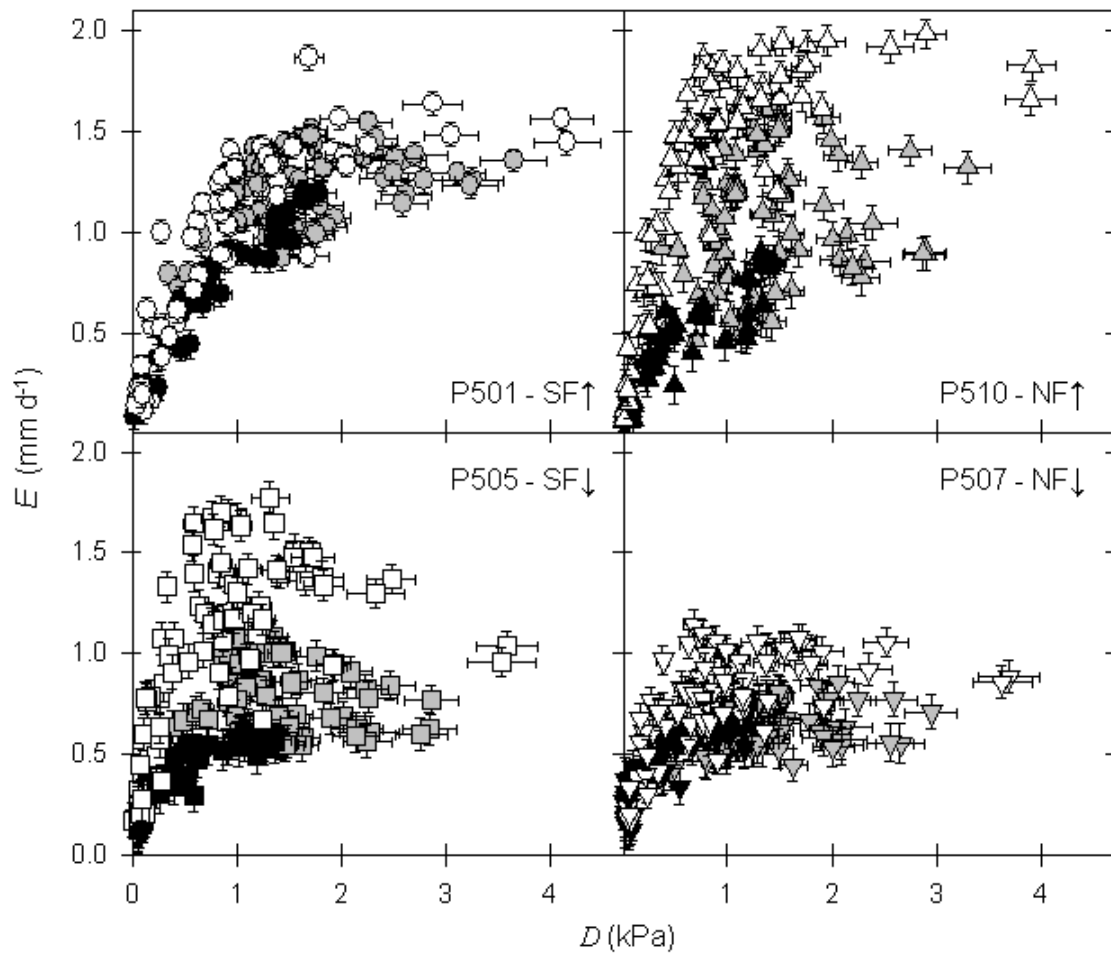


Figure 3-3: The relationship between mean 0800-1430  $D$  and  $E$  for early (DOY 100-181; open symbols), mid- (DOY 182-256; gray symbols), and late (DOY 257-300; black symbols) growing season. Error bars = standard error.

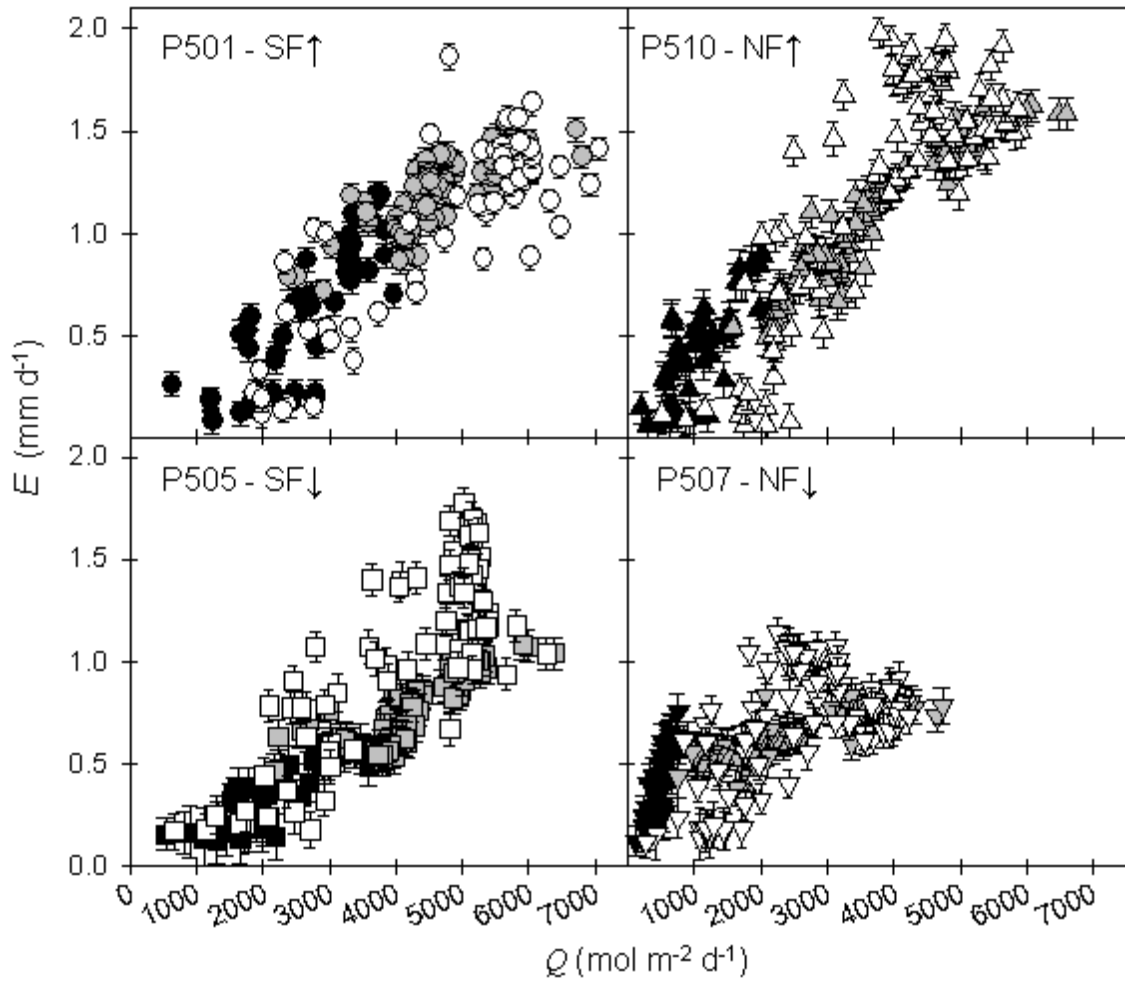


Figure 3-4: The relationship between total daily  $Q$  and  $E$  for early (DOY 100-181; open symbols), mid- (DOY 182-256; gray symbols), and late (DOY 257-300; black symbols) growing season. Error bars = standard error.

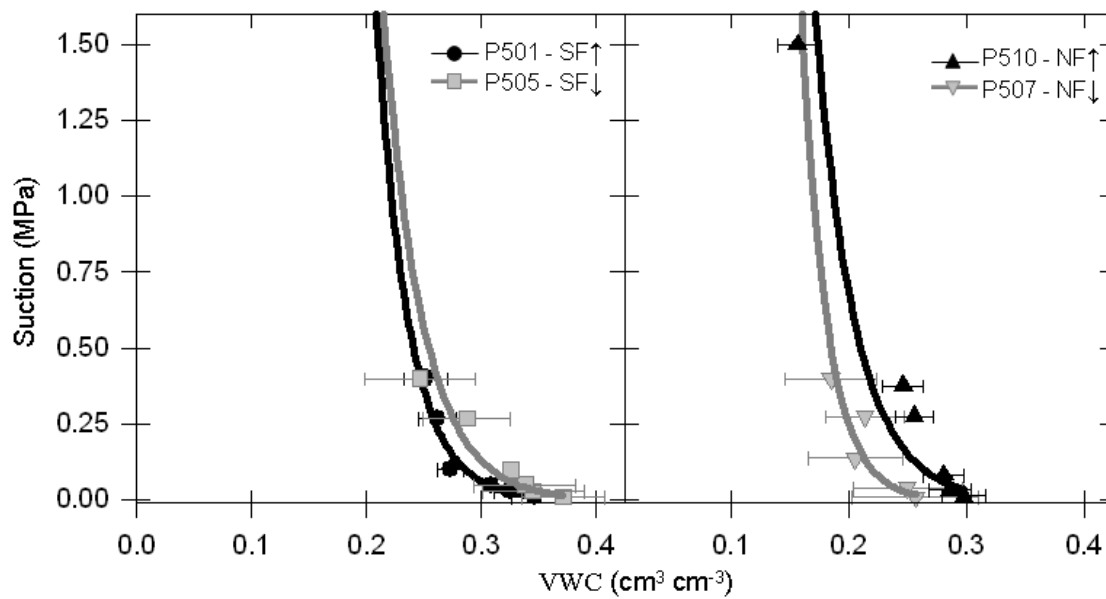


Figure 3-5: Soil moisture retention curves for the four study plots. Error bars = standard error.

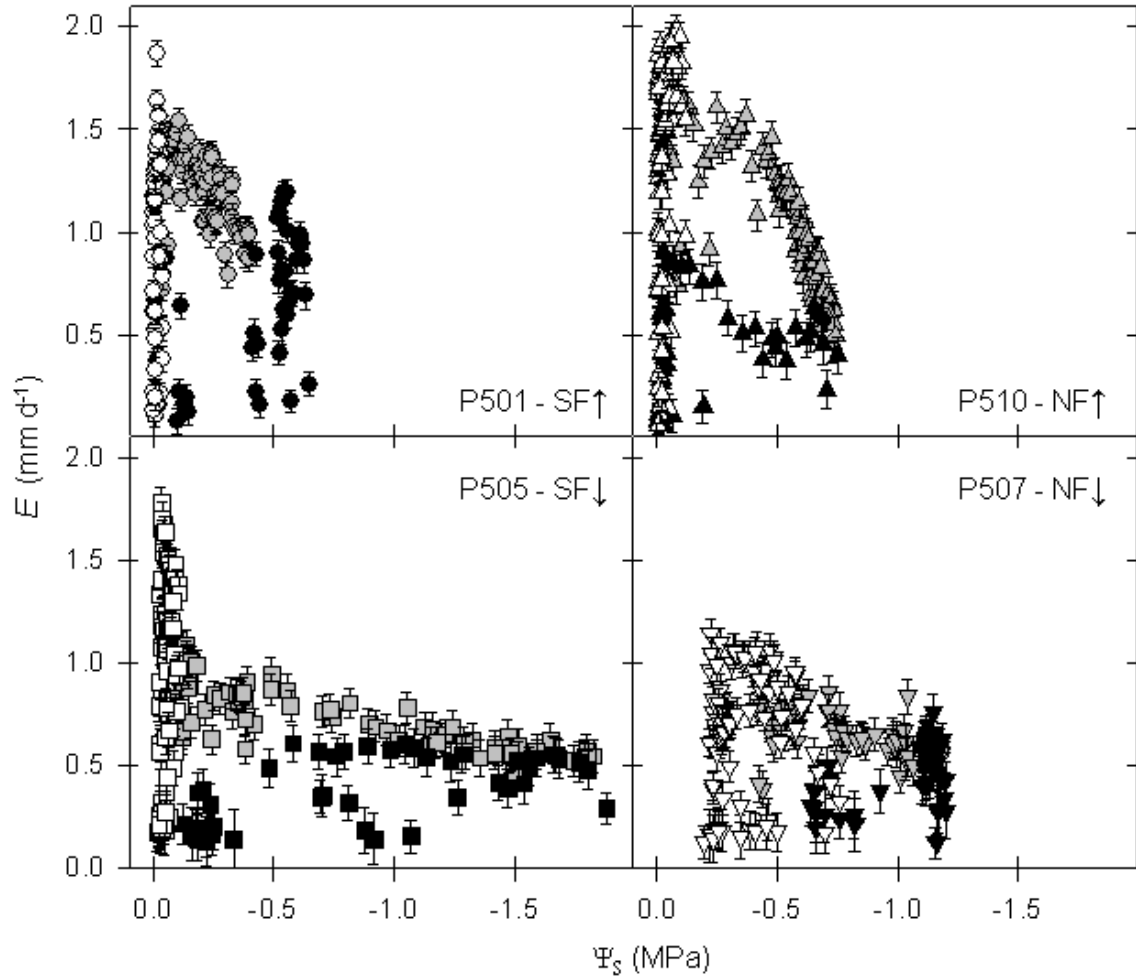


Figure 3-6: The relationship between  $\Psi_s$  at 30 cm depth and  $E$  for early (DOY 100-181; open symbols), mid- (DOY 182-256; gray symbols), and late (DOY 257-300; black symbols) growing season. Error bars = standard error.

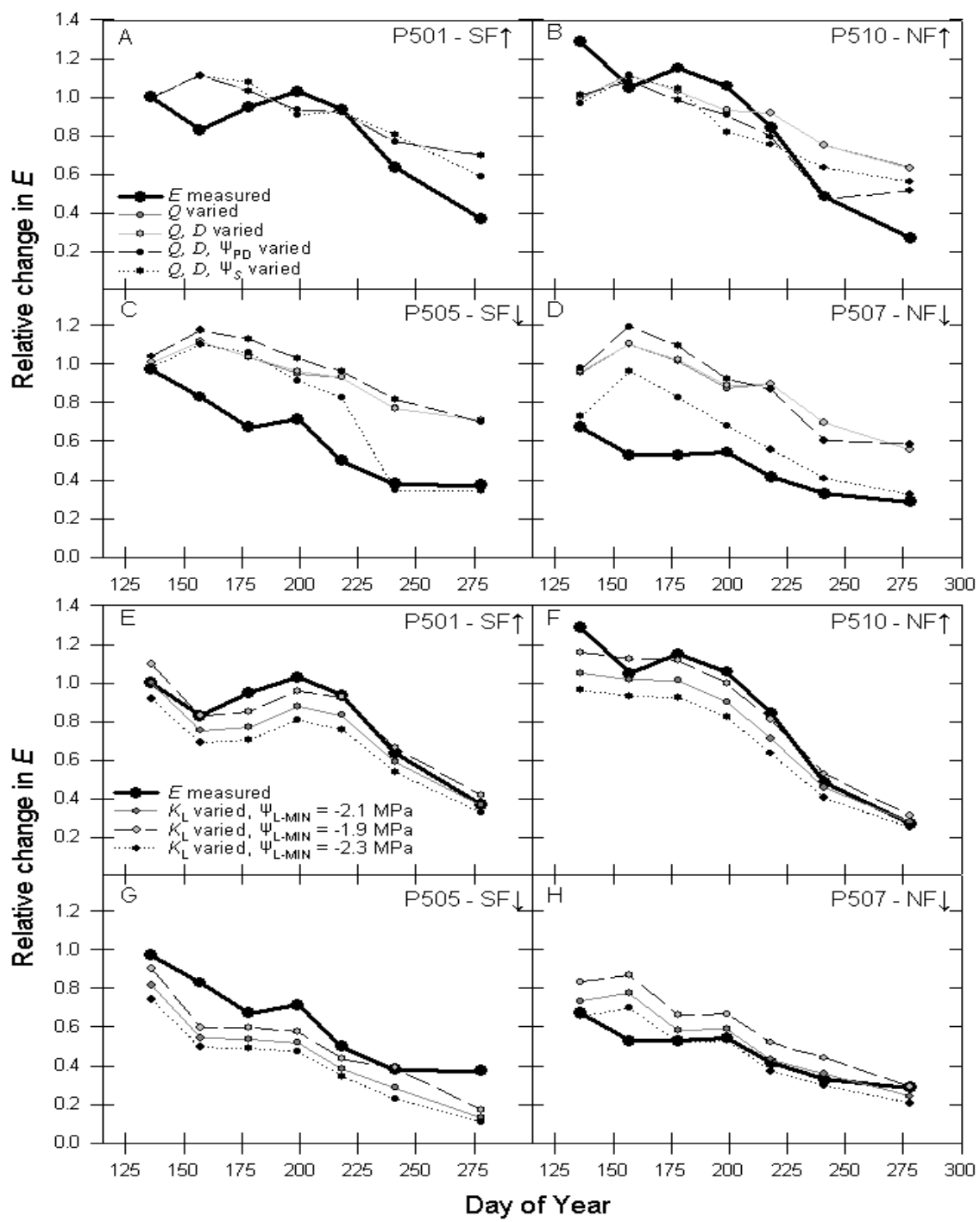


Figure 3-7: Results of the Bond-Kavanagh model for six model scenarios (see Table 3-2) examining the relative decline in  $E$  through time for each of the four study plots. The SF↑ plot is the reference base case where all parameters in the model were set equal to their plot-specific value measured in the field.

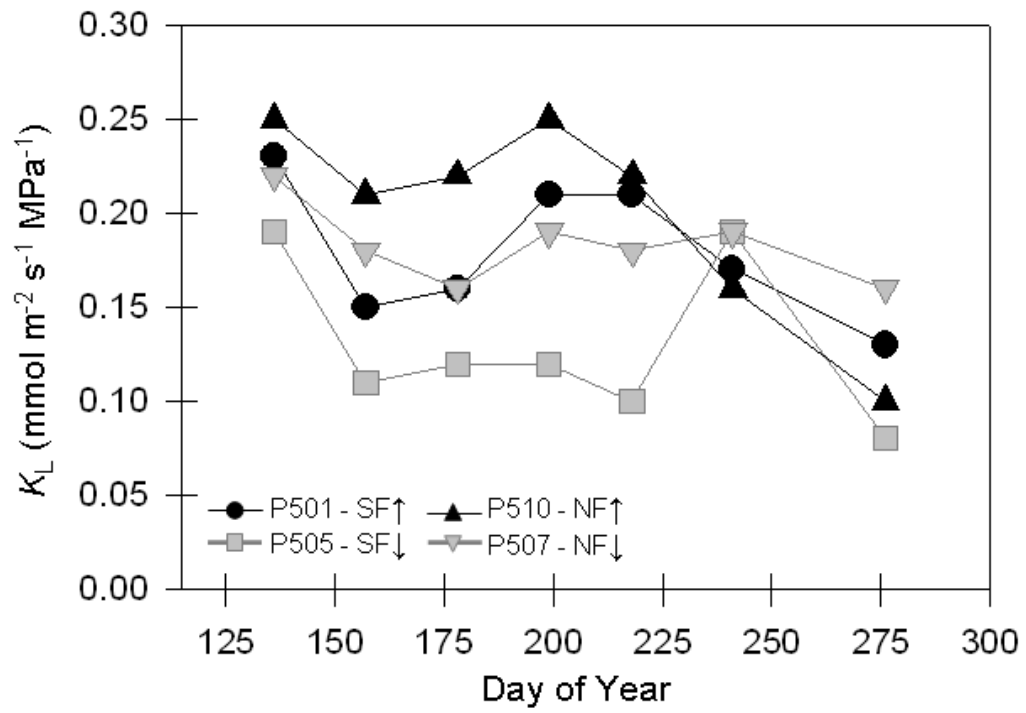


Figure 3-8: Estimated mid-day  $K_L$  through time for each of the four study plots.

**Chapter 4 A dual isotope ( $^{13}\text{C}$  and  $^{18}\text{O}$ ) approach to infer annual aboveground biomass increment in young Douglas-fir.**

## Introduction

Stable isotopes ratios in tree rings are powerful tools in environmental research because they indicate key physiological processes and record them over time. While several studies have clearly shown that the isotopic composition of tree rings can be a valuable source of information for the reconstruction of both plant water relations and environmental variability, most investigations to date have been based on independent analysis of  $\delta^{13}\text{C}$  or  $\delta^{18}\text{O}$  (McCarroll and Loader, 2004). In recent years, the theory behind changes in stable oxygen isotopes ratio ( $\delta^{18}\text{O}$ ) in plants has advanced significantly and the examination of the inter-relationships between  $\delta^{13}\text{C}$ ,  $\delta^{18}\text{O}$ , and tree ring width has the potential to illuminate valuable physiological and environmental information (Saurer et al., 1997, Farquhar et al., 1998, Anderson et al., 1998, Scheidegger et al., 2000, Barbour, 2007a). Theory and empirical evidence suggests that  $\delta^{13}\text{C}$  and  $\delta^{18}\text{O}$  in plant cellulose may provide a relative index of biomass accumulation because  $\delta^{13}\text{C}$  is strongly influenced by the rate of photosynthesis ( $A$ ) and stomatal conductance ( $g_s$ ) and  $\delta^{18}\text{O}$  enrichment cellulose is influenced by  $g_s$ , but not  $A$ . Indeed, experiments in controlled environments concur with expectations where  $\delta^{18}\text{O}$  has been shown to be correlated with  $g_s$  (Barbour and Farquhar, 2000, Grams et al., 2007). However, in natural environments,  $\delta^{13}\text{C}$  and  $\delta^{18}\text{O}$  can be influenced by many factors in addition to  $A$  and  $g_s$ , therefore obscuring relationships that may exist between biomass accumulation and the two isotopes (Katul et al., 2000). In addition, while  $A$  and biomass accumulation are clearly related, other factors also affect their correlation (Wong et al., 1985, Ehleringer and Cerling, 1995, Dawson et al., 2004). We conducted a field study under natural conditions to examine the extent to which temporal variations in annual aboveground biomass increment of a single species are related to  $\delta^{13}\text{C}$  and  $\delta^{18}\text{O}$  in annual rings.

The theory and practical interpretation behind carbon isotopes in plant material has been well established (see Appendix A: Stable Isotope Theory for details). Carbon isotopes are frequently used to estimate an integrated measure of photosynthesis relative to stomatal conductance ( $A/g_s$ ), which is a measure of the intrinsic water use efficiency – iWUE) (Farquhar et al., 1989, Lloyd and Farquhar, 1994, Feng and Epstein, 1995, Bert et al., 1997, Duquesnay et al., 1998). Unlike  $\delta^{13}\text{C}$ , the interpretation of  $\delta^{18}\text{O}$  largely

remains uncertain because variation can be caused through several independent mechanisms (see Appendix A). The  $\delta^{18}\text{O}$  of plant material can be influenced by differences in  $\delta^{18}\text{O}$  of source water, variation in  $\delta^{18}\text{O}$  of water vapor in the air, and the evaporative gradient at sites of evaporation inside the leaf (Barbour, 2007a). With careful study design, some of these sources of variation can be eliminated. For example, if source water for trees in close proximity to each other is the same, then inter-tree variation in cellulose  $\delta^{18}\text{O}$  ( $\delta^{18}\text{O}_{\text{cell}}$ ) is due to tree physiological processes. A growing number of studies have reported that when plants have the same water source, variation in  $\delta^{18}\text{O}_{\text{cell}}$  is correlated with  $g_s$  (Flanagan et al., 1991, Barbour and Farquhar, 2000, Barbour et al., 2000, Siegwolf et al., 2001, Barbour et al., 2004, Farquhar et al., 2007).

Because  $^{18}\text{O}$  enrichment in tree ring cellulose is influenced by  $g_s$  (and evaporative demand) and not by photosynthesis, the combined analysis of  $\delta^{13}\text{C}$  and  $\delta^{18}\text{O}$  has the potential to elucidate whether shifts in  $i\text{WUE}$  ( $A/g_s$ ) are the result of shifts in the tree's photosynthetic capacity or shifts in  $g_s$  driven by environmental variables. Studies examining the relationship between  $\delta^{13}\text{C}$  and  $\delta^{18}\text{O}$  largely have used a qualitative approach that describes the long-term effects of environmental factors on leaf-level gas exchange (Saurer et al., 1997, Brandes et al., 2006, Scheidegger et al., 2000). Scheidegger et al. (2000) provided a conceptual model for deducing changes in  $g_s$  and average maximum net photosynthesis ( $A_{\text{max}}$ ) through examining the isotopic shifts in tree ring cellulose through time (Figure 4-1). Changes in environmental conditions from one time period (in our case, represented by annual tree rings) to the next can cause higher ( $\uparrow$ ), lower ( $\downarrow$ ) or similar ( $\approx$ )  $\delta^{13}\text{C}$  and  $\delta^{18}\text{O}$  values (Scheidegger et al., 2000, Saurer and Siegwolf, 2007). The assumptions of the Scheidegger model are: 1) changes in  $\delta^{18}\text{O}_{\text{cell}}$  is primarily due to changes in leaf water enrichment caused by variation in air humidity between time periods, 2) the  $\delta^{18}\text{O}$  of source water and water vapor is the same between investigation periods, and 3) a negative relationship exist between  $\delta^{13}\text{C}_{\text{cell}}$  and  $[\text{CO}_2]$  inside the stomatal cavity ( $c_i$ ). Based on these assumptions, the model predicts "the most likely case" for the response of  $g_s$  and  $A_{\text{max}}$  (Scheidegger et al., 2000).

Recently, more quantitative approaches have been employed to explore the relationship between  $\delta^{18}\text{O}_{\text{cell}}$  and  $g_s$ . Using  $\delta^{13}\text{C}$  and  $\delta^{18}\text{O}$  of leaf cellulose, Grams et al., (2007), demonstrated that under controlled environmental conditions, reductions in  $g_s$

was associated with increases in  $\delta^{18}\text{O}$  of leaf cellulose in juvenile *Fagus* and *Picea* trees. The direct relationship between  $g_s$  and  $\delta^{18}\text{O}_{\text{cell}}$  was further inferred by Brooks and Coulombe (2009). By examining pre- and post- treatment  $\delta^{18}\text{O}_{\text{cell}}$  and  $\delta^{13}\text{C}_{\text{cell}}$  in contrast to control  $\delta^{18}\text{O}_{\text{cell}}$  and  $\delta^{13}\text{C}_{\text{cell}}$ , Brooks and Coulombe (2009) estimated that  $g_s$  was reduced by 30 % in the dry, late growing season as a result of increased leaf area following nitrogen fertilization in a Douglas-fir plantation. In addition, Marshall and Monserund (2006) found consistent differences in  $\delta^{18}\text{O}_{\text{cell}}$  over several decades between competing tree species growing in the same environmental conditions. The authors hypothesized that the differences in  $\delta^{18}\text{O}_{\text{cell}}$  may have been a result of changes in leaf function (such as changing  $g_s$ ) with tree size and age, or that competing species used water from depths of the soil that had distinct isotopic differences. While it is clear that the interpretation of  $\delta^{18}\text{O}_{\text{cell}}$  and  $\delta^{13}\text{C}_{\text{cell}}$  works under highly controlled conditions, the technique still has potential for further development in less controlled settings.

One possible way to improve our understanding of the linkage between  $\delta^{18}\text{O}_{\text{cell}}$  and  $\delta^{13}\text{C}_{\text{cell}}$  in less controlled environments is to use our understanding of within stand competition between trees, and known environmental gradients within canopies. For example,  $\delta^{13}\text{C}_{\text{cell}}$  has been found to increase with increasing vapor pressure difference and irradiance (Farquhar et al., 1989, Francey and Farquhar, 1982). Both of these factors can vary throughout the canopy profile and between crown dominance classes. In addition, dominant trees within a stand tend to increase in the use of resources (i.e., water, light, nutrients) as forest stand develop and, in some cases, dominant trees use these resources more efficiently than intermediate or suppressed trees (Oliver and Larson, 1990, Smith and Long, 2001, Binkley et al., 2002).

Here we apply a dual isotope ( $^{13}\text{C}$  and  $^{18}\text{O}$ ) approach to infer physiological response of trees to changing environmental conditions. Our specific objectives were to 1) to test the hypothesis that aboveground net primary production is related to the product of  $A/g_s$  (derived from  $\delta^{13}\text{C}_{\text{cell}}$ ) and  $g_s$  (derived from  $\delta^{18}\text{O}_{\text{cell}}$ ), 2) to examine how  $\delta^{13}\text{C}_{\text{cell}}$  and  $\delta^{18}\text{O}_{\text{cell}}$  responds to environmental variations with regard to crown dominance within a stand, and 3) to compare our observed values of  $\delta^{13}\text{C}_{\text{cell}}$  and  $\delta^{18}\text{O}_{\text{cell}}$  to a qualitative conceptual model of the  $^{13}\text{C}$ - $^{18}\text{O}$  relationship as presented in Scheidegger et al. (2000). We used natural environmental gradients in a steep catchment dominated by a single

species to maximize variation in aboveground net primary production, while at the same time reducing the isotopic variation in source water and source CO<sub>2</sub>.

## Methods

### *Study site*

The study area was a 96 ha watershed (Watershed One - WS1), located in the H J Andrews Experimental Forest (HJA) in the western Cascades of central Oregon, USA (44.2 °N, 122.2 °W) (Figure 4-2). Elevations in WS1 range from 430 m at the watershed gauging station to a maximum of 1010 m at the eastern ridge line. The HJA is part of the Long Term Ecological Research program and has a continuous meteorological data record from 1958 to the present. The watershed is predominately covered by young, mature Douglas-fir (*Pseudotsuga menzeii* (Mirb.) Franco) replanted following clear-cut harvesting in the late 1960s and contains smaller components of western hemlock (*Tsuga heterophylla* (Raf.) Sarg) and hardwood species (Moore et al., 2004). At the time of our study, the maximum height of canopy ranged from approximately 22 to 31 m. The HJA has a Mediterranean climate, with wet, mild winters and dry summers. Average annual rainfall is 2220 mm, of which about 80% falls between October and April (Rothacher et al., 1967). Soils have Andic properties, and are silty loam to gravelly clay loam in texture (Swanson and James, 1975a). Perpendicular to the axis of the valley, a transect of eight plots (four on each slope) with a radius of 10 m were established in the spring of 2005 (Figure 4-2).

### *Tree ring sampling and processing*

To maximize the differences in crown class within each study plot and in local environment within the watershed, six trees within each study plot (three south facing plots and two north facing plots) were selected by establishing six rays uniformly distributed around the plot center and selecting a tree along that ray from within the randomly assigned dominance class (two from each crown class: dominant, co-dominant and intermediate). For each tree, diameter at breast height (DBH) and height were measured, and four 5-mm cores were obtained from the four cardinal directions near

chest height. DBH was measured using diameter tape while standing on the uphill side of tree at a height of 1.4 m.

We selected an eight-year period (2000-2007) for isotopic analysis because these years contained a large range of year to year environmental variation and had the advantage of concurrent auxiliary data collected in 2005 and 2006. Ring widths were measured along the entire core (~1974 to 2007). Cores were sanded only enough to clearly observe earlywood and latewood boundaries. All cores were aged and cross-dated using marker rings to insure accurate dating. We measured ring width using a tree-ring analysis system (WinDENDRO, Reg 2005c, Regent Instruments Inc. Quebec, Canada) attached to a digital scanner (Epson Expression, 10000 XL supplied and calibrated by Regent Instruments). Cores were scanned at 2400 dpi and measured for annual ring boundaries to 0.001 mm accuracy. Each tree-ring image was visually inspected and manually adjusted for accurate boundary detection. To verify the ring widths measurements made using WinDendro, we measured a subset of the tree cores using traditional unislide-linear measurement equipment (Velmex, Inc, Bloomfield, NY, USA). Ring width measurements from the two methods were comparable and averaged within 1% of each other (n=131 rings). Basal area increment (BAI) was estimated using diameter measurements adjusted for bark thickness, and the average ring-width of the 4 cores from each tree.

Recent studies have suggested that earlywood in tree rings is synthesized, at least partially, from stored photosynthates that were assimilated during the previous year(s) and as a result, stable isotopes in earlywood may not be representative of current physiological process; whereas, latewood is formed almost entirely from current photosynthate (Helle and Schleser, 2004, McCarroll and Loader, 2004). As well, environmental conditions can change markedly between the early and late growing season which could obscure the relationship between isotopes and environmental variables if combined in one isotopic measurement per annual ring. For these reasons, we separated earlywood from latewood within each annual ring. Earlywood was distinguished from latewood by change in color and wood density. After cores were dated and measured, each year for each core was cut into early- and latewood sections and combined into one early and one late sample per year, per tree (5 plots x 6 trees x 8

years x 2 wood densities). Samples were ground to a fine power using a ball mill (Spex 5300, Metuchen, New Jersey, USA). Due to the size of many samples being insufficient for isotopic analysis, ground samples from the two trees within a crown class in the same plot were combined in equal amounts. All 240 samples (5 plots x 3 crown classes x 8 years x 2 wood densities) were extracted to  $\alpha$ -cellulose (Leavitt and Danzer, 1993, Sternberg, 1989).

### *Xylem water sampling*

We sampled water from the xylem of trees within each study plot to determine if the  $\delta^{18}\text{O}$  of the source water spatially varied. Xylem water was assumed to reflect soil source water from because trees do not fractionate water during uptake (White et al., 1985, Dawson, 1993). At each plot, xylem samples were collected from suberized branches located in the sunlit, upper half of the canopy of 3 trees. Samples were collected every 3 weeks throughout the growing seasons during 2006. Xylem samples were collected in glass vials with polyseal cone inserts in the cap and sealed to prevent evaporation. Water was extracted from the samples using cryogenic vacuum distillation (Ehleringer et al., 2000).

### *Isotope analysis*

Stable isotope composition of the  $\alpha$ -cellulose was measured on 0.3-2.5 mg subsamples that were either combusted in an elemental analyzer (ECS 4010, Costech, Valencia, CA) for  $\delta^{13}\text{C}$ , or pyrolyzed in a high temperature conversion elemental analyzer (TC/EA ThermoQuest Finnigan, Bremen Germany) for  $\delta^{18}\text{O}$  and the resulting gases were analyzed on an isotope ratio mass spectrometer (IRMS, Finnigan MAT Delta Plus XL or XP, Bremen, Germany) located at the Integrated Stable Isotope Research Facility at the Western Ecology Division of the EPA, Corvallis Oregon. Xylem water samples were also analyzed for  $\delta^{18}\text{O}$  using the TC/EA and IRMS. All  $\delta^{13}\text{C}$  and  $\delta^{18}\text{O}$  values are expressed relative to their respective standard (PDB, V-SMOW) in ‰:

$$\delta = \left( \frac{R_{\text{sample}}}{R_{\text{standard}}} - 1 \right) 1000 \quad (1)$$

where R is the ratio of  $^{13}\text{C}$  to  $^{12}\text{C}$  atoms or  $^{18}\text{O}$  to  $^{16}\text{O}$  atoms of the sample and the standard. Measurement precision was better than 0.1 ‰ for  $\delta^{13}\text{C}$  and 0.25 ‰ for  $\delta^{18}\text{O}$  as determined from repeated measure of internal QC standards and from sample replicates.

#### *Environmental variables*

Because environmental variables theoretically influence tree ring isotopes, we measured canopy air temperature (T) and relative humidity (RH) in each study plot. At each plot, T and RH were measured at mid-canopy (HMP45c, Campbell-Scientific Inc.) and recorded by a datalogger (CR23X, Campbell-Scientific Inc.) every 15 s and averaged over 15 minute intervals. Plot-specific T and RH data were not available prior to 2005; therefore, we used long-term meteorological data sets provided by the Forest Science Data Bank (a partnership between Oregon State University and the U.S. Forest Service Pacific Northwest Research Station) to predict T and RH for 2000 to 2005. Long-term data (T, RH, and precipitation) were available from a nearby weather station (HJA Primary Meteorological Station (PRIMET)) located within 0.75 km of the study area. To predict T and RH for each plot for years prior to 2005, we used the linear relationship between simultaneous measurements made at PRIMET versus each plot individually during 2005 and 2006, and used the calculated linear relationships to predict plot level T and RH ( $R^2$  ranged from 0.92 to 0.99 for T, and 0.81 to 0.93 for RH).

#### *Estimating $g_s$ from environmental data and $\delta^{18}\text{O}$ data*

We followed methods similar to Brooks and Coulombe (2009) to calculate relative changes in  $g_s$  from  $\delta^{18}\text{O}$  values of xylem water and  $\delta^{18}\text{O}_{\text{cell}}$  using steady-state models for estimating the enrichment of bulk leaf water above source water ( $\Delta^{18}\text{O}_l$ ) and  $g_s$ . For each year, we divided plot-level environmental data into two time periods that were assumed to represent environmental conditions during earlywood and latewood growth conditions. Earlywood environmental conditions were equal to the average T and RH for April through mid-July, and latewood conditions were defined as occurring from mid-July through the end of September each year. Only T and RH from 0700 to 1400 each day were used to calculate the average for each time period because leaf level physiological processes ( $A$  and  $g_s$ ) are most active during this time period.

First, we used measured values of the enrichment of cellulose  $^{18}\text{O}$  above source water ( $\Delta^{18}\text{O}_{\text{cell}}$ ) of equation 8 (Appendix A) to estimate  $\Delta^{18}\text{O}_l$ . Once we estimated  $\Delta^{18}\text{O}_l$  for both earlywood and latewood for each crown class within each plot, we back calculated  $g_s$  values using  $e^*$ ,  $e_a/e_i$ ,  $g_b$ ,  $L$ , and vapor pressure deficit (VPD). We used the environmental data to calculate  $e_a/e_i$  and used the equations in Barbour (2007a) to estimate  $\varepsilon^*$  and equation 5 (Appendix A) to estimate  $\varepsilon_k$  where  $g_b$  was estimated as 2 (Brooks and Coulombe, 2009). We used values from Brooks and Coulombe (2009) for  $L$  (3.25 cm) and estimated  $\varepsilon_o$  to equal 27. Following Brooks and Coulombe (2009) methods, we expanded equation 6 (Appendix A) with equation 4, 5, and 7 and represented  $E$  as  $g_s \cdot \text{VPD}$  to express  $\Delta^{18}\text{O}_l$  as a function of  $g_s$  and then solved for  $g_s$  using a nonlinear procedure (PROC NLIN) in SAS (Version 9.1, Cary, NC, USA).

*Estimating  $A$  from  $\delta^{13}\text{C}_{\text{cell}}$  and  $g_s$  derived from  $\delta^{18}\text{O}_{\text{cell}}$*

We calculated isotope derived values of  $A$  to compare with estimates of aboveground net primary production. To do this, we first calculated  $^{13}\text{C}$  discrimination using equation 1, Appendix A (where  $\delta_{\text{plant}}$  is equal to  $\delta^{13}\text{C}_{\text{cell}}$ ). We assumed  $\delta_a$  to be -8‰ (Farquhar et al., 1989). Next, we calculated  $c_i$  by re-arranging equation 2 (Appendix A) and set  $c_a$  equal to 360 ppm. Using equation 3, we calculated  $A/g_s$  from our estimates of  $c_i$  and  $c_a$ . Last, we multiplied  $A/g_s$  derived from  $\delta^{13}\text{C}_{\text{cell}}$  by  $g_s$  derived from  $\delta^{18}\text{O}_{\text{cell}}$ .

*Aboveground biomass and leaf area estimates*

We used aboveground biomass increment (BMI) as a proxy for annual aboveground net primary production. We estimated BMI and leaf area ( $A_L$ ) for each of the cored trees for the years 2000-2007. We estimated DBH for the years prior to 2007 by subtracting all radial growth that occurred after the target year of interest. BMI and leaf mass were estimated using DBH-dependent allometric equations specific to Douglas-fir from Gholz et al. (1979). We estimated  $A_L$  by multiplying the leaf mass predicted from the Gholz et al. (1979) equations by a published ratio of  $A_L$  to leaf mass ( $\text{cm}^2/\text{g}$ ) which is equal to 60 (Waring et al., 1980, Binkley, 1984).

### *Foliar Nitrogen*

Because nitrogen content is strongly correlated with foliar  $\delta^{13}\text{C}$  and photosynthetic capacity, we examined the variability in foliar nitrogen content within our experimental plots (Duursma and Marshall, 2006). We sampled current-year and one-year-old foliage from the upper half of the canopy from three trees in each of plots sampled for tree cores in August of 2005 and 2006. All samples were ground to a fine powder using a mortar and pestle and then air dried. For each sample, up to 2 g of ground material was analyzed for carbon and nitrogen content. Analyses were performed using a CNS analyzer (CNS-2000 Macro Analyzer, Leco Corp., St. Joseph, MI, USA), which simultaneously determines carbon and nitrogen content of the solid samples.

### *Application of the Scheidegger Conceptual Model*

We used the conceptual framework proposed by Scheidegger et al. (2000) to evaluate  $\delta^{13}\text{C}_{\text{cell}}$  and  $\delta^{18}\text{O}_{\text{cell}}$  differences found in our samples to the theoretical predictions in  $g_s$  and  $A$  based on the two isotopes (Figure 4-1). We used this framework to examine how the theoretical physiology responded to dominance class, to changes in RH over time, to spatial differences in leaf nitrogen, and to seasonal changes. For each analysis, we normalized the isotope data differently to eliminate other sources of variance. First, we examined how the dominance classes differed from a grand mean for each isotope for the early and late season. For each season, we calculated a mean for all years, all plots and crown classes (separate means for early and latewood), then subtracted that mean from the individual  $\delta^{13}\text{C}_{\text{cell}}$  or  $\delta^{18}\text{O}_{\text{cell}}$  values. We used Pearson's correlation coefficients to quantify the relationship between  $\delta^{13}\text{C}_{\text{cell}}$  and  $\delta^{18}\text{O}_{\text{cell}}$  difference of the mean for each tree crown class. If  $A_{\text{max}}$  is constant throughout the eight years of our time series, we expect that there will be a positive correlation between  $\delta^{13}\text{C}_{\text{cell}}$  and  $\delta^{18}\text{O}_{\text{cell}}$  difference from the means as result of changing  $g_s$ , because  $\delta^{18}\text{O}_{\text{cell}}$  becomes enriched when  $g_s$  declines, but if  $A_{\text{max}}$  remains the same then  $A/g_s$  and thus  $\delta^{13}\text{C}_{\text{cell}}$  would be higher based on current isotope theory. We regarded a negative relationship between  $\delta^{13}\text{C}_{\text{cell}}$  and  $\delta^{18}\text{O}_{\text{cell}}$  to represent a change in photosynthetic capacity.

Because RH varied temporally but not spatially, we normalize isotope values for each crown class within each study plot with respect to time. For each crown class

within each study plot, we calculated the mean of all eight year for each isotope (again, separate means for early- and latewood). We then subtracted the mean from each individual year's isotope value. We ranked the mean RH for each year (separate RH for each season) into three classes: high, medium and low) and assigned those classes to the samples. Last, we examined the relationship between normalized  $\delta^{13}\text{C}_{\text{cell}}$  and  $\delta^{18}\text{O}_{\text{cell}}$  within the conceptual framework of the Scheidegger model.

Since we only had leaf nitrogen values for 1 year, we had spatial nitrogen data and not temporal nitrogen data. We made the assumption that although the absolute value of N content is likely to change from one year to the next within a single sample plot the relative ranking between sample plots is likely to stay the same through time in a closed canopy forest such as our study site (Powers and Reynolds, 1999, R. Powers personal communication 2009). Thus, we normalized the data to minimize temporal variance and emphasize spatial variance. We calculated a mean  $\delta^{13}\text{C}_{\text{cell}}$  and mean  $\delta^{18}\text{O}_{\text{cell}}$  for each of the eight years for each dominance class (separate late- and earlywood means) and subtracted those from the appropriate  $\delta^{13}\text{C}_{\text{cell}}$  and  $\delta^{18}\text{O}_{\text{cell}}$  values. We ranked the study plots by their foliar N content from low to high and assigned the N-ranking to all tree ring samples from a given plot. We calculated the correlation between  $\delta^{13}\text{C}_{\text{cell}}$  difference from the mean and N rank. Within the context of the conceptual model, we anticipated that samples more enriched with  $^{13}\text{C}$  would correspond with higher foliar N content.

Last, we calculated the difference between late- and earlywood values of both  $\delta^{13}\text{C}_{\text{cell}}$  and  $\delta^{18}\text{O}_{\text{cell}}$  to examine if shifts in the isotopic composition might be explained by seasonal changes in  $g_s$ . Pypker et al. (2008) observed seasonal declines in canopy conductance in the same plots where our measurements were taken. If declines in  $g_s$  were responsible for isotopic shifts between late- and earlywood, we would expect both isotopes to be more enriched in latewood relative to earlywood and for a positive correlation between the two isotopes. We plotted the difference between late- and earlywood values of both isotopes against each other to visually examine the relationship within the Scheidegger framework.

### *Statistics*

We performed repeated measures ANOVA to determine differences in  $\delta^{13}\text{C}_{\text{cell}}$ ,  $\delta^{18}\text{O}_{\text{cell}}$ , and BAI with respect to time and Sidak Multiple Comparisons tests to determine differences between crown classes (Ott, 1993). We examined the relationship between climate variables and shifts in isotopic composition by using Pearson product-moment correlation analysis. Because we were interested in the shifts in isotope values and not absolute values for correlations, we normalized isotope values for plot level differences by subtracting the mean isotope value for all eight years within a given plot from each individual value. All statistics were performed using SPSS (Version 15.0, SPSS Inc. Chicago, IL, USA).

### **Results**

#### *Time series of $\delta^{13}\text{C}_{\text{cell}}$ , $\delta^{18}\text{O}_{\text{cell}}$ , and BAI*

The isotopic composition of earlywood samples was relatively consistent over time for  $\delta^{13}\text{C}_{\text{cell}}$  ( $p = 0.37$ ) with little variability between crown classes (Figure 4-3 G), and even though the temporal patterns of  $\delta^{18}\text{O}_{\text{cell}}$  appear to vary with time, the pattern was not significant (Figure 4-3 E,  $p = 0.46$ ). The changes in isotopic composition with respect to time were not significant ( $p = 0.37$  and  $0.46$  for  $\delta^{13}\text{C}_{\text{cell}}$  and  $\delta^{18}\text{O}_{\text{cell}}$ , respectively). Crown class was not significant in determining the response of isotopic composition with regard to time ( $p = 0.51$  and  $0.95$  for  $\delta^{13}\text{C}_{\text{cell}}$  and  $\delta^{18}\text{O}_{\text{cell}}$ , respectively). Post-hoc comparisons using Sidak Multiple Comparisons test indicated that mean isotopic composition between the three crown classes was not significantly different for both  $\delta^{13}\text{C}_{\text{cell}}$  and  $\delta^{18}\text{O}_{\text{cell}}$  ( $p = 0.35$  to  $0.97$  for all comparisons).

The isotopic composition of latewood cellulose changed significantly through time for both  $\delta^{13}\text{C}_{\text{cell}}$  and  $\delta^{18}\text{O}_{\text{cell}}$  (Figure 4-3F, H). Both isotopes significantly increased between 2001 and 2002, and significantly decreased from 2003 to 2004 ( $p < 0.05$  for all comparisons). These changes negatively corresponded with shifts in mean RH, where both  $\delta^{13}\text{C}_{\text{cell}}$  and  $\delta^{18}\text{O}_{\text{cell}}$  increased when RH declined and  $\delta^{13}\text{C}_{\text{cell}}$  and  $\delta^{18}\text{O}_{\text{cell}}$  decreased when RH increased (Figure 4-3D). All three crown classes had the same pattern in isotopes over time for both  $\delta^{13}\text{C}_{\text{cell}}$  and  $\delta^{18}\text{O}_{\text{cell}}$  ( $p = 0.56$  and  $0.33$ , respectively). Post-hoc comparisons indicated that mean  $\delta^{18}\text{O}_{\text{cell}}$  of dominant trees was significantly greater

than the mean of co-dominant trees ( $p = 0.02$ ); however, no differences were detected between dominant trees and intermediate trees ( $p = 0.32$ ) or between co-dominant and intermediate trees ( $p = 0.33$ ). Differences in mean  $\delta^{13}\text{C}_{\text{cell}}$  between crown classes were not significant ( $p = 0.66$ ).

Basal area increment was remarkably consistent over time in spite of large year to year variation in precipitation (Figure 4-4). Basal area increment significantly increased from 2003 to 2004 ( $p = 0.04$ ). The changes in BAI with respect to time did not differ among the three crown classes ( $p = 0.87$ ). However, as expected the crown classes grew at significantly different rates ( $p = 0.03$ ). Post-hoc comparisons indicated that BAI of dominant trees was significantly greater than that of intermediate trees ( $p = 0.04$ ); however, no differences were detected between dominant trees and co-dominant trees ( $p = 0.14$ ) or between co-dominant and intermediate trees ( $p = 0.84$ ).

#### *A derived from $\delta^{13}\text{C}_{\text{cell}}$ and $\delta^{18}\text{O}_{\text{cell}}$ versus BMI*

We examined the relationship between  $A$  derived from  $\delta^{13}\text{C}_{\text{cell}}$  and  $\delta^{18}\text{O}_{\text{cell}}$  and estimates of BMI across the three dominance classes of trees for all sample years. Not every unit of foliage contributes to net primary production equally; therefore, the functional leaf area (the amount of leaf area that is contributing the most to net primary production) is less than total leaf area of a tree (Cermak, 1989, Brooks et al., 2003). Because the functional leaf area for each of the trees is not known, we did not attempt to scale results from  $A$  derived from  $\delta^{13}\text{C}_{\text{cell}}$  and  $\delta^{18}\text{O}_{\text{cell}}$  from the leaf to the tree level. Instead, we examined values of both isotope derived  $A$  (for both earlywood and latewood) and BMI relative to their maximum computed value (Figure 4-5 A-B). Because isotope derived  $A$  is calculated at the leaf-level scale, we also examined the relationship between isotope derived  $A$  and BMI per unit leaf area ( $\text{kg m}^{-2}$ , Figure 6 C-D).

The mean  $\delta^{18}\text{O}$  of the source water, as indicated by xylem water, did not vary spatially during the 2006 growing season. The difference in mean  $\delta^{18}\text{O}$  of the source water between sample plots was less than the analytical precision of the measurement and the mean  $\delta^{18}\text{O}$  of the source water ranged from -10.73 to -10.51 ‰. Our analysis assumed that all sample years were similar to 2006 and  $\delta^{18}\text{O}$  of the source water did not

vary spatially. This assumption is backed by annual estimates of precipitation  $\delta^{18}\text{O}$  based on weekly precipitation isotope measurements in Corvallis, OR. Annual estimates over six years from Corvallis, OR, did not vary over 1 ‰, and xylem water analysis from a nearby watershed averaged 10.4 ‰ in both 2004 and 2005 (J. R. Brooks, unpublished data).

For earlywood, we found isotope derived  $A$  to be significantly correlated to BMI only for dominant trees ( $r = 0.36$ ,  $p = 0.02$ ). Isotope derived  $A$  was not significantly correlated to BMI per unit leaf area for any crown class ( $r = 0.06$  to  $0.22$ ,  $p = 0.20$  to  $0.71$ ). For latewood, isotope derived  $A$  from dominant trees was significantly correlated to both BMI ( $r = 0.54$ ,  $p < 0.01$ ) and BMI per unit leaf area ( $r = 0.37$ ,  $p = 0.02$ ). Co-dominant and intermediate trees had a significant correlation between isotope derived  $A$  and BMI ( $r = 0.55$ ,  $p < 0.01$ ,  $r = 0.45$ ,  $p < 0.01$ , respectively), the relationships were not significant when correlating isotope derived  $A$  and BMI per unit leaf area ( $r = 0.23$ ,  $p = 0.17$ ,  $r = 0.17$ ,  $p = 0.31$ , respectively).

#### *Correlations between environmental variables and $\delta^{13}\text{C}_{\text{cell}}$ , $\delta^{18}\text{O}_{\text{cell}}$ , and BAI*

Table 4-1 presents Pearson's correlation coefficients and p-values for environmental variables, tree ring normalized isotopes, and BAI. Given the relatively small sample size ( $N \leq 40$ ), significant correlations are identified at both the  $\alpha = 0.05$  and  $\alpha = 0.10$  level. Earlywood  $\delta^{13}\text{C}_{\text{cell}}$  for all crown classes increased with decreased early season RH. This relationship was the strongest for co-dominant trees ( $r = -0.65$ ), and weakest for intermediate trees ( $r = -0.31$ ). Normalized, earlywood  $\delta^{18}\text{O}_{\text{cell}}$  also increased with decreased early season RH for dominant and co-dominant trees, but the relationship was not significant for intermediate trees. Earlywood  $\delta^{18}\text{O}_{\text{cell}}$  also tended to increase with decreased summer PPT for all crown classes. Data did not indicate that early season T, annual PPT, or BAI were valuable indicators of shifts in isotopic composition in earlywood cellulose.

Latewood isotope values were also significantly correlated with RH. However, isotopes of intermediate trees did not have a significant relationship with RH (Figure 4-7). For the dominant and co-dominant crown classes, both  $\delta^{13}\text{C}_{\text{cell}}$  and  $\delta^{18}\text{O}_{\text{cell}}$  increased with decreased late season RH and decreased summer PPT. In addition,  $\delta^{13}\text{C}_{\text{cell}}$  increased

with increased late season T for dominant and co-dominant trees ( $p < 0.01$  and  $0.08$ , respectively).

We did not find any isotopic value or environmental variable with the exception of late season T to be significantly related to BAI indicating that stable isotope values in tree ring cellulose are more sensitive to environmental variables than growth.

#### *Conceptual Model of $\delta^{13}\text{C}_{\text{cell}}$ and $\delta^{18}\text{O}_{\text{cell}}$ relationships*

The  $\delta^{13}\text{C}_{\text{cell}}$  increased with increased  $\delta^{18}\text{O}_{\text{cell}}$  for both earlywood and latewood samples (but not always significantly) across all crown classes (Figure 4-6). Dominant trees had the strongest correlation for both earlywood and latewood ( $r = 0.43$  and  $0.53$ , respectively and  $p < 0.01$  for both correlations, Figure 4-6 A, D). The strength of the relationship between  $\delta^{13}\text{C}_{\text{cell}}$  and  $\delta^{18}\text{O}_{\text{cell}}$  varied between earlywood and latewood for co-dominant and intermediate trees. For earlywood, the correlation was not significant for co-dominant trees ( $r = 0.20$ ,  $p = 0.22$ ), but intermediate trees were significant ( $r = 0.39$ ,  $p = 0.02$ ). For latewood, co-dominant trees were significantly correlated ( $r = 0.38$ ,  $p = 0.02$ ), but intermediate trees were not ( $r = 0.14$ ,  $p = 0.41$ ). According to the Scheidegger model, a positive correlation between  $\delta^{13}\text{C}_{\text{cell}}$  and  $\delta^{18}\text{O}_{\text{cell}}$  indicates that  $A$  was relatively stable regardless of changes in  $g_s$  through time and space for a crown class. This interpretation is because  $\delta^{18}\text{O}_{\text{cell}}$  becomes enriched when  $g_s$  declines, but if  $A$  remains the same then  $A/g_s$  and thus  $\delta^{13}\text{C}_{\text{cell}}$  would be higher based on isotope theory. We regarded a negative relationship between  $\delta^{13}\text{C}_{\text{cell}}$  and  $\delta^{18}\text{O}_{\text{cell}}$  to represent a change in photosynthetic capacity over time and space and not stomatal limitations on photosynthesis.

Foliar nitrogen content ranged from 0.88 % to 1.11 % for 1-yr-old foliage and from 0.69 to 1.13 % for current yr foliage (Table 4-2). Both dominant and intermediate trees demonstrated a significant relationship between  $\delta^{13}\text{C}_{\text{cell}}$  and the rank of foliar N content, where  $\delta^{13}\text{C}_{\text{cell}}$  was more enriched relative to the mean when foliar N was higher (Figure 4-8). Correlation coefficients for dominant trees were 0.58 ( $p < 0.01$ ) and 0.63 ( $p < 0.01$ ) for earlywood and latewood, respectively. Intermediate sized trees had increased  $\delta^{13}\text{C}_{\text{cell}}$  with higher foliar N content in both earlywood ( $r = 0.72$ ,  $p < 0.01$ ) and latewood ( $r = 0.70$ ,  $p < 0.01$ ). Surprisingly, in co-dominant trees,  $\delta^{13}\text{C}_{\text{cell}}$  was not related to foliar N content in earlywood ( $r = 0.10$ ,  $p = 0.57$ ) or latewood ( $r = -0.08$ ,  $p = 0.63$ ).

We calculated the difference between late- and earlywood values of both  $\delta^{13}\text{C}_{\text{cell}}$  and  $\delta^{18}\text{O}_{\text{cell}}$  to determine if shifts in the isotopic composition might be explained by seasonal changes in  $g_s$ . Pypker et al. (2008) observed seasonal declines in canopy conductance in the same plots where our measurements were taken. If declines in  $g_s$  were responsible for isotopic shifts between late- and earlywood, we would expect both isotopes to be more enriched in latewood relative to earlywood and a positive correlation between the two isotopes. In the dominant crown class, practically every sample latewood  $\delta^{13}\text{C}_{\text{cell}}$  was enriched compared to the earlywood values, indicating that the dominant trees became more water-use efficient in the late season. In addition, 68 % of the latewood  $\delta^{18}\text{O}_{\text{cell}}$  were enriched relative to the earlywood values, indicating most dominant trees experienced a decline in stomatal conductance over the growing season. A positive relationship existed between the two isotopes ( $r = 0.30$ ,  $p = 0.06$ , Figure 4-9), indicating that water-use efficiency increased more with decreasing stomatal conductance which kept  $A$  relatively constant through the season. Interestingly, Co-dominant trees did not show a consistent increase in water-use efficiency or in stomatal closure through the season. Similarly to dominant trees, intermediate trees tended to increase water use efficiency over the growing season and decrease stomatal conductance.

## Discussion

*Can  $^{13}\text{C}$  and  $^{18}\text{O}$  be used to estimate aboveground net primary production?*

Recent experimental studies demonstrated that enrichment in  $\delta^{18}\text{O}$  leaf cellulose can be related to reductions in  $g_s$  if source water variation can be accounted for (Barbour et al., 2000, Barbour and Farquhar, 2000, Grams et al., 2007, Brooks and Coulombe, 2009). If  $\delta^{18}\text{O}_{\text{cell}}$  is related to changes in  $g_s$  then  $\delta^{18}\text{O}_{\text{cell}}$  coupled with  $\delta^{13}\text{C}_{\text{cell}}$  can be used to infer temporal changes in gross primary production by the product of  $A/g_s$  (derived from  $\delta^{13}\text{C}_{\text{cell}}$ ) and  $g_s$  (derived from  $\delta^{18}\text{O}_{\text{cell}}$ ). Taking it a step further to net primary productivity assumes a constant fraction for plant respiration as implied by Waring (1994), and similar allocation above and below ground each year. Our results provide weak evidence to support this hypothesis. We found the strongest relationship for all crown classes of trees to be between isotope derived  $A$  and BMI when  $A$  was derived

from latewood isotope values. However, when examining  $A$  derived from latewood versus BMI per unit leaf area, only dominant trees had a significant relationship. Theoretically,  $A$  derived from isotopes would represent the average photosynthetic rate of the canopy that contributed to the carbon in the cellulose. We might expect that dominant trees would have the highest average rate of photosynthesis; however, we found that trees in all crown classes spanned the entire range of calculated  $A$  rates, with the low end being only 40 % of the maximum rates. This variation in  $A$  was not related to annual production in the tree where we clearly saw crown class differences.

There are several reasons why isotope derived  $A$  may not be related to growth. Using  $\delta^{13}\text{C}_{\text{cell}}$  to predict  $A$ , assumes a linear relationship between  $A/g_s$  and  $c_i/c_a$ . As reported by Katul et al. (2000), the use  $\delta^{13}\text{C}_{\text{cell}}$  provides an assimilation-weighted approximation of  $c_i/c_a$ ; however, this approximation does not permit us to examine variability in  $A$  other than that due to  $g_s$ . The non-linear relationship in  $A$  versus  $c_i$  can result in an apparent disconnect between  $\delta^{13}\text{C}_{\text{cell}}$  and  $A$ . In *Pinus taeda*, Katul et al. (2000) found that canopy conductance decreased by two orders of magnitude, whereas  $c_i/c_a$  increased by only 20 %. In addition, McDowell et al. (2005) noted that mesophyll resistance to  $\text{CO}_2$  diffusion from within the stomatal cavity to the chloroplasts reduces the functional  $c_i$  and  $\delta^{13}\text{C}$  of foliar cellulose to be greater than expected from  $A$  and  $g_s$ . All of these differences will contribute to the isotopic composition of tree rings, thereby affecting the ability to use the bio-physiological equations we used to estimate  $A$ . Additional experiments at leaf level relating isotope derived  $A$  to measured net primary production are warranted.

#### *The relationship between $\delta^{13}\text{C}_{\text{cell}}$ , $\delta^{18}\text{O}_{\text{cell}}$ and environmental variables*

The results from this study support the hypothesis that  $\delta^{13}\text{C}_{\text{cell}}$  and  $\delta^{18}\text{O}_{\text{cell}}$  in tree ring chronologies can serve as proxies for a variety of environmental variables; however, our results highlight that stable isotopes in dominant trees were the most responsive to environmental variables. Latewood  $\delta^{13}\text{C}_{\text{cell}}$  and  $\delta^{18}\text{O}_{\text{cell}}$  of dominant trees had a significant correlation with all environmental variables except for annual precipitation. Both earlywood and latewood  $\delta^{13}\text{C}_{\text{cell}}$  and  $\delta^{18}\text{O}_{\text{cell}}$  were negatively correlated with relative humidity for dominant and co-dominant trees. These results are consistent with other

studies, where increases in humidity result in reduced leaf evaporative enrichment of  $^{18}\text{O}$  (Edwards et al., 2000, Barbour et al., 2002, Roden and Ehleringer, 2007). Early studies using  $\delta^{18}\text{O}$  of tree rings were focused on their use as a reconstructive tool for past temperature (Libby et al., 1976). In our study, only latewood of dominant trees were moderately correlated with temperature. Rebetez et al. (2003) noted that  $\delta^{18}\text{O}$  in tree rings was related only to temperature during the time period when the wood is formed.

Our results highlight the potential usefulness of stable isotopes in tree rings to be applied to dendroclimatology and dendrochronology. Tree rings in this study demonstrated relatively uniform growth over the time series and growth was not responsive to variation in environmental variables from one year to the next. Other authors have acknowledged the utility of stable isotopes under similar circumstances (McNulty and Swank, 1995, Robertson et al., 2008, Roden, 2008). Because we did not find BAI to be significantly related to any of the environmental variables that we considered, we conclude that variability in  $\delta^{13}\text{C}_{\text{cell}}$  and  $\delta^{18}\text{O}_{\text{cell}}$  is a more reliable indicator of climate than ring widths in young, Douglas-fir trees.

*Do variations in  $\delta^{13}\text{C}_{\text{cell}}$  and  $\delta^{18}\text{O}_{\text{cell}}$  correspond to the Scheidegger conceptual model?*

Scheidegger et al. (2000) conceptualized the relationship between  $\delta^{13}\text{C}$  and  $\delta^{18}\text{O}$  in plant material where changes in  $\delta^{18}\text{O}_{\text{cell}}$  is primarily due to changes in leaf water enrichment caused by variation in air humidity between time periods. They hypothesize that the  $\delta^{18}\text{O}$  of source water and water vapor is the same between investigation periods and the relationship between  $\delta^{13}\text{C}_{\text{cell}}$  and  $c_i$  is negative. Based on these assumptions, Scheidegger et al. (2000) were able to predict “the most likely case” for the response of  $g_s$  and  $A_{\text{max}}$ . The Scheidegger model provides the means for deducing changes in  $g_s$  and average photosynthesis ( $A$ ) through examining the isotopic shifts in tree ring cellulose through time.

In this study, the relationship between variations in  $\delta^{13}\text{C}_{\text{cell}}$  and  $\delta^{18}\text{O}_{\text{cell}}$  for dominant trees was consistent with the Scheidegger conceptual framework in both earlywood and latewood. We found a strong positive relationship between  $\delta^{13}\text{C}_{\text{cell}}$  and  $\delta^{18}\text{O}_{\text{cell}}$  for dominant trees and can deduce from the conceptual model that  $A_{\text{max}}$  was relatively unaffected through time and the response of  $\delta^{13}\text{C}_{\text{cell}}$  and  $\delta^{18}\text{O}_{\text{cell}}$  is driven by

changes in  $g_s$ . When making comparisons between the  $\delta^{13}\text{C}_{\text{cell}} - \delta^{18}\text{O}_{\text{cell}}$  relationship of earlywood and latewood of dominant trees, it is interesting to note that latewood values fall within a quadrant that represents increased WUE ( $A_{\text{max}}$  remain constant and  $g_s$  declines), whereas earlywood samples are more uniformly distributed. This shift between earlywood and latewood is likely due to seasonal reductions in  $g_s$ .

In addition, we found that foliar N content can be incorporated into the conceptual model to make additional interpretations. For dominant trees, our results indicated that variations in  $\delta^{13}\text{C}_{\text{cell}}$  were strongly related to foliar N content. This is not surprising because it is well documented that high foliar N content generally increases  $A_{\text{max}}$  (Field and Mooney, 1986, Chapin III et al., 2002, Duursma and Marshall, 2006). Our study does not include temporal variations in foliar N; however, our results suggest that temporal measurements of foliar N may aid in interpreting the relationship between  $\delta^{13}\text{C}_{\text{cell}}$  and  $\delta^{18}\text{O}_{\text{cell}}$  within the framework of the conceptual model.

#### *On the importance of stand dominance in tree ring isotope research*

In general, one would expect to find variations in the isotopic composition of tree rings between dominance classes due to vertical gradients in light,  $\delta^{13}\text{C}_{\text{air}}$ , or RH (Elias et al., 1989, Buchmann et al., 1997, Hanba et al., 1997). However, we did not expect to find the differences between dominant and co-dominant trees that we observed. Previous studies have shown that  $\delta^{13}\text{C}$  of leaves becomes more depleted lower in that canopy as light limits photosynthesis, thus decreasing  $A/g_s$  with canopy depth (Duursma and Marshall, 2006, Hanba et al., 1997). The observed decrease in  $\delta^{13}\text{C}$  of leaves has been attributed to increases in  $c_i$  and consequently, increased carbon isotope discrimination with decreases in light (Farquhar et al., 1989, Zimmerman and Ehleringer, 1990). We found that both co-dominant and intermediate trees had lower  $\delta^{13}\text{C}_{\text{cell}}$  in comparison to dominant trees, although differences were not significant. It is reasonable to assume that the canopies of co-dominant and intermediate trees would experience lower light levels than dominant trees and as a result, the integration of leaf  $\delta^{13}\text{C}$  represented by  $\delta^{13}\text{C}_{\text{cell}}$  would be lower.

We observed the biggest difference between dominant trees and other crown classes when examining latewood  $\delta^{18}\text{O}_{\text{cell}}$ . Our results, along with previous studies, show

a strong correlation between  $\delta^{18}\text{O}_{\text{cell}}$  and RH (Edwards et al., 2000, Barbour et al., 2002, Roden and Ehleringer, 2007). If RH alone was responsible for the difference in  $\delta^{18}\text{O}_{\text{cell}}$  between dominant trees and other crown classes, we would infer that the canopy of dominant trees is exposed to lower RH conditions than those of co-dominant or intermediate trees within the same stand. Coniferous forests tend to be well coupled to the atmosphere and we do not expect large vertical gradients of RH to exist in our study plots, especially within the upper canopy, during the daytime (Jarvis et al., 1976, Jarvis and McNaughton, 1986, Monteith, 1995). We hypothesize that the difference in  $\delta^{18}\text{O}_{\text{cell}}$  between dominant trees and other crown classes is due to reductions in  $g_s$ . A reduction of  $g_s$  in dominant trees could be due increased water stress of foliage at the top of the canopy. Stress inducing mechanisms include increased leaf temperature which in turn increases the leaf-to-air vapor pressure deficit and increased limitation to water transport as trees grow taller (Ryan and Yoder, 1997, Martin et al., 1999, Niinemets et al., 2004, Duursma and Marshall, 2006). Our study does not have the required data to suggest which of these mechanisms might be responsible for a decline in  $g_s$  in dominant trees. However, the difference in late- and earlywood  $\delta^{13}\text{C}_{\text{cell}}$  and  $\delta^{18}\text{O}_{\text{cell}}$  in dominant trees within the Scheidegger conceptual model suggests that seasonal reductions in  $g_s$  are at least partially responsible for enrichment in  $\delta^{18}\text{O}_{\text{cell}}$ . Additional work examining the vertical profiles of  $\delta^{18}\text{O}$  of leaf with regard to  $g_s$  is necessary to further our ability to interpret  $\delta^{18}\text{O}_{\text{cell}}$ .

### *Conclusion*

We used natural environmental gradients in a steep catchment dominated by a single species to further our understanding of the relationship between  $\delta^{13}\text{C}_{\text{cell}}$  and  $\delta^{18}\text{O}_{\text{cell}}$ , physiological processes and environmental variables. Our results provide weak evidence to support that  $\delta^{18}\text{O}_{\text{cell}}$  coupled with  $\delta^{13}\text{C}_{\text{cell}}$  can be used to infer temporal changes in net primary production by the product of  $A/g_s$  (derived from  $\delta^{13}\text{C}_{\text{cell}}$ ) and  $g_s$  (derived from  $\delta^{18}\text{O}_{\text{cell}}$ ). The relationship between  $\delta^{18}\text{O}$  of plant material and  $g_s$  versus RH is still subject to investigation and debate (Sheshshayee et al., 2005, Farquhar et al., 2007). Using a qualitative conceptual model of the  $^{13}\text{C}$ - $^{18}\text{O}$  relationship as presented in Scheidegger et al. (2000), we found evidence of  $\delta^{18}\text{O}_{\text{cell}}$  being related to both  $g_s$  and RH;

however, the relationship with RH most apparent. We found that dominant trees behaved differently from sub-dominant trees within the same stand and provide isotopic results that are most consistent with current isotope theory. The correlation of stable isotopes in tree rings with environmental variables can be particularly useful for assessing the impacts of environmental change on vegetation over short time series. However, future studies should pay close attention to tree dominance when sampling tree rings for isotopes and drawing conclusion from data.

## References

- Barbour, M. M. (2007) Stable oxygen isotope composition of plant tissue: a review. *Functional Plant Biology*, **34**, 83-94.
- Barbour, M. M. & Farquhar, G. D. (2000) Relative humidity- and ABA-induced variation in carbon and oxygen isotope ratios of cotton leaves. *Plant, Cell and Environment*, **23**, 473-485.
- Barbour, M. M., Fischer, R. A., Sayre, K. D. & Farquhar, G. D. (2000) Oxygen isotope ratio of leaf and grain material correlates with stomatal conductance and grain yield in irrigated wheat. *Australian Journal of Plant Physiology*, **27**, 625-637.
- Barbour, M. M., Roden, J. S., Farquhar, G. D. & Ehleringer, J. R. (2004) Expressing leaf water and cellulose oxygen isotope ratios as enrichment above source water reveals evidence of a Peclet effect. *Oecologia*, **138**, 426-435.
- Barbour, M. M., Walcroft, A. S. & Farquhar, G. D. (2002) Seasonal variation in  $\delta^{13}\text{C}$  and  $\delta^{18}\text{O}$  of cellulose from growth rings of *Pinus radiata*. *Plant, Cell and Environment*, **25**, 1483-1499.
- Bert, D., Leavitt, S. W. & Dupouey, J.-L. (1997) Variations in wood  $\delta^{13}\text{C}$  and water-use efficiency of *Abies alba* during the last century. *Ecology*, **78**, 1588-1596.
- Binkley, D. (1984) Douglas-fir stem growth per unit leaf area increased by interplanted Sitka alder and red alder. *Forest Science*, **30**, 259-263.
- Binkley, D., Stape, J. L., Ryan, M. G., Barnard, H. R. & Fownes, J. H. (2002) Age-related decline in forest ecosystem growth: An individual-tree, stand-structure hypothesis. *Ecosystems*, **5**, 58-67.
- Brandes, E., Kodama, N., Whittaker, K., Weston, C., Rennenberg, H., Keitel, C., Adams, M. A. & Gessler, A. (2006) Short-term variation in the isotopic composition of organic matter allocated from the leaves to the stem of *Pinus sylvestris*: effects of photosynthetic and postphotosynthetic carbon isotope fractionation. *Global Change Biology*, **12**, 1922-1936.
- Brooks, J. R. & Coulombe, R. (2009) Physiological responses to fertilization recorded in tree rings: isotopic lessons from a long-term fertilization trial. *Ecological Applications* **19**, 1044-1060.
- Brooks, J. R., Schulte, P. J., Bond, B. J., Coulombe, R., Domec, J. C., Hinckley, T. M., McDowell, N. G. & Phillips, N. (2003) Does foliage on the same branch compete for the same water? Experiments on Douglas-fir trees. *Trees*, **17**, 101-108.
- Buchmann, N., Kao, W.-Y. & Ehleringer, J. R. (1997) Influence of stand structure on carbon-13 of vegetation, soils, and canopy air within deciduous and evergreen forests in Utah, United States. *Oecologia*, **110**, 109-119.
- Cermak, J. (1989) Solar equivalent leaf area as the efficient biometrical parameter of individual leaves, trees and stands. *Tree Physiology*, **5**, 269-289.
- Chapin III, F. S., Matson, P. A. & Mooney, H. A. (2002) *Principles of Terrestrial Ecosystem Ecology*. Springer, New York.
- Dawson, T. E. (1993) Water sources of plants as determined from xylem-water isotopic composition: perspectives on plant competition, distribution, and water relations. *Stable Isotopes and Plant Carbon-Water Relations* (eds J. R. Ehleringer, A. E. Hall & G. D. Farquhar), pp. 465-496. Academic Press, Inc., New York.

- Dawson, T. E., Ward, J. K. & Ehleringer, J. R. (2004) Temporal scaling of physiological responses from gas exchange to tree rings: a gender-specific study of *Acer negundo* (Boxelder) growing under different conditions. *Functional Ecology*, **18**, 212-222.
- Duquesnay, A., Breda, N., Stievenard, M. & Dupouey, J. L. (1998) Changes of tree-ring  $\delta^{13}\text{C}$  and water-use efficiency of beech (*Fagus sylvatica* L.) in north-eastern France during the past century. *Plant, Cell and Environ.*, **21**, 565-572.
- Duursma, R. A. & Marshall, J. D. (2006) Vertical canopy gradients in  $\delta^{13}\text{C}$  correspond with leaf nitrogen content in a mixed-species conifer forest. *Trees*, **20**, 496-506.
- Edwards, T. W. D., Graf, W., Trimborn, P., Stichler, W., Lipp, J. & Payer, H. D. (2000)  $\delta^{13}\text{C}$  response surface resolves humidity and temperature signals in trees. *Geochimica et Cosmochimica Acta*, **64**, 161-167.
- Ehleringer, J. R. & Cerling, T. E. (1995) Atmospheric  $\text{CO}_2$  and the ratio of intercellular to ambient  $\text{CO}_2$  concentrations in plants. *Tree Physiology*, **15**, 105-111.
- Ehleringer, J. R., Roden, J. S. & Dawson, T. E. (2000) Assessing ecosystem-level water relations through stable isotope ratio analyses. *Methods in Ecosystem Science* (eds O. E. Sala, R. B. Jackson, H. A. Mooney & R. W. Howarth), pp. 181-198. Springer, New York.
- Elias, P., I. Kratochvilova, D. Janous, M. Marek & Masarovicova., E. (1989) Stand microclimate and physiological activity of tree leaves in an oak-hornbeam forest. I. stand microclimate. *Trees*, **4**, 234-240.
- Farquhar, G. D., Cernusak, L. A. & Barnes, B. (2007) Heavy water fractionation during transpiration. *Plant Physiology*, **143**, 11-18.
- Farquhar, G. D., Ehleringer, J. R. & Hubick, K. T. (1989) Carbon isotope discrimination and photosynthesis. *Annual Review of Plant Physiology and Plant Molecular Biology*, **40**, 503-537.
- Feng, X. & Epstein, S. (1995) Carbon isotopes of trees from arid environments and implications for reconstructing atmospheric  $\text{CO}_2$  concentration. *Geochimica et Cosmochimica Acta*, **59**, 2599-2608.
- Field, C. & Mooney, H. A. (1986) The photosynthesis-nitrogen relationship in wild plants. *On the Economy of Plant Form and Function* (ed T. J. Givnish), pp. 25-55. Cambridge University Press, Cambridge.
- Flanagan, L. B., Comstock, J. P. & Ehleringer, J. R. (1991) Comparison of modeled and observed environmental influences on the stable oxygen and hydrogen isotope composition of leaf water in *Phaseolus vulgaris* L. *Plant Physiology*, **96**, 588-596.
- Francey, R. J. & Farquhar, G. D. (1982) An explanation of  $^{13}\text{C}/^{12}\text{C}$  variations in tree rings. *Nature*, **297**, 28-31.
- Gholz, H. L., Grier, C. C., Campbell, A. G. & Brown, A. T. (1979) Equation for estimating biomass and leaf area of plants in the Pacific Northwest. pp. 1-36. Oregon State University, Forest Research Lab.
- Grams, T. E. E., Kozovits, A. R., Haberle, K.-H., Matyssek, R. & Dawson, T. E. (2007) Combining  $\delta^{13}\text{C}$  and  $\delta^{18}\text{O}$  analysis to unravel competition,  $\text{CO}_2$  and  $\text{O}_3$  effects on the physiological performance of different-aged trees. *Plant, Cell and Environment*, **30**, 1023-1034.

- Hanba, Y. T., Mori, S., Lei, T. T., Koike, T. & Wada, E. (1997) Variations in leaf  $\delta^{13}\text{C}$  along a vertical profile of irradiance in a temperate Japanese forest. *Oecologia*, **110**, 253-261.
- Helle, G. & Schleser, G. H. (2004) Beyond  $\text{CO}_2$ -fixation by Rubisco - an interpretation of  $^{13}\text{C}/^{12}\text{C}$  variations in tree rings from novel intra-seasonal studies on broad-leaf trees. *Plant, Cell and Environment*, **27**, 367-380.
- Jarvis, P. G., James, G. B. & Landsberg, J. J. (1976) Coniferous forest. *Vegetation and the Atmosphere* (ed J. L. Monteith), pp. 171-240. Academic Press, London.
- Jarvis, P. G. & McNaughton, K. G. (1986) Stomatal control of transpiration: scaling up from leaf to region. *Advances in Ecological Research*, **15**, 1-49.
- Leavitt, S. W. & Danzer, S. R. (1993) Methods for batch processing small wood samples to holocellulose for stable-carbon isotope analysis. *Anal. of Chemistry*, **65**, 87-89.
- Libby, L. M., Pandolfi, L. J., Payton, P. H., Marshall III, J., Becker, B. & Giertz-Siebenlist, V. (1976) Isotopic tree thermometers. *Nature*, **261**, 284-290.
- Marshall, J. D. & Monserud, R. A. (2006) Co-occurring species differ in tree-ring  $^{18}\text{O}$  trends. *Tree Physiology*, **26**, 1055-1066.
- Martin, T. A., Hinckley, T. M., Meizner, F. C. & Sprugel, D. G. (1999) Boundary layer conductance, leaf temperature and transpiration of *Abies amabilis* branches. *Tree Physiology*, **19**, 435-443.
- McCarroll, D. & Loader, N. J. (2004) Stable isotopes in tree rings. *Quaternary Science Reviews*, **23**, 771-801.
- McNulty, S. G. & Swank, W. T. (1995) Wood  $\delta^{13}\text{C}$  as a measure of annual basal area growth and soil water stress in a *Pinus strobus* forest. *Ecology*, **76**, 1581-1586.
- Monteith, J. L. (1995) A reinterpretation of stomatal responses to humidity. *Plant, Cell, and Environment*, **18**, 357-364.
- Moore, G. W., Bond, B. J., Jones, J. A., Phillips, N. & Meinzer, F. C. (2004) Structural and compositional controls on transpiration in a 40- and 450-yr-old riparian forest in western Oregon, USA. *Tree Physiology*, **24**, 481-491.
- Niinemets, U., Sonninen, E. & Tobias, M. (2004) Canopy gradients in leaf intercellular  $\text{CO}_2$  mole fractions revisited: interactions between leaf irradiance and water stress need consideration. *Plant, Cell and Environment*, **27**, 569-583.
- Oliver, C. D. & Larson, B. C. (1990) *Forest Stand Dynamics*. McGraw-Hill Inc., New York.
- Ott, R. L. (1993) *An introduction to statistical methods and data analysis*. Duxbury Press, Belmont, CA.
- Powers, R. F. & Reynolds, P. E. (1999) Ten-year responses of ponderosa pine plantations to repeated vegetation and nutrient control along an environmental gradient. *Canadian Journal of Forest Research*, **29**, 1027-1038.
- Pypker, T. G., Hauck, M. J., Sulzman, E. W., Unsworth, M. H., Mix, A. C., Kayler, Z., Conklin, D., Kennedy, A., Barnard, H. R., Phillips, C. & Bond, B. J. (2008) Toward using  $\delta^{13}\text{C}$  of ecosystem respiration to monitor canopy physiology in complex terrain. *Oecologia*, **158**.
- Rebetez, M., Saurer, M. & Cherubini, P. (2003) To what extent an oxygen isotopes in tree rings and precipitation be used to reconstruct past atmospheric temperature? A case study. *Climatic Change*, **61**, 237-248.

- Robertson, I., Leavitt, S., Loader, N. J. & Buhay, W. (2008) Progress in isotope dendroclimatology. *Chemical Geology* **252**, EX1-EX4.
- Roden, J. S. (2008) Cross-dating of tree ring  $\delta^{18}\text{O}$  and  $\delta^{13}\text{C}$  tie series. *Chemical Geology*, **252**, 72-79.
- Roden, J. S. & Ehleringer, J. R. (2007) Summer precipitation influences the stable oxygen and carbon isotopic composition of tree-ring cellulose in *Pinus ponderosa*. *Tree Physiology*, **27**, 491-501.
- Rothacher, J., Dyrness, C. T. & Fredriksen, F. L. (1967) Hydrologic and related characteristics of three small watersheds in the Oregon cascades. pp. 1-54. Forest Service, USDA.
- Ryan, M. G. & Yoder, B. J. (1997) Hydraulic limits to tree height and tree growth. *BioScience*, **47**, 235-242.
- Saurer, M., Aellen, K. & Siegwolf, R. (1997) Correlating  $\delta^{13}\text{C}$  and  $\delta^{18}\text{O}$  in cellulose of trees. *Plant, Cell, and Environment*, **20**, 1543-1550.
- Saurer, M. & Siegwolf, R. T. W. (2007) Human impacts on tree ring growth reconstruction from stable isotopes. *Stable Isotopes as Indicators of Ecological Change* (eds T. E. Dawson & R. T. W. Siegwolf), pp. 49-62. Elsevier, New York.
- Scheidegger, Y., Saurer, M., Bahn, M. & Siegwolf, R. (2000) Linking stable oxygen and carbon isotopes with stomatal conductance and photosynthetic capacity: a conceptual model. *Oecologia*, **125**, 350-357.
- Sheshshayee, M. S., Bindumadhava, H., Ramesh, R., Prasad, T. G., Lakshminarayana, M. R. & Udayakumar, M. (2005) Oxygen isotope enrichment ( $\Delta^{18}\text{O}$ ) as a measure of time-averaged transpiration rate. *Journal of Experimental Botany*, **56**, 3033-3039.
- Siegwolf, R. T. W., Matyssek, R., Saurer, M., Maurer, S., Günthardt-Georg, M. S., Schmutz, P. & Bucher, J. B. (2001) Stable isotope analysis reveals differential effects of soil nitrogen and nitrogen dioxide on the water use efficiency in hybrid poplar leaves. *New Phytologist*, **149**, 233-246.
- Smith, F. W. & Long, J. N. (2001) Age-related decline in forest growth: an emergent property. *Forest Ecology and Management*, **1-3**, 175-181.
- Sternberg, L. D. S. L. (1989) Oxygen and hydrogen isotope measurements in plant cellulose analysis. *Modern Methods of Plant Analysis: plant fibers* (eds H. F. Linskens & J. F. Jackson), pp. 89-99. Springer Verlag, Berlin.
- Swanson, F. J. & James, M. E. (1975) Geology and geomorphology of the H.J. Andrews Experimental Forest, Western cascades, Oregon. *Pacific Northwest Forest and Range Experiment Station, Forest Service, U.S.D.A., Research Paper PNW-188*, 1-14.
- Waring, R. H., Thies, W. G. & Muscato, D. (1980) Stem growth per unit of leaf area: A measure of tree vigor. *Forest Science*, **26**, 112-117.
- Waring, R. H., and W. B. Silvester (1994) Variation in foliar  $\delta^{13}\text{C}$  values within the crowns of *Pinus radiata* trees. *Tree Physiology*, **14**:1203-1213.
- White, J. W. C., Cook, E. R., Lawrence, J. R. & Broecker, W. S. (1985) The D/H ratios in trees: implications for water sources and tree ring D/H ratios. *Geochimica et Cosmochimica Acta*, **49**, 237-246
- Zimmerman, J. K. & Ehleringer, J. R. (1990) Carbon isotope ratios are correlated with irradiance levels in the Panamanian orchid *Catacetum viridiflavum*. *Oecologia*, **83**, 247-249.

Table 4-1: Pearson correlation coefficient (r), p-value (p), and number of observations (N) for the relationship between normalized cellulose  $\delta^{13}\text{C}_{\text{cell}}$ ,  $\delta^{18}\text{O}_{\text{cell}}$ , BAI, and climate variables for both earlywood and latewood. Significant correlations ( $\alpha \leq 0.10$ ) are in bold text.

		Earlywood					Latewood					
		BAI	Annual PPT (mm)	Summer PPT (mm)	T (°C)	RH (%)	BAI	Annual PPT (mm)	Summer PPT (mm)	T (°C)	RH (%)	
Dominant	$\delta^{13}\text{C}_{\text{cell}}$	r	-.08	.21	-.04	.25	<b>-.37</b>	.01	.12	<b>-.53</b>	<b>.47</b>	<b>-.46</b>
		p	.61	.20	.80	.12	.02	.99	.45	<.01	<.01	<.01
		N	40	40	40	40	40	40	40	40	40	40
	$\delta^{18}\text{O}_{\text{cell}}$	r	-.03	.22	<b>-.29</b>	.19	<b>-.51</b>	.10	.11	<b>-.40</b>	<b>.33</b>	<b>-.43</b>
		p	.85	.17	.07	.25	<.01	.54	.49	.01	.04	<.01
		N	39	39	39	39	39	40	40	40	40	40
	BAI	r		-.03	-.05	-.06	.28		-.03	-.05	.08	.12
		p		.86	.77	.74	.08		.86	.77	.64	.46
		N		40	40	40	40		40	40	40	40
Co-dominant	$\delta^{13}\text{C}_{\text{cell}}$	r	-.01	.10	-.25	<b>.38</b>	<b>-.65</b>	.03	-.04	<b>-.41</b>	<b>.28</b>	<b>-.31</b>
		p	.96	.53	.13	.02	<.01	.87	.79	.01	.08	.05
		N	38	38	38	38	38	40	40	40	40	40
	$\delta^{18}\text{O}_{\text{cell}}$	r	.02	.23	<b>-.27</b>	.06	<b>-.27</b>	.08	.11	<b>-.39</b>	.14	<b>-.30</b>
		p	.89	.15	.10	.70	.10	.63	.50	.01	.38	.07
		N	39	39	39	39	39	39	39	39	39	39
	BAI	r		-.02	-.05	.17	.14		-.02	-.05	.16	.07
		p		.93	.75	.31	.39		.93	.75	.32	.68
		N		40	40	40	40		40	40	40	40
Intermediate	$\delta^{13}\text{C}_{\text{cell}}$	r	.01	.02	<b>-.33</b>	.16	<b>-.31</b>	.01	.16	<b>-.42</b>	.26	-.21
		p	.95	.92	.05	.35	.06	.96	.32	.01	.11	.20
		N	37	37	37	37	37	40	40	40	40	40
	$\delta^{18}\text{O}_{\text{cell}}$	r	.09	.24	<b>-.31</b>	.16	-.12	.14	.15	-.13	.11	-.25
		p	.62	.16	.06	.34	.47	.39	.35	.44	.50	.12
		N	37	37	37	37	37	39	39	39	39	39
	BAI	r		-.01	-.05	.09	.02		-.01	-.05	<b>.34</b>	-.23
		p		.97	.75	.57	.91		.97	.75	.03	.15
		N		40	40	40	40		40	40	40	40

Table 4-2: The nitrogen composition (%) of current year (2006) foliage, 1-yr-old foliage (2005). \*Plot 504 values are from the 2005 growing season, where current year is 2005 and 1-yr-old is 2004 foliage.

Plot	Foliage N (S.E.)			
	Current yr	1-yr old	Average	Rank (low to high)
501	0.69 (0.03)	0.88 (0.02)	0.79	1
504*	0.94 (0.07)	0.94 (0.10)	0.94	3
505	1.13 (0.10)	1.11 (0.02)	1.12	4
507	0.81 (0.02)	0.97 (0.03)	0.89	2
510	0.80 (0.05)	1.07 (0.02)	0.94	3

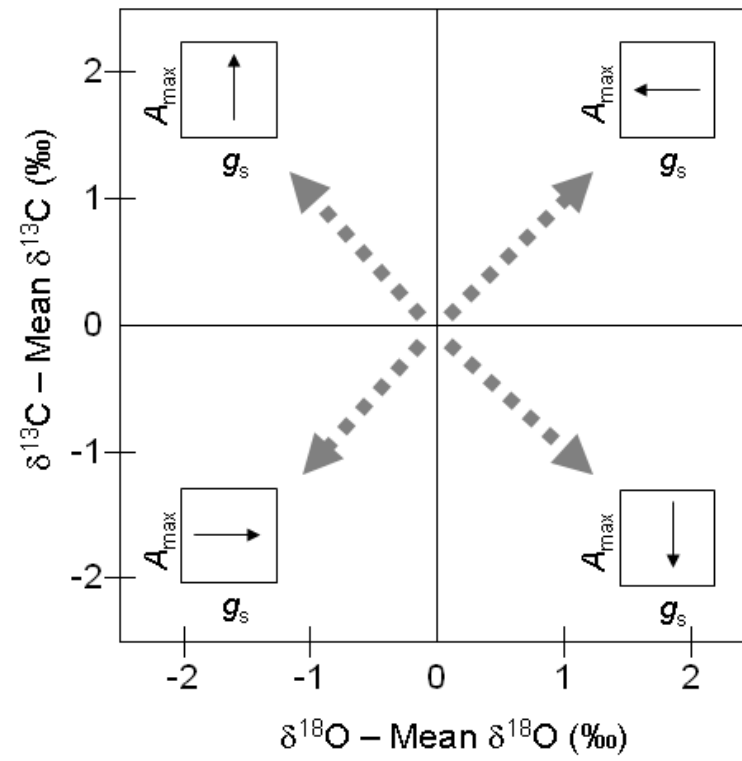


Figure 4-1: Conceptual application of the Scheidegger model (adapted from Scheidegger et al. (2000)).

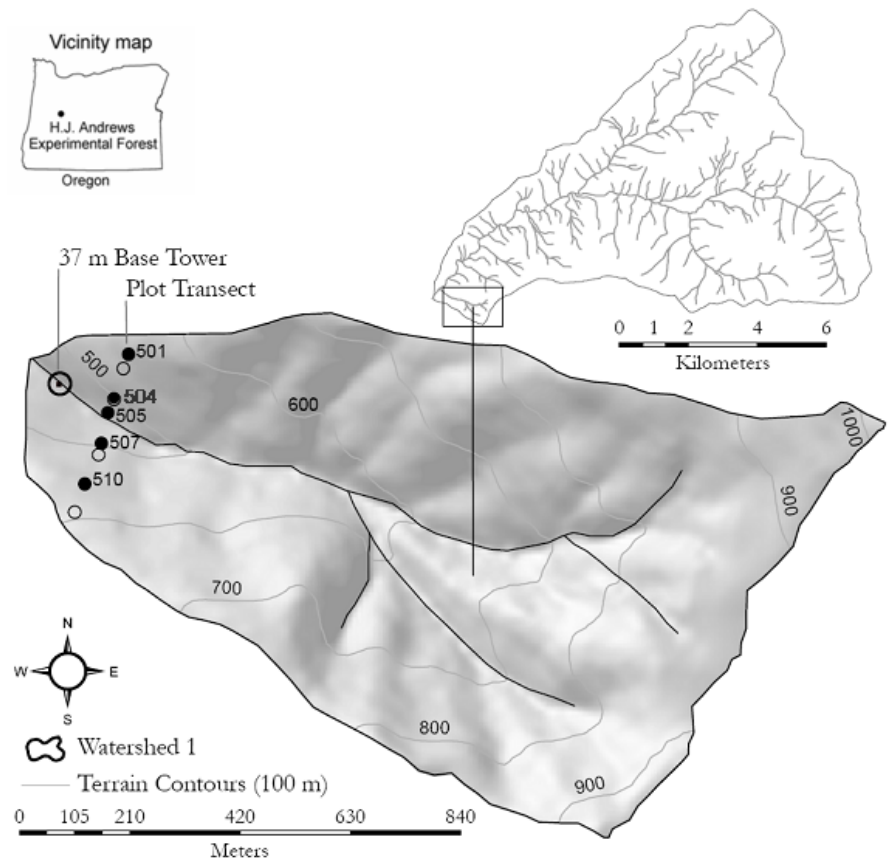


Figure 4-2: Map of the location of the HJ Andrews Experimental Forest and Watershed 1. The map of Watershed 1 shows the locations of the eight research plot along the transect. The dark circles indicate the five research plots along the transect that were used in this study.

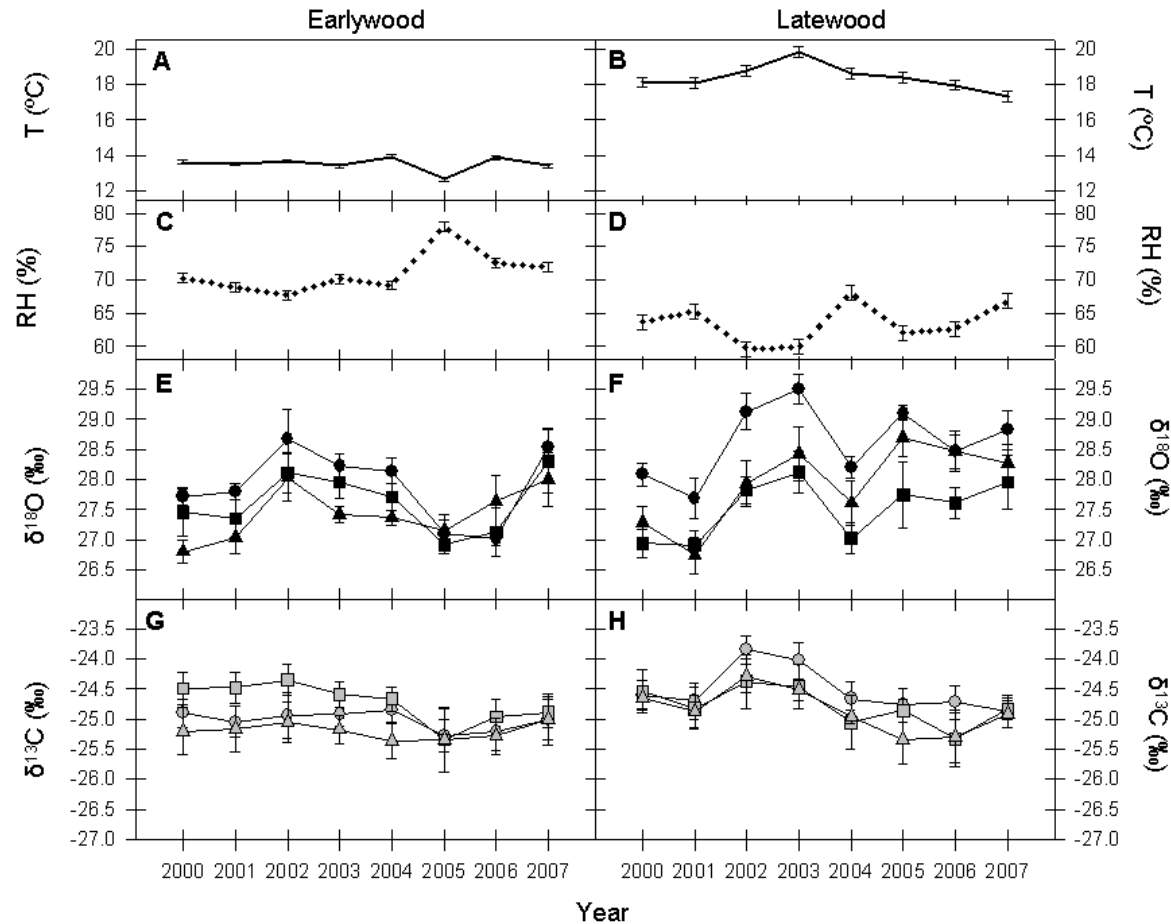


Figure 4-3: Temperature (T), relative humidity (RH),  $\delta^{18}\text{O}_{\text{cell}}$  and  $\delta^{13}\text{C}_{\text{cell}}$  through time. A-B: Mean temperature for 0700 – 1400 hrs for early season (DOY 90-194) and late season (DOY 195-275), C-D mean relative humidity 0700 – 1400 hrs for early season (DOY 90-194) and late season (DOY 195-275), E-F:  $\delta^{18}\text{O}_{\text{cell}}$  by crown class. Circles = dominant, Squares = co-dominant, triangles = intermediate. G-H:  $\delta^{13}\text{C}_{\text{cell}}$  by crown class with same symbols as above. Error bars equal the standard error of the means.

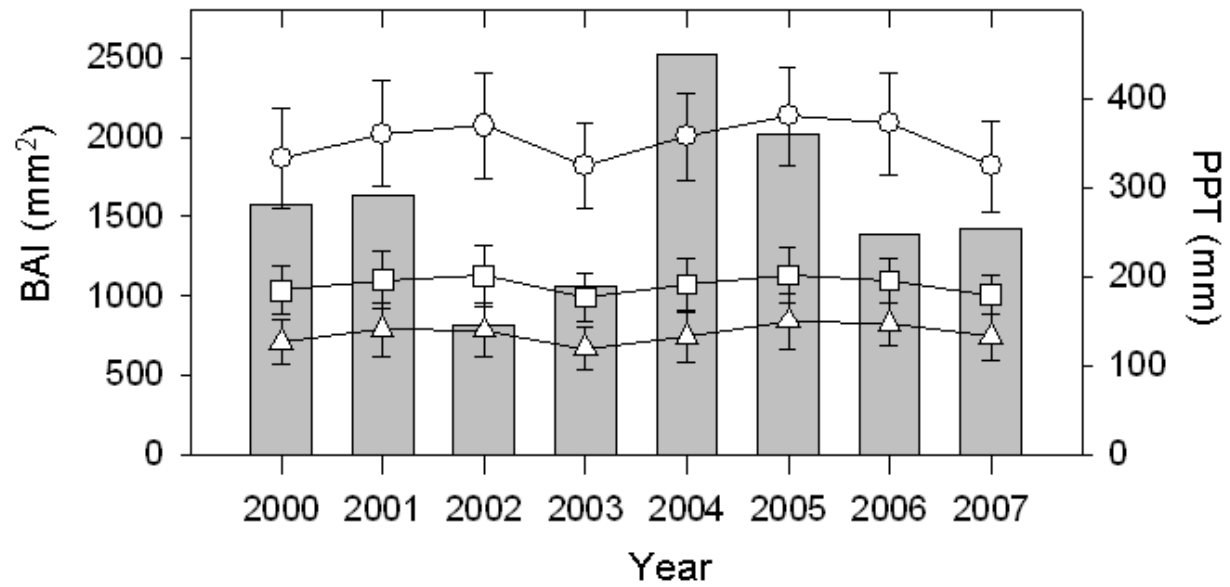


Figure 4-4: Annual basal area increment by crown class. Circles = dominant, Squares = co-dominant, triangles = intermediate, and summer precipitation (May-October). Error bars equal the standard error of the means.

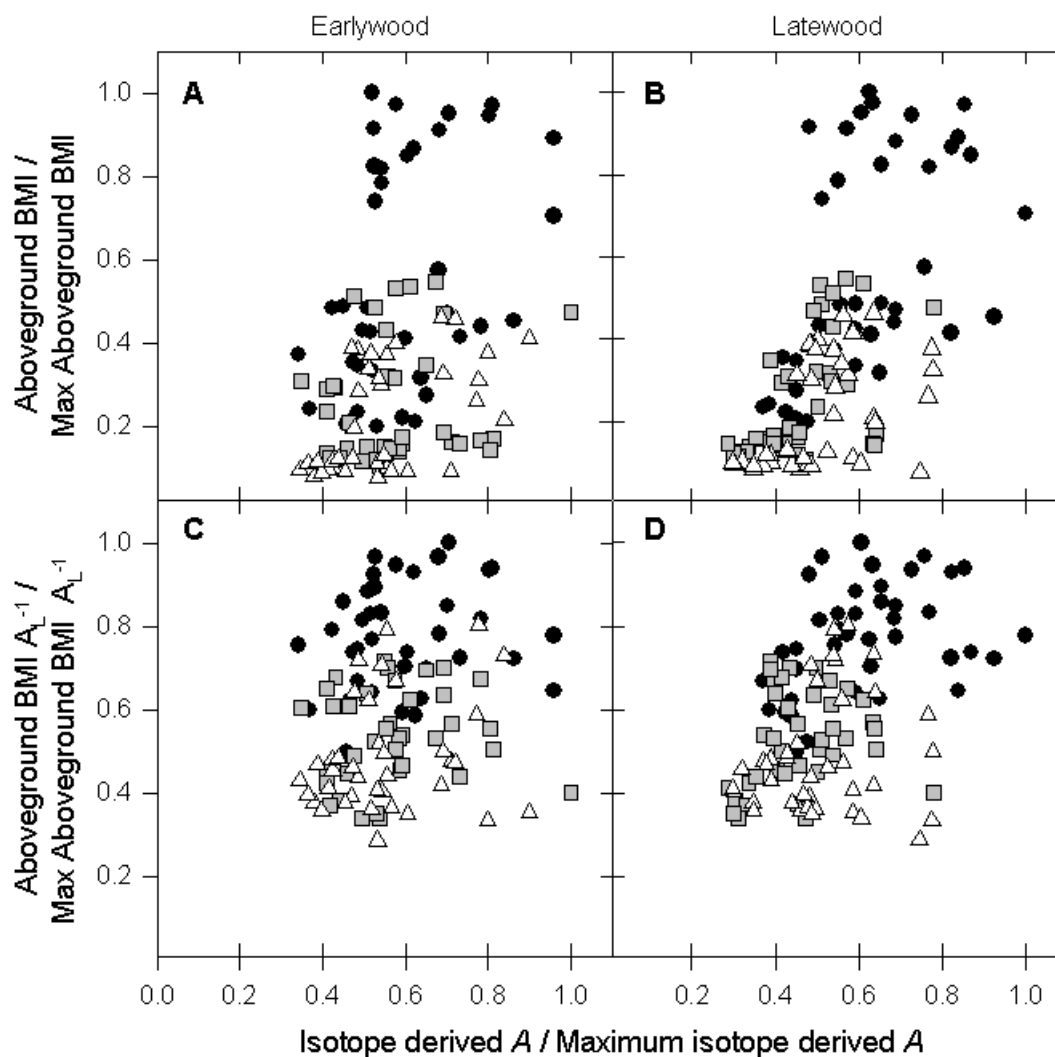


Figure 4-5: Aboveground biomass increment (BMI) relative to maximum aboveground BMI versus isotope derived  $A$  relative to maximum isotope derived  $A$  for earlywood (Panel A) and latewood (Panel B). Aboveground BMI  $A_L^{-1}$  relative to maximum aboveground BMI  $A_L^{-1}$  versus isotope derived  $A$  relative to maximum isotope derived  $A$  for earlywood (Panel C) and latewood (Panel D). Circles = Dominant, Squares = Co-dominant, Triangles = Intermediate

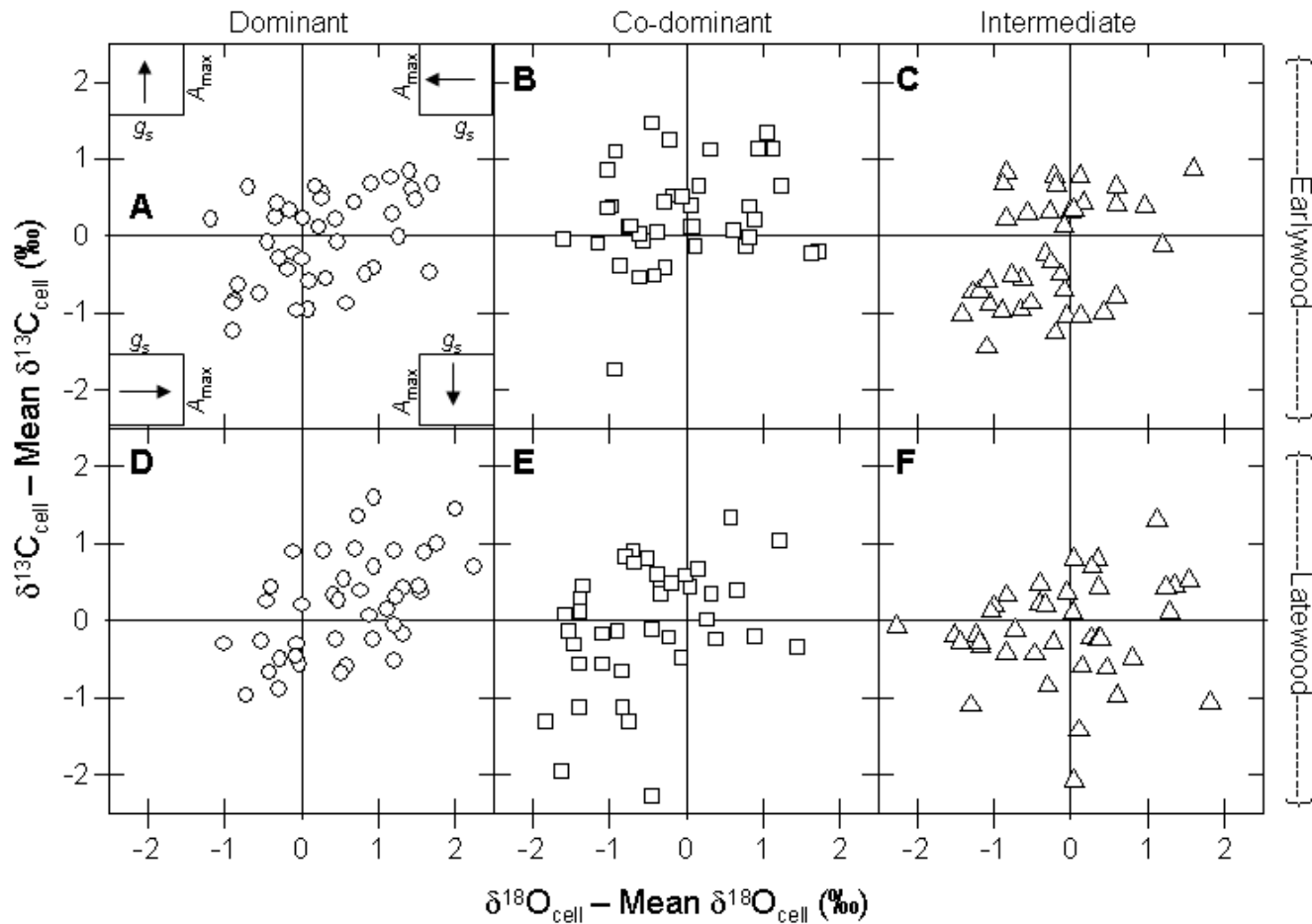


Figure 4-6:  $\delta^{13}\text{C}_{\text{cell}}$  and  $\delta^{18}\text{O}_{\text{cell}}$  Cellulose  $\delta^{13}\text{C}$  value minus the mean  $\delta^{13}\text{C}$  value for all samples versus  $\delta^{18}\text{O}$  minus mean  $\delta^{18}\text{O}$  for all samples for earlywood (Panels A-C) and latewood (Panel D-F). Circles, squares, and triangles are dominant, co-dominant, and intermediate crown classes, respectively.

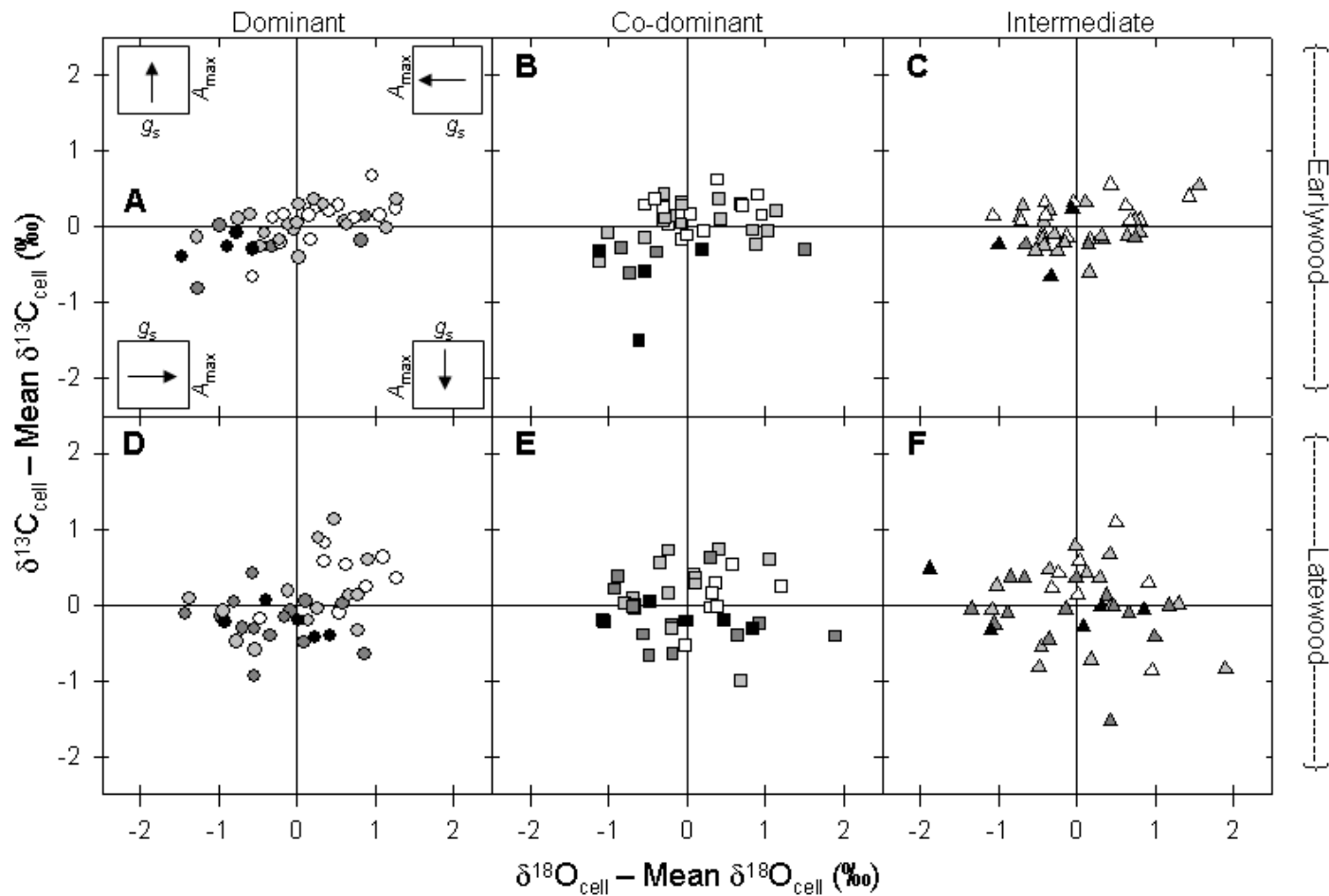


Figure 4-7:  $\delta^{13}\text{C}_{\text{cell}}$  minus mean  $\delta^{13}\text{C}_{\text{cell}}$  versus  $\delta^{18}\text{O}_{\text{cell}}$  minus mean  $\delta^{18}\text{O}_{\text{cell}}$  for earlywood (Panels A-C) and latewood (Panel D-F). Circles, squares, and triangles are dominant, co-dominant, and intermediate crown classes, respectively. Colors indicate relative humidity: black = highest N, white = lowest. Data was normalized to the mean of all years for each crown class.

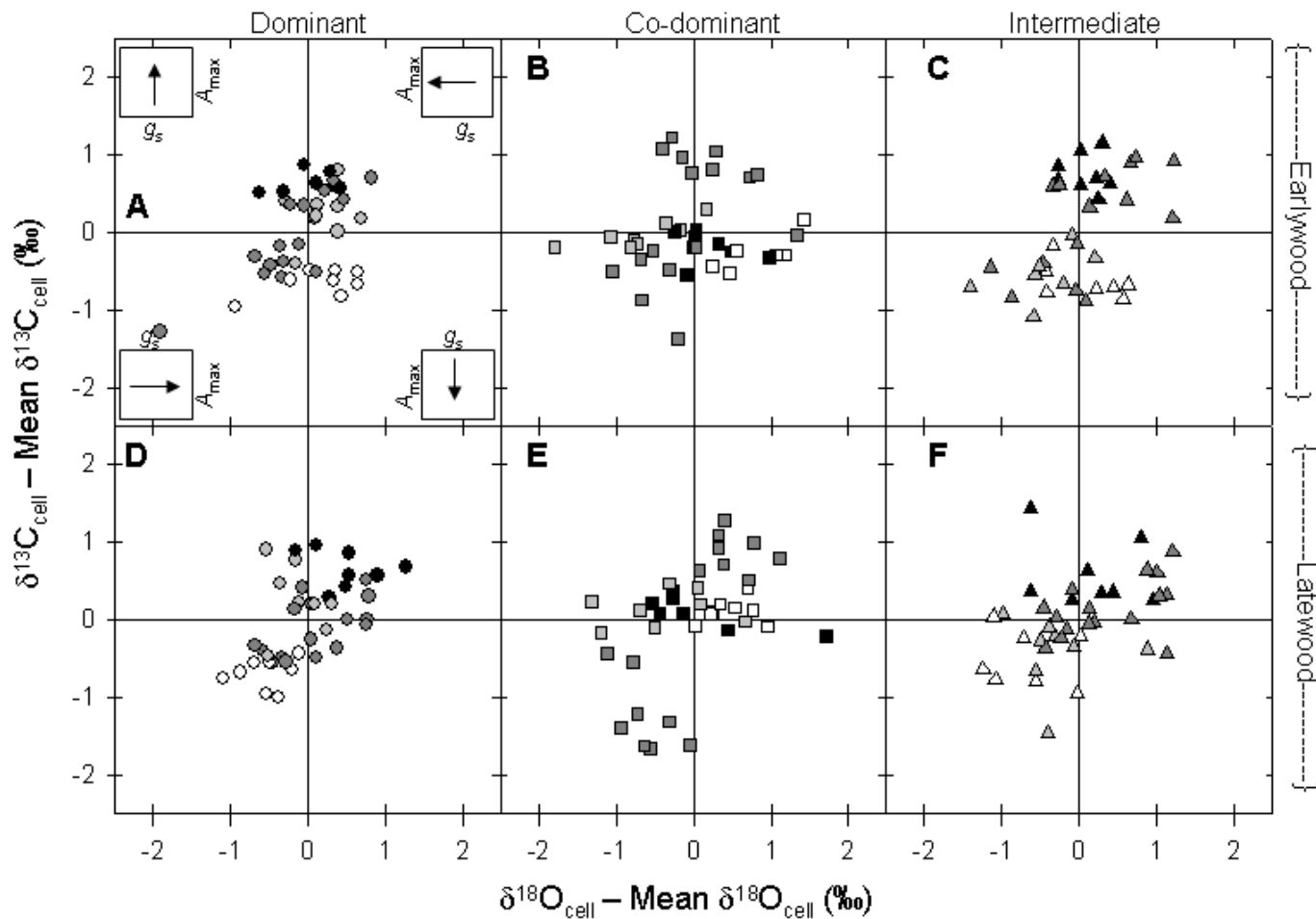


Figure 4-8:  $\delta^{13}\text{C}_{\text{cell}}$  minus mean  $\delta^{13}\text{C}_{\text{cell}}$  versus  $\delta^{18}\text{O}_{\text{cell}}$  minus mean  $\delta^{18}\text{O}_{\text{cell}}$  for earlywood (Panels A-C) and latewood (Panel D-F). Circles, squares, and triangles are dominant, co-dominant, and intermediate crown classes, respectively. Colors indicate rank of foliar nitrogen content (%): black = highest N, white = lowest N. Data was normalized to the mean of each year by crown class.

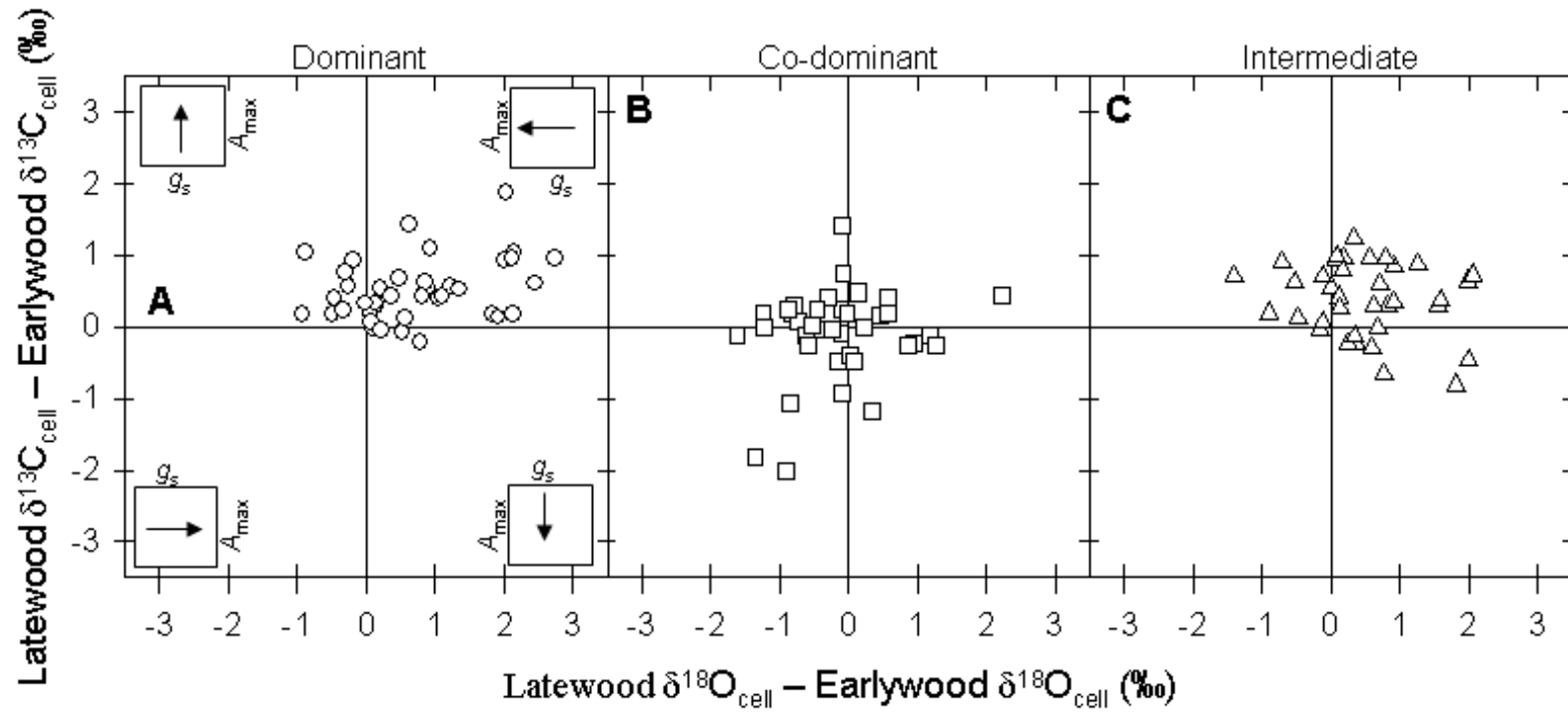


Figure 4-9: The difference between latewood and earlywood  $\delta^{13}\text{C}_{\text{cell}}$  and  $\delta^{18}\text{O}_{\text{cell}}$  for dominant (A), co-dominant (B), and intermediate (C) crown classes.

## **Chapter 5    Conclusion**

## **Conclusion**

### *Summary of main dissertation findings*

One of the grand challenges in humid and sub-humid land ecohydrology is identifying what roles topography, vegetation, and soil heterogeneity play in determining hydrological processes at the catchment scale (Rodriguez-Iturbe et al., 2007). The hydrological cycle involves mutually-dependent biological and physical processes that operate at multiple scales of time and space, and this principle is the foundation for research in ecohydrology. The research presented in this dissertation used multiple approaches to semi-mechanistically assess the inter-relationships between forest water use, hydrology, and climate.

In Chapter 2, we used a hillslope-scale irrigation experiment to examine the relationships of soil moisture, transpiration, and hillslope subsurface flow. Irrigation experiments at the hillslope scale provided an opportunity to isolate the relationships between hillslope transpiration and runoff from riparian and instream processes. By directly measuring hillslope discharge via a gauged trench at the hillslope-streambed interface, we observed time lags between maximum transpiration and minimum discharge on the hillslope scale that were similar to those reported for the whole catchment scale in a nearby basin (Bond et al., 2002). The time lags we observed were not likely caused by increases in transpiration rate in response to soil moisture. We speculated that the interactions of hillslope and soil properties with tree roots under different moisture regimes are responsible for the variation in lag time. This work represents one step forward in elucidating the linkages between vegetation water use and (sub) surface flow processes.

In Chapter 3, we observed that plot-scale transpiration across a steep topographic gradient could not be predicted from measured variations in environmental variables alone. Furthermore, spatial variations in soil moisture and soil matric potential did not conform to preconceived expectations based simply upon topographic gradients. Spatial variability in transpiration across even small distances can be high and it can not be assumed that a single, randomly selected plot will be representative of the catchment. In the case of this study, heterogeneity in biophysical drivers (photosynthetically active radiation and vapor pressure deficit), edaphic properties and

whole tree conductance control plot scale transpiration. Our results demonstrate that models of catchment hydrological processes should not assume that transpiration is spatially uniform or that biophysical drivers accurately predict transpiration.

Chapter 4 uses stable isotopes in tree rings to examine the inter-relationships between environmental variables and tree physiological function. We found weak evidence to support that stable isotopes of oxygen coupled with stable isotopes in tree ring cellulose can be used to infer temporal changes in net primary production. We found evidence of stable isotopes of oxygen being related to both stomatal conductance and relative humidity; however, the relationship with relative humidity most apparent. Our results demonstrated that the physiological interpretation of stable isotope in tree rings continues to be challenging in uncontrolled environments. Additional experiments at leaf level relating isotope derived physiological processes to measured net primary production are warranted.

#### *Future research*

This dissertation research provided a glimpse of the complex inter-relationships between vegetation, hydrology, and climate. Future research should focus on understanding the feedbacks between vegetation, hydrology, and climate beyond the plot or hillslope scale. A mechanistic understanding of the role forests play in controlling subsurface flow and streamflow patterns, and conversely, the role that biologically available water plays in determining ecosystem function is needed to further our understanding of ecohydrological processes in headwater catchments. The amount of biologically available water is arguably the central driver in plant processes (Newman et al., 2006). Biologically available water is determined by precipitation, runoff pathways and water use by vegetation. While many studies have examined the hydrological components of biologically available water (e.g. precipitation variation in time and space, runoff generation mechanisms), the role that vegetation water use (transpiration) plays within the forested ecosystem water balance is poorly understood. Knowledge in this area is important for modeling and predicting the consequences of global climate change, such as altered precipitation regimes and shifts in plant species composition. Future research topics may include:

- Partitioning of evaporation and transpiration. Although it is common for transpiration to be combined with surface evaporation as evapotranspiration (ET) in runoff assessment, combining these components limits our understanding of the relative importance of water used for biological processes versus water that evaporates and is not biologically available (Newman et al., 2006).
- Examining to what extent canopy interception and re-evaporation influences streamflow dynamics during storm events. Intra-storm isotopic variation of rainfall and the effect of interception loss by the forest canopy on the isotopic concentration of rainfall have often been neglected in hydrograph separation.
- How will land use change and/or invasive species encroachment change the water and carbon balance? Shifts in species composition and distribution can have drastic effects on water resources especially in semi-arid areas. Grazing and the introduction of non-native species are known to degrade sensitive riparian corridors. Even shifts in the distribution of native species can influence interception losses and soil moisture depletion. Further research is needed to examine how the long term carbon and water balance will be affected by these activities.

## References

- Bond, B. J., Jones, J. A., Moore, G., Phillips, N., Post, D. & McDonnell, J. J. (2002) The zone of vegetation influence on baseflow revealed by diel patterns of streamflow and vegetation water use in a headwater basin. *Hydrological Processes*, 16, 1671-1677.
- Newman, B. D., Wilcox, B. P., Archer, S. R., Breshears, D. D., Dahm, C. N., Duffy, C. J., McDowell, N. G., Phillips, F. M., Scanlon, B. R. & Vivoni, E. R. (2006) Ecohydrology of water-limited environments: a scientific vision. *Water Resources Research*, 42.
- Rodriguez-Iturbe, I., D'Odorico, P., Laio, F., Ridolfi, L. & Tamea, S. (2007) Challenges in humid land ecohydrology: Interactions of water table and unsaturated zone with climate, soil, and vegetation. *Water Resources Research*, 43, W09301.

## **Appendix A Stable isotope theory**

### Isotopic Theory

The isotopic theory of fractionation processes that occur within plants has been outlined nicely by several authors and is briefly described below (Marshall and Monserud, 2006, Barbour, 2007b, Grams et al., 2007, Sternberg, 2008, Bowling et al., 2008, Brooks and Coulombe, 2009). Changes in  $\delta^{13}\text{C}$  through time are recorded in tree rings as the photosynthate from leaves is biosynthesized into cellulose. Once cellulose is deposited in cell walls, it is immobile and therefore, the carbon isotope composition of cellulose ( $\delta^{13}\text{C}_{\text{cell}}$ ) in tree rings is a record of crown-scale WUE (Tans et al., 1978, McDowell et al., 2003). The  $\delta^{13}\text{C}$  of tree rings is influenced by both the variation in tree physiological processes and by variation in isotopic composition of atmospheric  $\text{CO}_2$  ( $\delta^{13}\text{C}_{\text{air}}$ ). Because many studies of  $^{13}\text{C}$  of plant tissues ( $\delta^{13}\text{C}_{\text{plant}}$ ) are interested in the physiological processes rather than  $\delta^{13}\text{C}_{\text{air}}$ , it is common for  $^{13}\text{C}$  composition to be reported as a carbon isotope discrimination against  $^{13}\text{C}$  ( $\Delta^{13}\text{C}$ ) relative to  $\delta^{13}\text{C}_{\text{air}}$  using the following equation (Farquhar et al., 1982):

$$\Delta^{13}\text{C} = \frac{\delta^{13}\text{C}_{\text{plant}} - \delta^{13}\text{C}_{\text{air}}}{1 + \delta^{13}\text{C}_{\text{plant}} / 1000} \quad (1)$$

The  $\Delta^{13}\text{C}$  of plant material is directly related to the ratio of internal  $[\text{CO}_2]$  to atmospheric  $[\text{CO}_2]$  as described by the equation:

$$\Delta^{13}\text{C} = a + (b - a) \left( \frac{c_i}{c_a} \right) \quad (2)$$

where,  $a$  and  $b$  are constants for fractionation due to diffusion (4.4‰) and carboxylation (~27‰), respectively, and  $c_i / c_a$  is the ratio  $[\text{CO}_2]$  inside the stomatal cavity to the  $[\text{CO}_2]$  of ambient air surrounding the leaf (Farquhar et al. 1982). The  $c_i / c_a$  ratio is influenced by the rate of photosynthesis ( $A$ ) which draws down  $c_i$  and stomatal conductance ( $g_s$ ) which allows  $\text{CO}_2$  into the leaf. Therefore,  $c_i$  and  $c_a$  are directly related to the intrinsic WUE which is estimated as:

$$\frac{A}{g_s} = \frac{(c_a - c_i)}{1.6} \quad (3)$$

where 1.6 is the ratio of diffusivities of water and CO<sub>2</sub> in air. Variation in  $\Delta^{13}\text{C}$  can result from changes in  $A$ ,  $g_s$ , or disproportional changes in both, but additional information would be needed to determine their relative influence.

Like  $\delta^{13}\text{C}$ ,  $\delta^{18}\text{O}$  of tree rings is influenced by both variation in plant physiological processes and by variation in the isotopic composition of the source. In the case of  $^{18}\text{O}$ , the source of oxygen atoms is the soil water that the plants take up (Anderson et al., 1998). Water is not fractionated as it enters roots and is carried to the leaves (White et al., 1985). However, as water exits the leaf, oxygen atoms from source water undergo evaporation and diffusion within the stomatal cavity during transpiration and biochemical fractionation during cellulose synthesis (Epstein et al., 1976, Farquhar et al., 1998, Barbour, 2007b). Enrichment under steady state conditions at the site of evaporation was described by the following model (Craig and Gordon, 1965, Farquhar and Lloyd, 1993):

$$\Delta^{18}\text{O}_e = \varepsilon^* + \varepsilon_k + (\Delta^{18}\text{O}_v - \varepsilon_k) \frac{e_a}{e_i} \quad (4)$$

where  $\Delta^{18}\text{O}_e$  and  $\Delta^{18}\text{O}_v$  represent the isotopic difference between source water and either leaf water at the site of evaporation, or atmospheric water vapor, respectively.  $e_a$  and  $e_i$  are atmospheric and inter-cellular vapor pressures, respectively.  $\varepsilon^*$  is the equilibrium fractionation factor for exchange between water liquid and vapor.  $\varepsilon_k$  is the kinetic fractionation that occurs during diffusion and can be calculated using  $g_s$  and boundary layer conductance ( $g_b$ ) to water vapor using the following equation (Barbour, 2007b):

$$\varepsilon_k = \frac{32g_s^{-1} + 21g_b^{-1}}{g_s^{-1} + g_b^{-1}} \quad (5)$$

$\Delta^{18}\text{O}_e$  can be used to estimate the enrichment of bulk leaf water above source water ( $\Delta^{18}\text{O}_l$ ) using the following two equations (Barbour 2007):

$$\Delta^{18}\text{O}_l = \frac{\Delta^{18}\text{O}_e (1 - e^{-\wp})}{\wp} \quad (6)$$

where  $\wp$  represents the Péclet effect, a dimensionless ratio of convection to diffusion:

$$\wp = \frac{LE}{CD} \quad (7)$$

where  $L$  is the effective path length (m),  $E$  is transpiration ( $\text{mol m}^{-2} \text{s}^{-1}$ ),  $C$  is the molar density of water ( $55.5 \times 10^3 \text{ mol m}^{-3}$ ), and  $D$  is the diffusivity of H<sub>2</sub><sup>18</sup>O ( $2.66 \times 10^{-9} \text{ m}^2 \text{ s}^{-1}$ )

<sup>1</sup>). The incorporation of  $\Delta^{18}\text{O}_l$  into tree ring cellulose ( $\Delta^{18}\text{O}_{\text{cell}}$ ) is based on empirical estimates of biochemical fractionation and proportional oxygen exchange (Barbour and Farquhar, 2000):

$$\Delta^{18}\text{O}_{\text{cell}} = \Delta^{18}\text{O}_l (1 - p_{\text{ex}} p_x) + \varepsilon_o \quad (8)$$

where  $p_{\text{ex}}$  is the proportional exchangeable oxygen and  $p_x$  is the proportion of unenriched water (xylem water) at the site of cellulose formation, which for tree cores collected from the main trunk is equivalent to 1. According to Sternberg et al. (1986),  $\varepsilon_o$  is +27‰ and according to Roden et al. (2000),  $p_{\text{ex}}$  for oxygen in xylem cellulose is 0.42. There is no exchange between the oxygen atoms of water and of cellulose after cellulose formation (Lang and Mason, 1959).

Separating source effects from plant processes is more challenging for  $\delta^{18}\text{O}$  than  $\delta^{13}\text{C}$ , because the isotopic signature of soil water can vary dramatically both temporally and spatially. However, if source water for trees in close proximity to each other is the same, then inter-tree variation in cellulose  $\delta^{18}\text{O}$  is due to tree physiological processes.

## References

- Anderson, W. T., Bernasconi, S. M., McKenzie, J. A. & Saurer, M. (1998) Oxygen and carbon isotopic record of climatic variability in tree ring cellulose (*Picea abies*): an example from Switzerland (1913 - 1995). *Journal of Geophysical Research*, **103(D24)**, 625-631,636.
- Barbour, M. M. (2007) Stable oxygen isotope composition of plant tissue: a review. *Functional Plant Biology*, **34**, 83-94.
- Barbour, M. M. & Farquhar, G. D. (2000) Relative humidity- and ABA-induced variation in carbon and oxygen isotope ratios of cotton leaves. *Plant, Cell and Environment*, **23**, 473-485.
- Bowling, D. R., Pataki, D. E. & Randerson, J. T. (2008) Carbon isotopes in terrestrial ecosystem pools and CO<sub>2</sub> fluxes. *New Phytologist*, **178**, 24-40.
- Brooks, J. R. & Coulombe, R. (2009) Physiological responses to fertilization recorded in tree rings: isotopic lessons from a long-term fertilization trial. *Ecological Applications* **19**, 1044-1060.
- Craig, H. & Gordon, L. I. (1965) Deuterium and oxygen 18 variations in the ocean and the marine atmosphere. *Stable isotopes in oceanographic studies and paleotemperatures*, pp. 9-130. Spoleto.
- Epstein, S., Yapp, C. Y. & Hall, J. H. (1976) The determination of D/H ratio of nonexchangeable hydrogen in cellulose extracted from aquatic and land plants. *Earth and Planetary Science Letters*, **30**, 241-251.
- Farquhar, G. D., Barbour, M. M. & Henry, B. K. (1998) Interpretation of oxygen isotope composition of leaf material. *Stable isotopes: integration of biological, ecological and geochemical processes* (ed H. Griffiths), pp. 27-61. BIOS Scientific Publishers, Oxford.
- Farquhar, G. D. & Lloyd, J. (1993) Carbon and oxygen isotopes effects in the exchange of carbon dioxide between terrestrial plants and the atmosphere. *Stable Isotopes and Plant Carbon-Water Relations* (eds J. R. Ehleringer, A. E. Hall & G. D. Farquhar), pp. 47-70. Academic Press, New York.
- Farquhar, G. D., O'Leary, M. H. & Berry, J. A. (1982) On the relationship between carbon isotope discrimination and the intercellular carbon dioxide concentration in leaves. *Australian Journal of Plant Physiology*, **9**, 121-137.
- Grams, T. E. E., Kozovits, A. R., Haberle, K.-H., Matyssek, R. & Dawson, T. E. (2007) Combining  $\delta^{13}\text{C}$  and  $\delta^{18}\text{O}$  analysis to unravel competition, CO<sub>2</sub> and O<sub>3</sub> effects on the physiological performance of different-aged trees. *Plant, Cell and Environment*, **30**, 1023-1034.
- Lang, A. R. G. & Mason, S. G. (1959) The exchange of oxygen-18 between cellulose, adsorbed water, and water vapor. *CANADIAN JOURNAL OF CHEMISTRY*, **37**, 1829-1833.
- Marshall, J. D. & Monserud, R. A. (2006) Co-occurring species differ in tree-ring <sup>18</sup>O trends. *Tree Physiology*, **26**, 1055-1066.
- McDowell, N., Brooks, J. R., Fitzgerald, S. A. & Bond, B. (2003) Carbon isotope discrimination and growth response of old *Pinus ponderosa* trees to stand density reductions. *Plant, Cell, and Environment*, **26**, 631-644.

- Roden, J. S., Lin, G. & Ehleringer, J. (2000) A mechanistic model for interpretation of hydrogen and oxygen isotope ratios in tree-ring cellulose. *Geochimica et Cosmochimica Acta*, **64**, 21-35.
- Sternberg, L., DeNiro, M. J. & Savidge, R. A. (1986) Oxygen isotope exchange between metabolites and water during biochemical reactions leading to cellulose synthesis. *Plant Physiology*, **82**, 423-427.
- Sternberg, L. D. S. L. (2008) Oxygen stable isotope ratios of tree-ring cellulose: the next phase of understanding. *New Phytologist*.
- Tans, P. P., deJong, A. F. M. & Mook, W. G. (1978) Chemical pre-treatment and radial flow of  $^{14}\text{C}$  in tree rings. *Nature*, **271**, 234-235.
- White, J. W. C., Cook, E. R., Lawrence, J. R. & Broecker, W. S. (1985) The D/H ratios in trees: implications for water sources and tree ring D/H ratios. *Geochimica et Cosmochimica Acta*, **49**, 237-246

## **Bibliography**

- Addington, R. N., Mitchell, R. J., Oren, R. & Donovan, L. A. (2004) Stomatal sensitivity to vapor pressure deficit and its relationship to hydraulic conductance in *Pinus palustris*. *Tree Physiology*, **24**, 561-569.
- Adelman, J. D., Ewers, B. E. & Mackay, D. S. (2008) Use of temporal patterns in vapor pressure deficit to explain spatial autocorrelation dynamics in transpiration. *Tree Physiology*, **28**, 647-658.
- Anderson, W. T., Bernasconi, S. M., McKenzie, J. A. & Saurer, M. (1998) Oxygen and carbon isotopic record of climatic variability in tree ring cellulose (*Picea abies*): an example from Switzerland (1913 - 1995). *Journal of Geophysical Research*, **103(D24)**, 625-631,636.
- Aubinet, M., Heinesch, B. & Yernaux, M. (2003) Horizontal and vertical CO<sub>2</sub> advection in a sloping forest. *Boundary-Layer Meteorology*, **108**, 397-417.
- Barbour, M. M. (2007a) Stable oxygen isotope composition of plant tissue: a review. *Functional Plant Biology*, **34**, 83-94.
- Barbour, M. M. (2007b) Stable oxygen isotope composition of plant tissue: a review. *Functional Plant Biology*, **34**, 83-94.
- Barbour, M. M. & Farquhar, G. D. (2000) Relative humidity- and ABA-induced variation in carbon and oxygen isotope ratios of cotton leaves. *Plant, Cell and Environment*, **23**, 473-485.
- Barbour, M. M., Fischer, R. A., Sayre, K. D. & Farquhar, G. D. (2000) Oxygen isotope ratio of leaf and grain material correlates with stomatal conductance and grain yield in irrigated wheat. *Australian Journal of Plant Physiology*, **27**, 625-637.
- Barbour, M. M., Roden, J. S., Farquhar, G. D. & Ehleringer, J. R. (2004) Expressing leaf water and cellulose oxygen isotope ratios as enrichment above source water reveals evidence of a Peclet effect. *Oecologia*, **138**, 426-435.
- Barbour, M. M., Walcroft, A. S. & Farquhar, G. D. (2002) Seasonal variation in  $\delta^{13}\text{C}$  and  $\delta^{18}\text{O}$  of cellulose from growth rings of *Pinus radiata*. *Plant, Cell and Environment*, **25**, 1483-1499.
- Barnard, H. R. & Ryan, M. G. (2003) A test of the hydraulic limitation hypothesis in fast-growing *Eucalyptus saligna*. *Plant, Cell and Environment*, **26**, 1235-1245.
- Bauerle, W. L., Hinckley, T. M., Cermak, J., Kucera, J. & Bible, K. (1999) The canopy water relations of old-growth Douglas-fir trees. *Trees*, **13**, 211-217.
- Berry, S. L., Farquhar, G. D. & Roderick, M. L. (2005) Co-evolution of climate, vegetation, soil and air. *Encyclopedia of Hydrological Sciences*, pp. 177-192. John Wiley & Sons Inc., Hoboken, NJ.
- Bert, D., Leavitt, S. W. & Dupouey, J.-L. (1997) Variations in wood  $\delta^{13}\text{C}$  and water-use efficiency of *Abies alba* during the last century. *Ecology*, **78**, 1588-1596.
- Binkley, D. (1984) Douglas-fir stem growth per unit leaf area increased by interplanted Sitka alder and red alder. *Forest Science*, **30**, 259-263.
- Binkley, D., Stape, J. L., Ryan, M. G., Barnard, H. R. & Fownes, J. H. (2002) Age-related decline in forest ecosystem growth: An individual-tree, stand-structure hypothesis. *Ecosystems*, **5**, 58-67.
- Bond, B. J. (2003) Hydrology and ecology meet - and the meeting is good. *Hydrological Processes*, **17**, 2087-2089.
- Bond, B. J., Jones, J. A., Moore, G., Phillips, N., Post, D. & McDonnell, J. J. (2002) The zone of vegetation influence on baseflow revealed by diel patterns of streamflow

- and vegetation water use in a headwater basin. *Hydrological Processes*, **16**, 1671-1677.
- Bond, B. J. & Kavanagh, K. L. (1999) Stomatal behavior of four woody species in relation to leaf-specific hydraulic conductance and threshold water potential. *Tree Physiology*, **19**, 502-510.
- Bosch, J. M. & Hewlett, J. D. (1982) A review of catchment experiments to determine the effect of vegetation changes on water yield and evapotranspiration. *Journal of Hydrology*, **55**, 3-23.
- Bowling, D. R., Pataki, D. E. & Randerson, J. T. (2008) Carbon isotopes in terrestrial ecosystem pools and CO<sub>2</sub> fluxes. *New Phytologist*, **178**, 24-40.
- Brandes, E., Kodama, N., Whittaker, K., Weston, C., Rennenberg, H., Keitel, C., Adams, M. A. & Gessler, A. (2006) Short-term variation in the isotopic composition of organic matter allocated from the leaves to the stem of *Pinus sylvestris*: effects of photosynthetic and postphotosynthetic carbon isotope fractionation. *Global Change Biology*, **12**, 1922-1936.
- Bren, L. J. (1997) Effects of slope vegetation removal on the diurnal variations of a small mountain stream. *Water Resources Research*, **33**, 321-331.
- Brooks, J. R. & Coulombe, R. (2009) Physiological responses to fertilization recorded in tree rings: isotopic lessons from a long-term fertilization trial. *Ecological Applications* **19**, 1044-1060.
- Brooks, J. R., Schulte, P. J., Bond, B. J., Coulombe, R., Domec, J. C., Hinckley, T. M., McDowell, N. G. & Phillips, N. (2003) Does foliage on the same branch compete for the same water? Experiments on Douglas-fir trees. *Trees*, **17**, 101-108.
- Brooks, J. R., Sprugel, D. G. & Hinckley, T. M. (1996) The effects of light acclimation during and after foliage expansion on photosynthetic function of *Abies amabilis* foliage within the canopy. *Oecologia*, **107**, 21-32.
- Buchmann, N., Kao, W.-Y. & Ehleringer, J. R. (1997) Influence of stand structure on carbon-13 of vegetation, soils, and canopy air within deciduous and evergreen forests in Utah, United States. *Oecologia*, **110**, 109-119.
- Calder, I. R. (1998) Water use by forests, limits and controls. *Tree Physiology*, **18**, 625-631.
- Campbell, G. S. & Norman, J. M. (1998) *An introduction to environmental biophysics*. Springer, New York.
- Cermak, J. (1989) Solar equivalent leaf area as the efficient biometrical parameter of individual leaves, trees and stands. *Tree Physiology*, **5**, 269-289.
- Chapin III, F. S., Matson, P. A. & Mooney, H. A. (2002) *Principles of Terrestrial Ecosystem Ecology*. Springer, New York.
- Chen, X. (2007) Hydrologic connections of a stream-aquifer-vegetation zone in south-central Platte River valley, Nebraska. *Journal of Hydrology* **333**, 554-568.
- Cochard, H., Breda, N. & Granier, A. (1996) Whole tree hydraulic conductance and water loss regulation in *Quercus* during drought: evidence for stomatal control of embolism. *Annales Des Sciences Forestières*, **53**, 197-206.
- Cosandey, C., Andreassian, V., Martin, C., Didon-Lescot, J., Lavabre, J., Folton, N., Mathys, N. & Richard, D. (2005) The hydrologic impact of the Mediterranean forest: a review of French research. *Journal of Hydrology*, **301**, 235-249.

- Craig, H. & Gordon, L. I. (1965) Deuterium and oxygen 18 variations in the ocean and the marine atmosphere. *Stable isotopes in oceanographic studies and paleotemperatures*, pp. 9-130. Spoleto.
- Czarnomski, N. M., Moore, G. W., Pypker, T. G., Licata, J. & Bond, B. J. (2005) Precision and accuracy of three alternative soil water content instruments in two forest soils of the Pacific Northwest. *Canadian Journal of Forest Research*, **35**, 1867-1876.
- Dawson, T. E. (1993) Water sources of plants as determined from xylem-water isotopic composition: perspectives on plant competition, distribution, and water relations. *Stable Isotopes and Plant Carbon-Water Relations* (eds J. R. Ehleringer, A. E. Hall & G. D. Farquhar), pp. 465-496. Academic Press, Inc., New York.
- Dawson, T. E., Burgess, S. S. O., Tu, K. P., Oliveira, R. S., Santiago, L. S., Fisher, J. B., Simonin, K. A. & Ambrose, A. R. (2007) Nighttime transpiration in woody plants from contrasting ecosystems. *Tree Physiology*, **27**, 561-575.
- Dawson, T. E., Ward, J. K. & Ehleringer, J. R. (2004) Temporal scaling of physiological responses from gas exchange to tree rings: a gender-specific study of *Acer negundo* (Boxelder) growing under different conditions. *Functional Ecology*, **18**, 212-222.
- Deming, W. E. (1950) *Some theory of sampling*. Wiley and Sons, New York.
- Domec, J.-C., Warren, J. M., Meinzer, F. C., Brooks, J. R. & Coulombe, R. (2004) Native root xylem embolism and stomatal closure in stands of Douglas-fir and ponderosa pine: mitigated by hydraulic redistribution. *Oecologia*, **141**, 7-16.
- Domec, J. C., Meinzer, F. C., Gartner, B. L. & Woodruff, D. (2006) Transpiration-induced axial and radial tension gradients in trunks of Douglas-fir trees. *Tree Physiology* **26**, 275-284.
- Donovan, L. A., Richards, J. H. & Linton, M. J. (2003) Magnitude and mechanisms of disequilibrium between predawn plant and soil water potentials. *Ecology*, **84**, 463-470.
- Dunford, E. G. & Fletcher, P. W. (1947) Effect of removal of stream-bank vegetation upon water yield. *Eos transactions, American Geophysical Union* **28**, 105-110.
- Duquesnay, A., Breda, N., Stievenard, M. & Dupouey, J. L. (1998) Changes of tree-ring  $\delta^{13}\text{C}$  and water-use efficiency of beech (*Fagus sylvatica* L.) in north-eastern France during the past century. *Plant, Cell and Environ.*, **21**, 565-572.
- Duursma, R. A. & Marshall, J. D. (2006) Vertical canopy gradients in  $\delta^{13}\text{C}$  correspond with leaf nitrogen content in a mixed-species conifer forest. *Trees*, **20**, 496-506.
- Edwards, T. W. D., Graf, W., Trimborn, P., Stichler, W., Lipp, J. & Payer, H. D. (2000)  $\delta^{13}\text{C}$  response surface resolves humidity and temperature signals in trees. *Geochimica et Cosmochimica Acta*, **64**, 161-167.
- Ehleringer, J. R. & Cerling, T. E. (1995) Atmospheric  $\text{CO}_2$  and the ratio of intercellular to ambient  $\text{CO}_2$  concentrations in plants. *Tree Physiology*, **15**, 105-111.
- Ehleringer, J. R., Roden, J. S. & Dawson, T. E. (2000) Assessing ecosystem-level water relations through stable isotope ratio analyses. *Methods in Ecosystem Science* (eds O. E. Sala, R. B. Jackson, H. A. Mooney & R. W. Howarth), pp. 181-198. Springer, New York.

- Elias, P., I. Kratochvilova, D. Janous, M. Marek & Masarovicova., E. (1989) Stand microclimate and physiological activity of tree leaves in an oak-hornbeam forest. I. stand microclimate. *Trees*, **4**, 234-240.
- Epstein, S., Yapp, C. Y. & Hall, J. H. (1976) The determination of D/H ratio of nonexchangeable hydrogen in cellulose extracted from aquatic and land plants. *Earth and Planetary Science Letters*, **30**, 241-251.
- Ewers, B. E., Gower, S. T., Bond-Lamberty, B. & Wang, C. K. (2005) Effects of stand age and tree species on canopy transpiration and average stomatal conductance of boreal forests. *Plant, Cell and Environment*, **28**, 660-678.
- Farquhar, G. D., Barbour, M. M. & Henry, B. K. (1998) Interpretation of oxygen isotope composition of leaf material. *Stable isotopes: integration of biological, ecological and geochemical processes* (ed H. Griffiths), pp. 27-61. BIOS Scientific Publishers, Oxford.
- Farquhar, G. D., Cernusak, L. A. & Barnes, B. (2007) Heavy water fractionation during transpiration. *Plant Physiology*, **143**, 11-18.
- Farquhar, G. D., Ehleringer, J. R. & Hubick, K. T. (1989) Carbon isotope discrimination and photosynthesis. *Annual Review of Plant Physiology and Plant Molecular Biology*, **40**, 503-537.
- Farquhar, G. D. & Lloyd, J. (1993) Carbon and oxygen isotopes effects in the exchange of carbon dioxide between terrestrial plants and the atmosphere. *Stable Isotopes and Plant Carbon-Water Relations* (eds J. R. Ehleringer, A. E. Hall & G. D. Farquhar), pp. 47-70. Academic Press, New York.
- Farquhar, G. D., O'Leary, M. H. & Berry, J. A. (1982) On the relationship between carbon isotope discrimination and the intercellular carbon dioxide concentration in leaves. *Australian Journal of Plant Physiology*, **9**, 121-137.
- Federer, C. A. (1973) Forest transpiration greatly speeds streamflow recession. *Water Resources Research*, **9**, 1599-1604.
- Feng, X. & Epstein, S. (1995) Carbon isotopes of trees from arid environments and implications for reconstructing atmospheric CO<sub>2</sub> concentration. *Geochimica et Cosmochimica Acta*, **59**, 2599-2608.
- Field, C. & Mooney, H. A. (1986) The photosynthesis-nitrogen relationship in wild plants. *On the Economy of Plant Form and Function* (ed T. J. Givnish), pp. 25-55. Cambridge University Press, Cambridge.
- Flanagan, L. B., Comstock, J. P. & Ehleringer, J. R. (1991) Comparison of modeled and observed environmental influences on the stable oxygen and hydrogen isotope composition of leaf water in *Phaseolus vulgaris* L. *Plant Physiology*, **96**, 588-596.
- Ford, C. R., Hubbard, R. M., Kloeppel, B. D. & Vose, J. M. (2007) A comparison of sap flux based evapotranspiration estimates with catchment-scale water balance. *Agricultural and Forest Meteorology*, **145**, 176-185.
- Francey, R. J. & Farquhar, G. D. (1982) An explanation of <sup>13</sup>C/<sup>12</sup>C variations in tree rings. *Nature*, **297**, 28-31.
- Gholz, H. L., Grier, C. C., Campbell, A. G. & Brown, A. T. (1979) Equation for estimating biomass and leaf area of plants in the Pacific Northwest. pp. 1-36. Oregon State University, Forest Research Lab.
- Grams, T. E. E., Kozovits, A. R., Haberle, K.-H., Matyssek, R. & Dawson, T. E. (2007) Combining  $\delta^{13}\text{C}$  and  $\delta^{18}\text{O}$  analysis to unravel competition, CO<sub>2</sub> and O<sub>3</sub> effects on

- the physiological performance of different-aged trees. *Plant, Cell and Environment*, **30**, 1023-1034.
- Granier, A. (1985) Une nouvelle méthode pour la mesure du flux de sève brute dans le tronc des arbres. *Annales Des Sciences Forestieres*, **42**, 193-200.
- Granier, A. (1987) Evaluation of transpiration in a Douglas-fir stand by means of sap flow measurements. *Tree Physiology*, **3**, 309-320.
- Gribovszki, Z., Kalicz, P., Szilágyi, J. & Kucsara, M. (2008) Riparian zone evapotranspiration estimation from diurnal groundwater fluctuations. *Journal of Hydrology* **349**, 6-17.
- Hacke, U. G., Sperry, J. S., Ewers, B. E., Ellsworth, D. S., Schafer, K. V. R. & Oren, R. (2000) Influence of soil porosity on water use in *Pinus taeda*. *Oecologia*, **124**, 495 - 505
- Hanba, Y. T., Mori, S., Lei, T. T., Koike, T. & Wada, E. (1997) Variations in leaf  $\delta^{13}\text{C}$  along a vertical profile of irradiance in a temperate Japanese forest. *Oecologia*, **110**, 253-261.
- Harr, R. D. (1977) Water flux in soil and subsoil on a steep forested slope. *Journal of Hydrology*, **33**, 37-58.
- Harr, R. D. & McCorison, F. M. (1979) Initial effects of clearcut logging on size and timing of peak flows in a small watershed in western Oregon. *Water Resources Research*, **15**, 90-94.
- Helle, G. & Schleser, G. H. (2004) Beyond CO<sub>2</sub>-fixation by Rubisco - an interpretation of  $^{13}\text{C}/^{12}\text{C}$  variations in tree rings from novel intra-seasonal studies on broad-leaf trees. *Plant, Cell and Environment*, **27**, 367-380.
- Hewlett, J. D. (1982) *Principles of forest hydrology*. The University of Georgia Press, Athens.
- Hinckley, T. M., Lassoie, J. P. & Running, S. W. (1978) Temporal and spatial variations in the water status of forest trees. *Forest Science*, **24**, 72.
- Hjerdt, K. N., McDonnell, J. J., Seibert, J. & Rodhe, A. (2004) A new topographic index to quantify downslope controls on local drainage. *Water Resources Research*, **40**, W05602, doi:10.1029/2004WR003130.
- Hooper, R. P., Aulenbach, B. T., Burns, D. A., McDonnell, J., Freer, J., Kendall, C. & Beven, K. (1998) Riparian control of stream-water chemistry: implications for hydrochemical basin models. *Conference HeadWater '98 Conf.* (eds K. Kovar, U. Tappeiner, N. Peters & R. Craig), pp. 451-458. IAHS, Meran, Italy.
- Huxman, T. E., Wilcox, B. P., Breshears, D. D., Scott, R. L., Snyder, K. A., Small, E. E., Hultine, K., Pockman, W. T. & Jackson, R. B. (2005) Ecohydrological implications of woody plant encroachment. *Ecology*, **86**, 308-319.
- Irvine, J., Perks, M. P., Magnani, F. & Grace, J. C. (1998) The response of *Pinus sylvestris* to drought: stomatal control of transpiration and hydraulic conductance. *Tree Physiology*, **18**, 393-402.
- Jarvis, P. G., James, G. B. & Landsberg, J. J. (1976) Coniferous forest. *Vegetation and the Atmosphere* (ed J. L. Monteith), pp. 171-240. Academic Press, London.
- Jarvis, P. G. & McNaughton, K. G. (1986) Stomatal control of transpiration: scaling up from leaf to region. *Advances in Ecological Research*, **15**, 1-49.

- Katul, G. G., Ellsworth, D. S. & Lai, C.-T. (2000) Modelling assimilation and intercellular CO<sub>2</sub> from measured conductance: a synthesis of approaches. *Plant, Cell and Environment*, **23**, 113-1328.
- Kavanagh, K. L., Pangle, R. & Schotzko, A. D. (2007) Nocturnal transpiration causing disequilibrium between soil and stem predawn water potential in mixed conifer forests of Idaho. *Tree Physiology*, **27**, 621-629.
- Klute, A. (1986) Water Retention: Laboratory Methods. *Methods of Soil Analysis Part 1 - Physical and Mineralogical Methods* (ed A. Klute), pp. 635-662. Soil Science Society of America, Inc., Madison, WI.
- Kobayashi, D., Suzuki, K. & Nomura, M. (1990) Diurnal fluctuations in streamflow and in specific electric conductance during drought periods. *Journal of Hydrology*, **115**, 105-114.
- Lang, A. R. G. & Mason, S. G. (1959) The exchange of oxygen-18 between cellulose, adsorbed water, and water vapor. *CANADIAN JOURNAL OF CHEMISTRY*, **37**, 1829-1833.
- Lassoie, J., Scott, D. & Fritschen, L. (1977) Transpiration Studies in Douglas-fir Using the Heat Pulse Technique. *Forest Science*, **23**, 377-390.
- Leavitt, S. W. & Danzer, S. R. (1993) Methods for batch processing small wood samples to holocellulose for stable-carbon isotope analysis. *Anal. Chem.*, **65**, 87-89.
- Libby, L. M., Pandolfi, L. J., Payton, P. H., Marshall III, J., Becker, B. & Giertz-Siebenlist, V. (1976) Isotopic tree thermometers. *Nature*, **261**, 284-290.
- Lloyd, J. & Farquhar, G. D. (1994) C-13 Discrimination during CO<sub>2</sub> assimilation by the terrestrial biosphere. *Oecologia*, **99**, 201-215.
- Loheide, S. P. (2008) A method for estimating subdaily evapotranspiration of shallow groundwater using diurnal water table fluctuations. *Ecohydrology*, **1**, 59-66.
- Loranty, M. M., Mackay, D. S., Ewers, B. E., Adelman, J. D. & Kruger, E. L. (2008) Environmental drivers of spatial variation in whole-tree transpiration in an aspen-dominated upland-to-wetland forest gradient. *Water Resources Research*, **44**, W02441, doi:10.1029/2007WR00627, 2008.
- Ludwig, J. A., Wilcox, B. P., Breshears, D. D., Tongway, D. J. & Imeson, A. C. (2005) Vegetation patches and runoff-erosion as interacting ecohydrological processes in semiarid landscapes. *Ecology*, **85**, 288-297.
- Marshall, J. D. & Monserud, R. A. (2006) Co-occurring species differ in tree-ring <sup>18</sup>O trends. *Tree Physiology*, **26**, 1055-1066.
- Martin, T. A., Hinckley, T. M., Meizner, F. C. & Sprugel, D. G. (1999) Boundary layer conductance, leaf temperature and transpiration of *Abies amabilis* branches. *Tree Physiology*, **19**, 435-443.
- McCarroll, D. & Loader, N. J. (2004) Stable isotopes in tree rings. *Quaternary Science Reviews*, **23**, 771-801.
- McDonnell, J. J. & Tanaka, T. (2001) Hydrology and biogeochemistry of forested catchments. *Hydrological Processes*. John Wiley & Sons, New York.
- McDowell, N., Brooks, J. R., Fitzgerald, S. A. & Bond, B. (2003) Carbon isotope discrimination and growth response of old *Pinus ponderosa* trees to stand density reductions. *Plant, Cell, and Environment*, **26**, 631-644.
- McDowell, N., Licata, J. & Bond, B. J. (2005) Environmental sensitivity of gas exchange in different-sized trees. *Oecologia*.

- McDowell, N. G., Phillips, N., Lunch, C., Bond, B. J. & Ryan, M. G. (2002) An investigation of hydraulic limitation and compensation in large, old Douglas-fir trees. *Tree Physiology*, **22**, 763-774.
- McGuire, K. J. (2004) *Water residence time and runoff generation in the western Cascades of Oregon*. PhD Dissertation, Oregon State University, Corvallis.
- McGuire, K. J., McDonnell, J. J. & Weiler, M. (2007) Integrating tracer experiments with modeling to infer water transit times. *Advances in Water Resources*, **30**, 824-837.
- McNulty, S. G. & Swank, W. T. (1995) Wood  $\delta^{13}\text{C}$  as a measure of annual basal area growth and soil water stress in a *Pinus strobus* forest. *Ecology*, **76**, 1581-1586.
- Meinzer, F. C. (2003) Functional convergence in plant responses to the environment. *Oecologia*, **134**, 1-11.
- Meinzer, F. C., Brooks, J. R., Bucci, S., Goldstein, G., Scholtz, F. G. & Warren, J. M. (2004) Converging patterns of uptake and hydraulic redistribution of soil water in contrasting woody vegetation types. *Tree Physiology*, **24**, 919-928.
- Monteith, J. L. (1995) A reinterpretation of stomatal responses to humidity. *Plant, Cell, and Environment*, **18**, 357-364.
- Monteith, J. L. & Unsworth, M. H. (2008) *Principles of Environmental Physics*. Academic Press, New York.
- Moore, G. W., Bond, B. J., Jones, J. A., Phillips, N. & Meinzer, F. C. (2004) Structural and compositional controls on transpiration in a 40- and 450-yr-old riparian forest in western Oregon, USA. *Tree Physiology*, **24**, 481-491.
- Neter, J., Kutner, M. H., Nachsheim, C. J. & Wasserman, W. (1996) *Applied Linear Statistical Models*. Irwin, Chicago, IL.
- Newman, B. D., Wilcox, B. P., Archer, S. R., Breshears, D. D., Dahm, C. N., Duffy, C. J., McDowell, N. G., Phillips, F. M., Scanlon, B. R. & Vivoni, E. R. (2006) Ecohydrology of water-limited environments: a scientific vision. *Water Resources Research*, **42**.
- Niinemets, U., Sonninen, E. & Tobias, M. (2004) Canopy gradients in leaf intercellular  $\text{CO}_2$  mole fractions revisited: interactions between leaf irradiance and water stress need consideration. *Plant, Cell and Environment*, **27**, 569-583.
- Nuttle, W. K. (2002) Is ecohydrology one idea or many? *Hydrological Sciences*, **47**, 805-807.
- Oke, T. R. (1992) *Boundary Layer Climates*. Routledge, New York.
- Oliver, C. D. & Larson, B. C. (1990) *Forest Stand Dynamics*. McGraww-Hill Inc., New York.
- Ott, R. L. (1993) *An introduction to statistical methods and data analysis*. Duxbury Press, Belmont, CA.
- Phillips, N., Bond, B., McDowell, N. & Ryan, M. G. (2002) Canopy and hydraulic conductance in young, mature, and old Douglas-fir trees. *Tree Physiology*, **22**, 205-211.
- Phillips, N., Oren, R. & Zimmerman, R. (1996) Radial patterns of xylem sap flow in non-diffuse and ring-porous tree species. *Plant Cell and Environment*, **19**, 983-990.
- Phillips, N., Ryan, M. G., Bond, B. J., McDowell, N. G., Hinkley, T. M. & Ęermák, J. (2003) Reliance on stored water increases with tree size in three species in the Pacific Northwest. *Tree Physiology*, **23**, 237-245.

- Pierson, F., Carlson, D. & Spaeth, K. (2002) Impacts of wildfire on soil hydrologic properties of steep sagebrush-stepp rangeland. *International Journal of Wildland Fire* **11**, 145-151.
- Powers, R. F. & Reynolds, P. E. (1999) Ten-year responses of ponderosa pine plantations to repeated vegetation and nutrient control along an environmental gradient. *Canadian Journal of Forest Research*, **29**, 1027-1038.
- Pypker, T. G., Hauck, M. J., Sulzman, E. W., Unsworth, M. H., Mix, A. C., Kayler, Z., Conklin, D., Kennedy, A., Barnard, H. R., Phillips, C. & Bond, B. J. (2008) Toward using  $\delta^{13}\text{C}$  of ecosystem respiration to monitor canopy physiology in complex terrain. *Oecologia*, **158**.
- Quinn, P. F., Beven, K. J., Chevallier, P. & Planchon, O. (1991) The prediction of hillslope flow paths for distributed hydrological modelling using digital terrain models. *Hydrological Processes*, **5**, 59-79.
- Ranken, D. W. (1974) *Hydrologic properties of soil and subsoil on a steep, forested slope*. M.S., Oregon State University, Corvallis.
- Rebetez, M., Saurer, M. & Cherubini, P. (2003) To what extent can oxygen isotopes in tree rings and precipitation be used to reconstruct past atmospheric temperature? A case study. *Climatic Change*, **61**, 237-248.
- Reich, P. B. & Hinckley, T. M. (1989) Influence of pre-dawn water potential and soil-to-leaf hydraulic conductance on maximum daily leaf diffusive conductance in two oak species. *Functional Ecology*, **3**, 719-726.
- Rich, L., Reynolds, H. & West, J. (1961) The Workman Creek experimental watershed. pp. 188.
- Richter, H. (1997) Water relations of plants in the field: some comments on the measurement of select parameters. *Journal of Experimental Botany*, **48**, 1-7.
- Robertson, I., Leavitt, S., Loader, N. J. & Buhay, W. (2008) Progress in isotope dendroclimatology. *Chemical Geology* **252**, EX1-EX4.
- Roden, J. S. (2008) Cross-dating of tree ring  $\delta^{18}\text{O}$  and  $\delta^{13}\text{C}$  tie series. *Chemical Geology*, **252**, 72-79.
- Roden, J. S. & Ehleringer, J. R. (2007) Summer precipitation influences the stable oxygen and carbon isotopic composition of tree-ring cellulose in *Pinus ponderosa*. *Tree Physiology*, **27**, 491-501.
- Roden, J. S., Lin, G. & Ehleringer, J. (2000) A mechanistic model for interpretation of hydrogen and oxygen isotope ratios in tree-ring cellulose. *Geochimica et Cosmochimica Acta*, **64**, 21-35.
- Rodriguez-Iturbe, I., D'Odorico, P., Laio, F., Ridolfi, L. & Tamea, S. (2007) Challenges in humid land ecohydrology: Interactions of water table and unsaturated zone with climate, soil, and vegetation. *Water Resources Research*, **43**, W09301.
- Rothacher, J., Dyrness, C. T. & Fredriksen, F. L. (1967) Hydrologic and related characteristics of three small watersheds in the Oregon cascades. pp. 1-54. Forest Service, USDA.
- Ryan, M. G. & Yoder, B. J. (1997) Hydraulic limits to tree height and tree growth. *BioScience*, **47**, 235-242.
- Saurer, M., Aellen, K. & Siegwolf, R. (1997) Correlating  $\delta^{13}\text{C}$  and  $\delta^{18}\text{O}$  in cellulose of trees. *Plant, Cell, and Environment*, **20**, 1543-1550.

- Saurer, M. & Siegwolf, R. T. W. (2007) Human impacts on tree ring growth reconstruction from stable isotopes. *Stable Isotopes as Indicators of Ecological Change* (eds T. E. Dawson & R. T. W. Siegwolf), pp. 49-62. Elsevier, New York.
- Saxton, K. E., Rawls, W. J., Romberger, J. S. & Papendick, R. I. (1986) Estimating generalized soil-water characteristics from texture. *Soil Science Society of America Journal*, **50**, 1031 - 1036.
- Scheidegger, Y., Saurer, M., Bahn, M. & Siegwolf, R. (2000) Linking stable oxygen and carbon isotopes with stomatal conductance and photosynthetic capacity: a conceptual model. *Oecologia*, **125**, 350-357.
- Selker, J. S., Keller, C. K. & McCord, J. T. (1999) *Vadose zone processes*. Lewis Publishers, Boca Raton, FL.
- Shanley, J. B., Hjerdt, K. N., McDonnell, J. J. & Kendall, C. (2003) Shallow water table fluctuations in relation to soil penetration resistance. *Ground Water*, **41**, 964 - 972.
- Sheshshayee, M. S., Bindumadhava, H., Ramesh, R., Prasad, T. G., Lakshminarayana, M. R. & Udayakumar, M. (2005) Oxygen isotope enrichment ( $\Delta^{18}\text{O}$ ) as a measure of time-averaged transpiration rate. *Journal of Experimental Botany*, **56**, 3033-3039.
- Shewhart, W. A. (1993) The role of statistical method in economic standardization. *Econometrica*, **1**, 23-25.
- Siegwolf, R. T. W., Matyssek, R., Saurer, M., Maurer, S., Günthardt-Georg, M. S., Schmutz, P. & Bucher, J. B. (2001) Stable isotope analysis reveals differential effects of soil nitrogen and nitrogen dioxide on the water use efficiency in hybrid poplar leaves. *New Phytologist*, **149**, 233-246.
- Smith, F. W. & Long, J. N. (2001) Age-related decline in forest growth: an emergent property. *Forest Ecology and Management*, **1-3**, 175-181.
- Sollins, P., Cromack, K. J., McCorison, F. M., Waring, R. H. & Harr, R. D. (1981) Changes in nitrogen cycling at an old-growth Douglas-fir site after disturbance. *Journal of Environmental Quality*, **10**, 37-42.
- Sperry, J. S., Adler, F. R., Campbell, G. S. & Comstock, J. P. (1998) Limitation of plant water use by rhizosphere and xylem conductance: results form a model. *Plant Cell and Environ.*, **21**, 347-359.
- Sperry, J. S. & Ikeda, T. (1997) Xylem cavitation in roots and stems of Douglas-fir and white fir. *Tree Physiology*, **17**, 275-280.
- Sternberg, L., DeNiro, M. J. & Savidge, R. A. (1986) Oxygen isotope exchange between metabolites and water during biochemical reactions leading to cellulose synthesis. *Plant Physiology*, **82**, 423-427.
- Sternberg, L. D. S. L. (1989) Oxygen and hydrogen isotope measurements in plant cellulose analysis. *Modern Methods of Plant Analysis: plant fibers* (eds H. F. Linskens & J. F. Jackson), pp. 89-99. Springer Verlag, Berlin.
- Sternberg, L. D. S. L. (2008) Oxygen stable isotope ratios of tree-ring cellulose: the next phase of understanding. *New Phytologist*.
- Swanson, F. J. & James, M. E. (1975a) Geology and geomorphology of the H.J. Andrews Experimental Forest, Western cascades, Oregon. *Pacific Northwest Forest and Range Experiment Station, Forest Service, U.S.D.A, Research Paper PNW-188*, 1-14.

- Swanson, F. J. & James, M. E. (1975b) Geology and geomorphology of the H.J. Andrews Experimental Forest, western Cascades, Oregon., pp. 14. U.S. Department of Agriculture, Forest Service, Pacific Northwest Forest and Range Experiment Station, Portland, OR.
- Szilágyi, J., Gribovszki, Z., Kalicz, P. & Kucsara, M. (2008) On diurnal riparian zone groundwater-level and streamflow fluctuations. *Journal of Hydrology*, **349**, 1-5.
- Taiz, L. & Zeiger, E. (1991) *Plant Physiology*. The Benjamin/Cummings Publishing Company, Inc., New York.
- Tans, P. P., deJong, A. F. M. & Mook, W. G. (1978) Chemical pre-treatment and radial flow of  $^{14}\text{C}$  in tree rings. *Nature*, **271**, 234-235.
- Tardieu, F. a. W. J. D. (1993) Integration of hydraulic and chemical signalling in the control of stomatal conductance and water status of droughted plants. *Plant, Cell, and Environ.*, **16:341-349**.
- Triska, F. J., Sedell, J. R., Cromack, K., Gregory, S. V. & McCorison, F. M. (1984) Nitrogen budget for a small coniferous forest stream. *Ecological Monographs*, **54**, 119-140.
- Tromp-van Meerveld, H. J. & McDonnell, J. J. (2006a) On the interrelations between topography, soil depth, soil moisture, transpiration rates and species distribution at the hillslope scale. *Advances in Water Resources*, **29**, 293-310.
- Tromp-van Meerveld, H. J. & McDonnell, J. J. (2006b) Threshold relations in subsurface stormflow: 2. The fill and spill hypothesis. *Water Resources Research*, **42**, doi:10.1029/2004WR003800.
- Troxell, M. C. (1936) The diurnal fluctuations in the groundwater and flow of the Santa Ana River and its meaning. *Eos transactions, American Geophysical Union* **17**, 496-504.
- Tyree, M. T. & Sperry, J. S. (1988) Do Woody plants operate near the point of catastrophic xylem dysfunction caused by dynamic water stress? *Plant Physiology*, **88**, 574-580.
- Unsworth, M. H., Phillips, N., Link, T. E., Bond, B. J., Falk, M., Harmon, M. E., Hinkley, T. M., Marks, D. & Paw U, K. (2004) Components and controls of water flux in an old-growth Douglas-fir/western hemlock ecosystem. *Ecosystems*, **7**, 468-481.
- van Verseveld, W. (2007) *Hydro-biogeochemical coupling at the hillslope and catchment scale*. PhD, Oregon State University, Corvallis.
- Waring, R. H., and W. B. Silvester (1994) Variation in foliar  $\delta^{13}\text{C}$  values within the crowns of *Pinus radiata* trees. *Tree Physiology*, **14:1203-1213**.
- Waring, R. H., Thies, W. G. & Muscato, D. (1980) Stem growth per unit of leaf area: A measure of tree vigor. *Forest Science*, **26**, 112-117.
- Warren, J. M., Meinzer, F. C., Brooks, J. R. & Domec, J. C. (2005) Vertical stratification of soil water storage and release dynamics in Pacific Northwest coniferous forests. *Agricultural and Forest Meteorology*, **130**, 39 - 58.
- White, J. W. C., Cook, E. R., Lawrence, J. R. & Broecker, W. S. (1985) The D/H ratios in trees: implications for water sources and tree ring D/H ratios. *Geochimica et Cosmochimica Acta*, **49**, 237-246

- White, W. N. (1932) A method of estimating ground-water supplies based on discharge by plants and evaporation from soil: Results of investigations in Escalante Valley, Utah. pp. 1-105.
- Whitehead, D. (1998) Regulation of stomatal conductance and transpiration in forest canopies. *Tree Physiology*, **18**, 633-644.
- Williams, D., Scott, R., Huxman, T. & Goodrich, D. (2005) Multi-scale eco-hydrology of riparian ecosystems in the desert southwest. *The 58th Annual Meeting, Society for Range Management*. Fort Worth, Texas.
- Wondzell, S. M., Gooseff, M. N. & McGlynn, B. L. (2007) Flow velocity and the hydrologic behavior of streams during baseflow. *Geophysical Research Letters*, **34**.
- Wong, S. C., Cowan, I. R. & Farquhar, G. D. (1985) Leaf conductance in relation to rate of CO<sub>2</sub> assimilation. III. Influences of water stress and photoinhibition. *Plant Physiology*, **78**, 830-834.
- Wullschlegel, S. D., Meinzer, F. C. & Vertessy, R. A. (1998) A review of whole-plant water use studies in trees. *Tree Physiology*, **18**, 499-512.
- Yoshinaga, S. & Ohnuki, Y. (1995) Estimation of soil physical properties from a handy cone penetrometer test. *Japan Society of Erosion Control Engineering*, **48**, 22-28.
- Zalewski, M. (2000) Ecohydrology – the scientific background to use ecosystem properties as management tools toward sustainability of water resources. *Ecological Engineering* **16**, 1-8.
- Zalewski, M. (2002) Ecohydrology - the use of ecological and hydrological processes for sustainable management of water resources. *Hydrological Sciences*, **47**, 823-832.
- Zimmerman, J. K. & Ehleringer, J. R. (1990) Carbon isotope ratios are correlated with irradiance levels in the Panamanian orchid *Catacetum viridiflavum*. *Oecologia*, **83**, 247-249.